

**STUDY OF MICROSTRUCTURE AND
MECHANICAL BEHAVIOUR OF ALUMINIUM
COPPER ALLOY FOR HIGH TEMPERATURE
APPLICATIONS**

**Thesis submitted
By
Sasmita Tripathy**

**Doctor of Philosophy
(Engineering)**

**Department of Mechanical Engineering
Faculty Council of Engineering & Technology
Jadavpur University Kolkata, India**

2022

JADAVPUR UNIVERSITY
KOLKATA-700032, INDIA

INDEX NO.112/15/E

1. Title of the Thesis

“Study of Microstructure and Mechanical Behaviour of Aluminium-Copper Alloy for High Temperature Applications”

2. Name, Designation & Institution of the Supervisors:

Prof. (Dr) Goutam Sutradhar Director,

NIT, Manipur, Imphal-795004, INDIA

[Lien at Department of Mechanical Engineering, Jadavpur University, Kolkata-32, WB]

3. List of Publication (Journal)

I. Tripathy S., Sutradhar G., (2022) “Effect of Copper Addition on Tensile Behaviour of Al-Cu Alloy Used in High Temperature Applications.” *International Journal of Surface Engineering and Interdisciplinary Materials Science (IJSEIMS)*, 10(1), 1-16. **SCOPUS**

II. Tripathy S., Sutradhar G., (2022) "Simulation Based Fluidity and Solidification Analysis of Aluminium-Copper Sand Cast Alloy" *International Conference on Modern Materials for Engineering and Research KEM*, **SCOPUS**

4. Contributed Book Chapter

I. Tripathy S., Sutradhar G., (2021) “Computer-Aided Analysis of Solidification Time and its Effect on Hardness for Aluminium Copper Alloy.” In *Recent Advances in Mechanical Engineering* (pp. 861-868). Springer, Singapore.

5. List of Patent: NIL

6. List of Presentations in National/International Conferences/Workshops

I. Tripathy S., Sutradhar G., Banerjee S., (2017) “Effect of Copper Addition in Al-Alloy Used for High Temperature Applications Using Solidification Simulation Software as a Tool” *International Conference on Sustainable Manufacturing, Automation and Robotics Technologies (IC-SMART), Held during Dec 15-16, 2017 at CMERI Durgapur.*

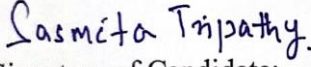
II. Tripathy S., Sutradhar G., (2018) “Computer Aided Study of Aluminium Alloy for Defect Free Casting” *1st International Conference on Mechanical Engineering (INCOM18), Held during Jan 4-6, 2018 at Jadavpur University, Kolkata-32*

III. Tripathy S., Sutradhar G., (2020) “Computer-Aided Analysis of Solidification Time and its Effect on Hardness for Aluminium Copper Alloy” *International Conference on Recent Advancements in Mechanical Engineering, Held during, Feb 07-09, at NIT, Silchar*

IV. Tripathy S., Sutradhar G., (2022) “Simulation Based Fluidity and Solidification Analysis of Aluminium-Copper Sand Cast Alloy” *International Conference on Modern Materials for Engineering and Research, (ICMMER 2022), Held during Oct 29-30 at Tiruchengode, Tamilnadu.*

“Statement of Originality”

I SASMITA TRIPATHY registered on 17th June 2015, do hereby declare that this thesis entitled “Study of Microstructure and Mechanical Behaviour of Aluminium-Copper Alloy for High Temperature Applications” contains literature survey and original research work done by the undersigned candidate as part of Doctoral studies. All information in this thesis has been obtained and presented in accordance with existing academic rules and ethical conduct. I declare that, as required by these rules and conduct, I have fully cited and referred all materials and results that are not original to this work. I also declare that I have checked this thesis as per the “Policy on Anti Plagiarism, Jadavpur University, 2019”, and the level of similarity as checked by iThenticate software is 9%.

Sasmita Tripathy.
Signature of Candidate:  01.12.22

Date:  01.12.22

Certified by Supervisor(s):

(Signature with date, seal)

Prof. (Dr.) Goutam Sutradhar
Director
National Institute of Technology
Manipur, Imphal, Manipur-735004
(Autonomous Inst. under MHRD, GOI)

1. _____

**DEPARTMENT OF MECHANICAL
ENGINEERING FACULTY OF ENGINEERING &
TECHNOLOGY JADAVPUR UNIVERSITY
KOLKATA, INDIA**

C E R T I F I C A T E

This is to certify that the thesis entitled, **“Study of Microstructure and Mechanical Behaviour of Aluminium-Copper Alloy for High Temperature Applications”** submitted by **SASMITA TRIPATHY**, who got her name registered on 17.06.2015 for the award of Ph.D. (Engineering) degree of Jadavpur University is absolutely based upon her own work under the supervision of Prof. (Dr) Goutam Sutradhar(Lien at Department of Mechanical Engineering ,JU,Kolkata-32) and that neither her thesis nor any part of the thesis has been submitted for any degree/diploma or any other academic award anywhere before.

1. 

29. 11. 22

Prof. (Dr.) Goutam Sutradhar
Director
National Institute of Technology
Manipur, Imphal, Manipur-736004
Autonomous Inst. under MHRD, GOI

Signature of the Supervisor and
date with official Seal

About the Author

Mrs Sasmita Tripathy, author of the thesis, was born in the year 1980 in Cuttack district of Odisha. Mrs Tripathy has completed her Secondary Education from Odisha Police High School, Cuttack in the year 1995 and Higher Secondary Education from Stewart Sc. College, Cuttack in the year 1997 under B.S.E and C.H.S.E, Odisha respectively. She graduated from Odisha Engineering College, Bhubaneswar with degree of B.E. in Mechanical Engineering in the year 2001 from Utkal University, Bhubaneswar, Odisha. After a carrier break due to marriage and motherhood she again pursued and completed her Master degree in Production and Design Engineering from NIT, Durgapur in the year 2010. Mrs Tripathy worked as an Assistant Professor (2011- 2013) in IMPS college of Engineering & Technology, Malda (WB). She was awarded with Women Scientist Fellowship WOS(A) by DST, New Delhi for the duration of 2014-2017. She has special interest in the field of synthesis of alloy and castings.

Page left blank intentionally

ACKNOWLEDGEMENT

The present thesis entitled, “Study of Microstructure and Mechanical Behaviour of Aluminium Copper Alloy for High Temperature Applications” is submitted for the degree of Doctor of Philosophy (Engineering) at Jadavpur University. The work has been carried out under the supervision of Prof. (Dr)Goutam Sutradhar, Director, NIT, Manipur [Lien at Department of Mechanical Engineering, Klokata-32]

It gives me immense pleasure to express my deep sense of gratitude to my supervisor Prof. (Dr) Goutam Sutradhar for his valuable guidance, motivation, constant inspiration, and advice that enabled me to bring up this thesis in the present form.

I would also express my thanks and gratitude to the HOD, Department of Mechanical Engineering, Secretary and office staff of the Faculty Council of Engineering and Technology, Jadavpur University, Kolkata-32, WB for their support and cooperation from the beginning of the programme.

I also acknowledge the funding agency “Department of Science and Technology, New Delhi” for financial support under their Women Scientist Scheme WOS-A. Sanction no: SR/WOS (A)/ET-82/2013.

I would especially like to thank Aligarh Muslim University, Aligarh, UP and Kalyani University, Kalyani, for providing testing facilities towards completing my research work. I would like to thank RITES, INDIA Ltd. for providing their testing facilities.

This journey would not have been possible without the support of my family and friends. I am incredibly grateful to my husband Mr. Jyotirmaya Panda (DGM, Indian Oil Corporation Limited) for his support and encouragement towards completing my Ph.D work. I am gratified to my kids, son Devjyoti [17] and especially daughter Devyanshi [6], for their love and sacrifice during my research work. I would like to thank my parents, brothers and in-laws for their blessings and love.

Above all I thank the Almighty for constantly giving me strength even during the most difficult time.

Place: Kolkata

Date:

SASMITA TRIPATHY

Dedicated to my parents

Mr. Gourikanta Tripathy

&

Mrs. Lavanya Tripathy

CONTENTS

RESEARCH PUBLICATIONS.....	ii
“STATEMENT OF ORIGINALITY”	iv
C E R T I F I C A T E	v
ABOUT THE AUTHOR.....	vi
A C K N O W L E D G E M E N T	viii
CONTENTS.....	x
LIST OF TABLES	xv
LIST OF FIGURES	xvi
ABBREVIATIONS	xviii
1. CHAPTER 1.....	1
INTRODUCTION.....	1
1.1Aluminium and its alloy	1
1.2Aluminium alloy for automotive, aerospace and high temperature applications (compared to ferrous alloy).....	3
1.3Alloys of aluminium.....	3
1.3.1Types of aluminium alloys.....	3
1.3.2Casting aluminium alloys	4
1.4Aluminium and silicon alloy	4
1.5Al-Cu alloy system	4
1.5.1Heat treatable Al-Cu alloy.....	5
1.5.2Metallurgical properties of Al-Cu alloy	5
1.5.3Mechanical properties Al-Cu alloy	5
1.5.4Castability of Al-Cu alloy	5
1.5.5High temperature applications and recent developments in Al-Cu alloy	6
1.6Computer aided analysis [Casting simulation software] for defect free casting.....	6
1.7Objective and Abstract.....	6
1.7.1 Objective	6
1.7.2 Abstract.....	8
1.8 Structure of thesis	8

2. CHAPTER 2	9
LITERATURE REVIEW	9
2.1 Aluminium alloy	9
2.1.1 Aluminium-copper alloy for high temperature applications	9
2.1.2 Al-Cu alloy and castability	10
2.2 Microstructure and metallurgy	11
2.2.1 Microstructure change due to copper addition	11
2.2.2 Microstructure due to change in solidification rate	12
2.2.3 Microstructure variation with casting processes.....	12
2.2.4 Microstructure variation with dimension change	13
2.2.5 Microstructure change after heat treatment	13
2.3 Mechanical properties	13
2.3.1 Copper addition and its effect on tensile behaviour.....	13
2.3.2 Copper addition and its effect on hardness	14
2.3.3 Tensile strength and micro hardness as function of microstructure	14
2.3.4 Copper addition and high temperature strength	14
2.4 Heat treatment	15
2.4.1 Solution heat treatment of Al-Cu alloy	15
2.4.2 Quenching process in heat treatment of Al-Cu alloy	15
2.4.3 Aging process in heat treatment of Al-Cu alloy	16
2.5 Wear properties of Al-Cu alloy	16
2.6 Casting simulation	16
2.6.1 Use of simulation software	16
2.6.2 Validation.....	17
3. CHAPTER 3	19
MATERIALS AND METHODS	19
3.1 Alloys and components development in the laboratory	19
3.1.1 Alloy development.....	20
3.1.2 Step-shape gravity die casting.....	21
3.1.3 Step-shape green-sand casting	23
3.1.4 Tensile test specimen preparation	24
3.1.5 Fluidity (spiral) test samples preparation:	24
3.1.6 Shrinkage volume calculation by water displacement method	25
3.2 Metallurgy and microstructure	25
3.2.1 Sample preparation for Optical micrograph (OM) and SEM	25
3.2.2 Grain morphology and grain size calculation.....	26

3.2.3	X-ray Diffraction (XRD) to study phase	26
3.2.4	Fractured surface microscopic test.....	26
3.3	Mechanical properties testing	26
3.3.1	Tensile strength test	26
3.3.2	Hardness test	27
3.3.3	SEM of fractured tensile and wear surface.....	28
3.4	Heat treatment	28
3.4.1	Solution heat treatment (SHT).....	28
3.4.2	Quenching	29
3.4.3	Aging	30
3.5	Pin-on-disc dry-sliding wear test	30
3.5.1	Dry-sliding pin-on-disc wear test.....	30
3.5.2	Taguchi method.....	31
3.5.3	SEM analysis of wear surface	32
3.6	Casting simulation with “Z-cast simulation software”	32
3.6.1	Use of simulation software.....	32
3.6.2	Solidification analysis	32
3.6.3	Cooling curve analysis	33
3.6.4	Iterations and defect free castings	33
4.	CHAPTER 4.....	35
	RESULTS AND DISCUSSIONS	35
4.1	Alloy and Cast-Components	35
4.1.1	Composition analysis	35
4.1.2	Macroscopic analysis results of gravity die cast step-shape component	35
	(varying copper wt%).....	35
4.1.3	Macroscopic analysis results of sand cast step-shape component (varying copper wt%)	36
4.1.4	Comparison (quantitative) of shrinkage defects for green sand-cast and gravity die-cast ‘step-shape’ components.....	37
4.1.5	External features of ‘step-shape’ cast components (varying section dimensions).....	38
4.1.6	Spiral /Fluidity test analysis	39
4.2	Metallographic results and analysis	40
4.2.1	Microstructure change for gravity die-cast components (variation of copper wt%) ..	40
4.2.2	Microstructure change for green sand cast component (varying copper wt%)	43
4.2.3	XRD of alloy A1, A2, A3.....	45
4.2.4	Comparison of grain size and change in copper wt%	46
4.2.5	Grain size variation with change in casting process	47
4.2.6	Grain size variation with change in thickness [Thickest S-1 & thinnest S-5].....	48

4.3Mechanical properties analysis.....	49
4.3.1Tensile test analysis of ‘step-shape’ component [gravity die casting].....	50
4.3.2Tensile test analysis of ‘step-shape’ component [green sand casting]	54
4.3.3Hardness of green sand cast and gravity die cast component [varying copper wt%] .	56
4.3.4Comparison of gravity die cast and green sand cast tensile results.....	57
4.3.5Comparison of Die cast and Sand cast hardness results.....	57
4.3.6 SEM images of fractured surface (Die cast)	58
4.3.7Micro hardness of sand cast and die cast alloys	59
4.4Heat treatment of Al-Cu alloy.....	60
4.4.1Tensile results of heat treated gravity die-casting [varying copper]	60
4.4.2Tensile results of heat treated green sand casting [varying copper].....	60
4.4.3SEM images of fractured tensile surface heat treated [green sand cast]	61
4.4.4SEM images of fractured tensile surface heat treated [gravity die cast].....	61
4.4.5Gravity die cast and green sand components [heat treated]	62
4.4.6Comparison of as cast & heat-treated tensile results [gravity die cast].....	63
4.4.7Comparison of grain size and tensile test results	63
4.5Tribo-mechanical analysis.....	64
4.5.1Results for dry-sliding wear properties with addition of copper	64
4.5.2Design of experiments	65
4.5.3Analysis of SEM images for wear properties [varying copper wt%]	67
4.6Casting Simulation Results	69
4.6.1Simulation results of green sand casting:.....	69
4.6.2Simulation results of gravity die casting	72
4.6.3Simulation and Experimental results discussion.....	80
4.6.4 Simulation results to make defect free cast components	80
4.6.5Simulation results for spiral [fluidity] tests	82
5. CHAPTER 5	86
5.1Variation in casting quality with varying composition.....	86
5.2Variation in mechanical properties with varying composition.....	86
5.3Wear properties	87
5.4Casting simulation.....	87
6. CHAPTER 6.....	88
FUTURE SCOPE OF WORK	88
REFERENCES	90

LIST OF TABLES

Table 1.1	Physical properties of Aluminium.....	1
Table 1.2	Area of car Portion of total Al used in car	4
Table 3.1	Green sand mold composition	23
Table 3.2	Wear test variables for dry-sliding wear test.....	30
Table 4.1	Al-Cu alloy composition for varying wt% of copper	35
Table 4.2	Comparison of shrinkage volume	38
Table 4.3	Simulation and actual spiral length comparison (in cm).....	40
Table 4.4	Grain size variation with change in casting process for	45
Table 4.5	Grain size and % area covered by θ -phase (die cast)	46
Table 4.6	UTS, YS, %EL for alloy composition A1, A2, A3	50
Table 4.7	Sand cast UTS, YS	54
Table 4.8	Hardness of sand cast and gravity die cast alloy	56
Table 4.9	Micro hardness of sand cast and die cast alloys A1, A2, A3	59
Table 4.10	UTS, YS, %EL for heat treated die cast samples	60
Table 4.11	UTS &YS of heat treated sand casting	60
Table 4.12	Mass loss with varying load for alloy A1, A2, A3[300rpm]	64
Table 4.13	Mass loss with varying speed for alloy A1, A2, A3[40N].....	64
Table 4.14	L9 Orthogonal array and S/N	65
Table 4.15	ANOVA response results and % contribution	67
Table 4.16	ANOVA model summary.....	67
Table 4.17	Comparison of actual and simulation SDAS	80
Table 4.18	Simulation shrinkage dimensions (in mm).....	84

LIST OF FIGURES

Figure 1.1 Aluminium cast alloy division.....	3
Figure 1.2 Phase diagram of Al-Cu alloy system	4
Figure 3.1 Patterns and die used for casting	19
Figure 3.2 Electrical Resistance Furnace.....	21
Figure 3.3 Gravity die casting set-up on the floor & Step casting developed from gravity die casting.....	22
Figure 3.4 Schematic diagram of gravity die cast component (all dimensions are in mm).....	23
Figure 3.5 Sand casting step shape (a) pattern with dimension(mm).....	24
Figure 3.6 Spiral-shape pattern and CO ₂ sand mold.....	25
Figure 3.7 Secondary dendrite arm spacing [SDAS].....	26
Figure 3.8 Universal Tensile Testing Machine.....	27
Figure 3.9 Schematic diagram of tensile test piece	27
Figure 3.10 Test pieces for SEM	28
Figure 3.11 Schematic diagram of the heat treatment process.....	29
Figure 3.12 Muffle Furnace.....	29
Figure 3.13 Test pieces (a) before and (b) after heat treatment.....	30
Figure 3.14 (a) Pin-On-Disc tribometer arrangements (b) monitor for readings [Courtesy: Tribology, AMU].....	31
Figure 4.1 Step components for gravity die casting.....	36
Figure 4.2 Green sand cast step-shape components (b) Schematic diagram showing S-1 to S-5	37
Figure 4.3 Shrinkage % comparisons for same copper wt%	38
Figure 4.4 Spiral-shape casting for fluidity analysis (a) A2 (b) A3	39
Figure 4.5 Optical Micrograph for (a) alloy A1 (b) alloy A2 (c) alloy A3.....	41
Figure 4.6 SEM images of (a) Alloy A1 (b) Alloy A2 (c) Alloy A3.....	42
Figure 4.7 % Area fraction covered by θ -phase (light colour in the image) (a) A1 (b) A2 (c) A3	43
Figure 4.8 Optical microscopy [200X] images (a) A1 (b) A2 (c) A3	44
Figure 4.9 XRD of alloy A1, A2, A3	45
Figure 4.10 Peak shift of alloy with varying copper wt %	46
Figure 4.11 Comparison of grain sizes and % area covered by θ -phase	47
Figure 4.12 Comparison of grain size for sand cast and die cast	47
Figure 4.13 Grain size variation for S-1 and S-5 for A2.....	48
Figure 4.14 Grain size variation for S-1 and S-5 for A3.....	49
Figure 4.15 Alloy A1 UTS & YS.....	51
Figure 4.16 Alloy A2 UTS & YS.....	51
Figure 4.17 Alloy A3 UTS & YS.....	52
Figure 4.18 Young's modulus of elasticity for A1.....	52
Figure 4.19 Young's modulus of elasticity for A2.....	53

Figure 4.20 Young's modulus of elasticity for A3	53
Figure 4.21 Comparison of UTS, YS and %EL of A1, A2, and A3	54
Figure 4.22 UTS, YS for step-shape component (a) A1 (b) A2(c) A3	55
Figure 4.23 Elastic modulus of sand cast alloy.....	56
Figure 4.24 Sand cast and gravity die cast tensile strength (varying copper wt%)	57
Figure 4.25 Hardness of sand casting and gravity die casting.....	58
Figure 4.26 Fracture surface SEM die cast (a) A1 (b) A2(c) A3	59
Figure 4.28 SEM-EDS of A2	61
Figure 4.27 SEM-EDS of A3.....	61
Figure 4.29 Fractured surface SEM of heat treated alloy (a) A1 (b) A2(c) A3	62
Figure 4.30 UTS of Gravity die casting & sand casting (heat treated).....	63
Figure 4.31 Comparison of as cast & heat treated tensile results	63
Figure 4.32 Comparison of UTS (as cast and heat treated) & grain size ...	64
Figure 4.33 S/N response table and graph	66
Figure 4.34 SEM of wear surface (1000X) for A1[load 20 N].....	68
Figure 4.35 SEM for wear (500X) of (a) A2 (b) A3	69
Figure 4.36 Sand casting simulation for A1	70
Figure 4.37 Sand casting simulation for A2.....	71
Figure 4.38 Sand casting simulation for A3.....	72
Figure 4.39 Die casting simulation for A1	74
Figure 4.40 Die casting simulation for A2.....	75
Figure 4.41 Die casting simulation for A3.....	76
Figure 4.42 Simulation cooling curve for A1	77
Figure 4.43 Simulation cooling curve for A2	78
Figure 4.44 Simulation cooling curve for A3	79
Figure 4.45 Solidification simulation iteration [sprue size change]	81
Figure 4.46 Solidification for modified riser base diameter	82
Figure 4.47 Simulation (a)cooling curve (b)length of spiral for A1	83
Figure 4.48 Simulation (a)cooling curve (b)length of spiral for A2	83
Figure 4.49 Simulation (a)cooling curve (b)length of spiral for A3	84

ABBREVIATIONS

Al-Cu: Aluminium – Copper
SEM: Scanning Electron Microscope
 V_m : Volume of mold cavity
 W_s : Water displaced by sand cast component
 W_d : Water displaced by die cast component
 SV_s : Shrinkage volume sand cast component
 SV_d : Shrinkage volume die cast component
SDAS: Secondary Dendrite Arm Spacing
YS: Yield Strength
UTS: Ultimate Tensile Strength
% EL: Percentage Elongation
HV: Vicker's hardness number
F: Test force
SHT: Solution heat treatment
HT: Heat treated
AC: As cast
DC: Gravity die casting
SC: Green sand casting
cc: Cooling curve
fdc: First derivative curve
S-1 to S-5: Section -1 to Section -5 of step component
DF: Degree of freedom

1. CHAPTER 1

INTRODUCTION

1.1 Aluminium and its alloy

Aluminium is a very strong electro-negative element and having high affinity toward oxygen. Aluminium is among six most widely spread metals on surface of earth but due to affinity towards oxygen it was not isolated till nineteenth century. In its pure state, aluminium is, however, a relatively soft metal with a yield strength of only 34.5 N/mm² (5,000 lb/in²) and a tensile strength of 90 N/mm²(13,000 lb/in²).

The versatile and unique combination of properties imparted by Aluminium and its alloys make it most commonly used metallic materials consisting of large range of applications. The application of aluminium and its alloys range from soft foil for wrapping to most complicate engineering components. Aluminium and its alloys also adapt a variety of manufacturing process. The most common manufacturing practice is casting. The unique combination of being nontoxic, lightweight and ease of manufacturing make it most used alloy till date. The father of the light metal industry was probably the French scientist, Henri Sainte-Claire Deville, who in 1850.

Two classes of alloys may be considered. The first are the 'cast alloys' which are cast directly into their desired forms by one of three methods (i.e., sand-casting, gravity die casting or pressure die casting), while the second class, the 'wrought alloys', are cast in ingots or billets and hot and cold worked mechanically into extrusions, forgings, sheet, foil, tube and wire.

Table 1.1 Physical properties of Aluminium

Aluminium	Al
Density	2.7g/cc
Melting temperature	660.3°C
Atomic weight	26.98amu
Thermal coefficient of expansion	(21-24)10⁻⁶ m/°C

Physical and chemical advantages of aluminium alloys for which they are preferred over other metal alloys are listed below:

Light weight

- The most used ferrous alloys for engineering applications are heavier compared to aluminium alloy. Light weight of aluminium alloys makes them easy and economical for transporting

High strength to weight ratio

This property of aluminium alloy the main reason for replacing heavy cast iron components especially in automotive industry. Strict norms of pollution control for vehicles are pushing manufacturer to search for lighter alternatives. The most preferred alloy and trending are alloys of aluminium.

Good strength at low or ambient temperature

- Most of the aluminium alloys exhibit strength comparable to ferrous alloy under ambient conditions. These qualities make them useful for cryogenics, LNG tankers etc.

Corrosion resistance

- Aluminium develops thin oxide film when exposed to air and this property imparts excellent corrosion resistant for this group of alloys.

Ease of manufacturing process

- Aluminium alloys can be manufactured at ease with many types of manufacturing process like casting, wrought, extrusion etc.

Non toxic

- Aluminium and its alloys are nontoxic for which foods are preferred to be packed in aluminium foil.

Thermal conductivity

- Aluminium is three times as thermal conductive as steel. So it is used in heat exchangers.

Electrical conductivity

- very good conductor of electricity

Other than the above properties aluminium and its alloys is noncombustible, spark proof and recyclable.

1.2 Aluminium alloy for automotive, aerospace and high temperature applications (compared to ferrous alloy)

- Aluminium alloy due to its low density are preferred for weight sensitive applications area such as automotive industry and aerospace. Aluminium provides high specific strength as compared to ferrous alloys used for such applications.
- Aluminium alloys are naturally oxidation resistant.
- Aluminium alloy has excellent corrosion resistance.
- Aluminium alloy can be manufactured to precision and adapt lots of manufacturing methods such as casting, extruding, forging etc.
- Aluminium posse's excellent weight to strength ratio.
- Aluminium alloys are cost effective as compared to alloy used for existing high temperature applications for example Ni-based and Ti-based alloy in aerospace and automotive industries.
- Aluminium alloys are environment friendly.
- All the above qualities are catching focus of researchers to replace ferrous alloy especially in automotive industries where environment norms are getting stringent and demand for high efficiency are building up.

1.3 Alloys of aluminium

1.3.1 Types of aluminium alloys

The chief alloying constituents added to aluminium are copper, magnesium, silicon, manganese, nickel and zinc. All of these are used to increase the strength of pure aluminium.

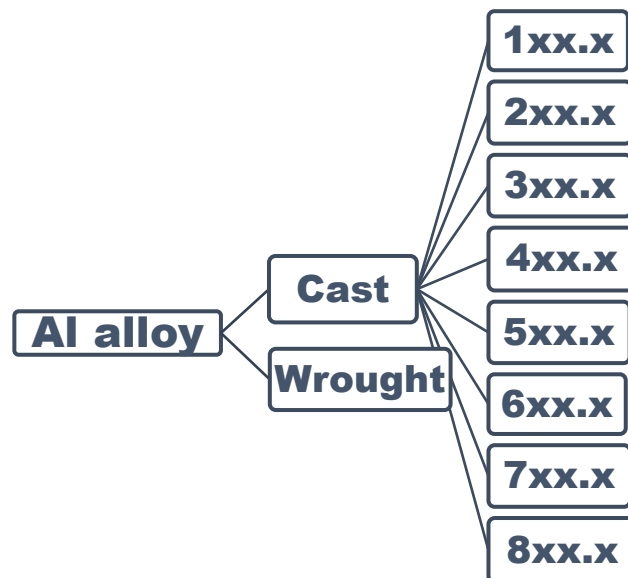


Figure 1.1 Aluminium cast alloy division

The Aluminium association designation system has following scheme for cast alloys of aluminium [Figure 1.1]. The cast alloy designation has assigned four numbers, where a decimal point between the third and fourth numbers. Letter precedes the numbers to indicate variations. The first three numbers indicate about the alloy, and the fourth is for the product form.

1xx.x- Controlled unalloyed compositions

2xx.x- Aluminium alloys containing copper as the major alloying element

3xx.x- Aluminium-silicon alloys are also containing magnesium and/or copper

4xx.x-Binary aluminium-silicon alloys

5xx.x- Aluminium alloys containing magnesium as the major alloying element

6xx.x- Currently unused

7xx.x- Aluminium alloys containing zinc as the major alloying element, usually also containing additions of either copper, magnesium, chromium, manganese or combinations of these elements.

8xx.x-Aluminium alloys containing tin as the major alloying element .

1.3.2Casting aluminium alloys

Use of cast part in automobile is gaining popularity. Data from reports reveal use of cast component from Aluminium alloy in engine and chassis is 90% compared to wrought aluminium alloy which is only 10%. [Table-1.2]

Table 1.2 Area of car Portion of total Al used in car

Area of car(%)	Portion of total Al used in car	(%) Cast Al-alloy	(%) Wrought Al-alloy
Engine Parts	50	90	10
Chassis	30	90	10
Body	15	20	80
Interior Fittings	5	40	60

[<https://www.researchgate.net/publication/306292368> Final Report on Scrap Management, Sorting and Classification of Aluminium Technical Report · December 2003]

1.4Aluminium and silicon alloy

The outstanding effect of silicon in aluminium alloys is the improvement of casting characteristics. Additions of silicon to pure aluminium dramatically improve fluidity, hot tear resistance, and feeding characteristics. The most prominently used compositions in all casting processes are those of the aluminium-silicon family. Commercial alloys span the hypoeutectic and hypereutectic ranges up to about 25% Si.

1.5Al-Cu alloy system

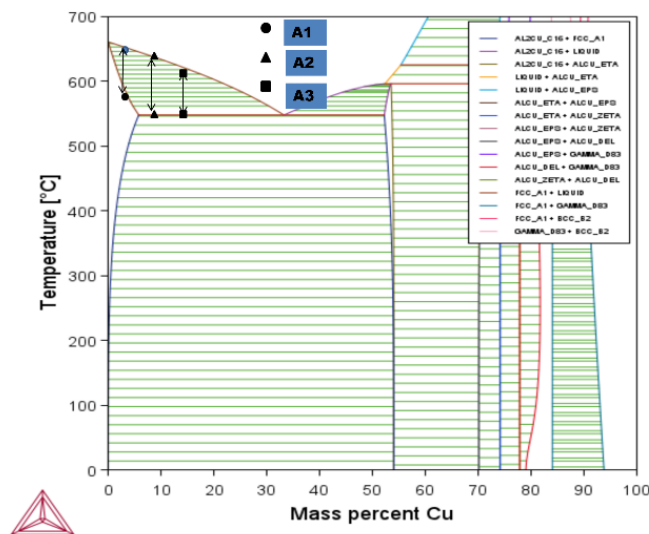


Figure 1.2 Phase diagram of Al-Cu alloy system

Aluminium alloys are the most used alloys in automotive industries. Among many other reasons of its use in automotive sectors light weight, high strength to weight ratio, ease in choice of manufacturing process is few. Developments in aluminium alloy and optimization of casting techniques have led to improved material properties and functional integration which enable aluminium castings to satisfy the new market requirements and have allowed replacing, in many cases, engine components made with heavy cast iron alloys. Phase diagram [Figure 1.2] of Al-Cu system mainly can be divided in to 3-parts:

- a. Hypoeutectic
- b. Eutectic
- c. Hyper-Eutectic

It is reported in the magazine “Aluminium Insider” in their [6th July 2018 issue] about the new material developed by using copper as an alloying element to sustain high temperature during engine operations. The report also mentioned about the difficulties that may arise due to copper addition during casting. The alloy was developed to address the issue of increasing efficiency without losing performance. The alloy developed with collaboration with “Oak Ridge National Laboratory and casting supplier Nematik” and FCA performed at high temperature with a nominal increase of 7% production cost.

Properties of Al-Cu cast alloy can be broadly classified as follows

1.5.1 Heat treatable Al-Cu alloy

Cast aluminium alloys have great response on heat-treatment because it is commonly used to alter the mechanical properties of the given alloy. Heat-treatment improves the strength of aluminium alloys. This improvement is possible through a process known as precipitation-hardening and it occurs due to the heating and cooling of an aluminium alloy. The alternate heating and cooling develop precipitates in the aluminium matrix.

Quenching-process and benefits: Quenching process description with emphasis on ambient quench temperature.

Aging-Process and benefits: Heat treatment improves hardness for improved machinability and eliminates any permanent changes in dimensions from residual growth due to aging at operating temperatures

1.5.2 Metallurgical properties of Al-Cu alloy

Aluminium-copper alloys having copper in excess precipitate as eutectic and intermetallic phase. This precipitation strengthening phase distribution is responsible for the improvement in mechanical behaviour at room as well as high temperature. The overall distribution of second phase in the aluminium primary phase and grain morphology depend upon many factors. Casting process, composition, cooling rate are some of the factors affecting the grain morphology of Al-Cu cast alloys.

1.5.3 Mechanical properties Al-Cu alloy

Aluminium casts are mainly alloyed to improve their mechanical properties depending upon the requirements. Copper is the most common alloying element when it comes to improvement of strength of aluminium alloy. The most commonly used Al-Cu alloy in automotive industry also contains silicon to improve castability. Silicon has lower thermal expansion. The intermetallics formed when silicon is present, during cooling are not preferable during high temperature applications. Aluminium alloyed with copper and not having silicon requires very carefully designed riser and gating system. Optimising the composition and design can result in components with high strength and sound casting.

1.5.4 Castability of Al-Cu alloy

Alloying aluminium with copper improves strength and with silicon improves castability. Alloy of aluminium with copper and in the absence of silicon is difficult to be casted. It is well known that adding silicon affect the strength at high temperature application but still to get

defect free cast components it is added with Al-Cu alloy.

1.5.5 High temperature applications and recent developments in Al-Cu alloy

The universal acceptance of aluminium pistons by all gasoline engine manufacturers in the United States can be attributed to their light weight and high thermal conductivity. Alloy 242-T571 is used in some heavy-duty pistons because of its higher thermal conductivity and superior properties at elevated temperatures. Other applications of aluminium alloys for elevated-temperature use include air-cooled cylinder heads for airplanes and motorcycles. The 10% Cu Alloy 222.0-T61 was used extensively for this purpose prior to the 1940s but has been replaced by the 242.0 and 243.0 compositions. The alloy 222.0-T6 contains Mg along with 10% Cu. But the use of the alloy is replaced by 242.0 and 243.0 which contain Si and copper in the range 3.5 to 4.5 %. Silicon addition improves fluidity. For use at moderate elevated temperatures (up to 175 °C, or 350 °F), Alloys 355 and C355 have been extensively used. These applications include aircraft motor and gear housings. Alloy A201.0 and the A206.0 type alloys have also been used in this temperature range when the combination of high strength at room temperatures and elevated temperatures is required. Aluminium alloy with copper always exhibits excellent strength, pressure tightness, light weight may be with or without silicon.

So, Al-Cu alloys are always preferred whenever strength at room and at elevated temperature is the priority. Compared to other alloying agents such as manganese and magnesium, rare earth elements used for elevated temperature use may not be cast effective when compared with copper.

1.6 Computer aided analysis [Casting simulation software] for defect free casting

Al-Cu alloys with somewhat higher copper contents (7 to 8%) were formerly the most commonly used aluminium casting alloys. Steadily been replaced by Al-Cu-Si alloys recently and are used to a very limited extent. The best attribute of higher-copper Al-Cu alloys is their insensitivity to impurities. However, these alloys display only fair castability. Also in limited use are Al-Cu alloys that contain 9 to 11% Cu, whose high-temperature strength and wear resistance are attractive for use in aircraft cylinder heads and in automotive (diesel) pistons and cylinder blocks. Very good high-temperature strength is an attribute of alloys containing copper, nickel, and magnesium, sometimes with iron in place of part of the nickel. When cost is a priority along with high temperature strength for selecting the major component to be used for alloy then copper with aluminium is the most desired material. Considering their fair castability and pressure to minimise rejections, use of “Casting simulation software” becoming unavoidable. The use of such software helps in saving time, labour material and money. Careful and accurate input parameters such as physical and thermal properties of alloy, dimension of the component, mold material and type of casting etc give very useful results to make defect free casting within a small-time frame. The use of casting simulation software to improve yield of alloy with fair castability and produce complex castings without defects are gaining popularity.

1.7 Objective and Abstract

1.7.1 Objective

Developing castable, precipitation strengthen and thermally stable Al-based alloy require alloying elements as having certain qualities such as capability of forming strengthening phase, low diffusibility in aluminium, ability to be casted conventionally and must have low solid solubility in aluminium. Considering copper as a major alloying element have all the above qualities developing Al-Cu alloy and not adding silicon to the system which is known to limit the high temperature applicability of the alloy is the main objective of the current research work. Al-Cu alloys are conventional alloy and one of the most studied alloy materials. The

need of recent analysis of these alloys is due to their versatile nature and adaptability to perform better under many conditions. Now a day lots of improved manufacturing techniques can be used to develop defect free components from this magic alloy economically which is the reason for the current study. The objective can be summarised as follows:

Part-I Development

- Development of the alloy system [without silicon]
- Casting components from the developed Al-Cu alloy. (Gravity die casting & Greensand casting) with varying dimensions.

Part-II Testing

- Study of microstructure and its effect on tensile behaviour for die cast and sand cast components developed from Al-Cu alloys.
- Effect of heat treatment (T6) on tensile behaviour of developed Al-Cu alloys.
- Wear properties of these developed Al-Cu alloys.
- Effect of solidification for different thickness under different manufacturing process.

Part-III Simulation

- Use and validation of casting simulation software to make defect free castings [“Z cast casting simulation software” used for the current study]. This is the improvement phase for improving the quality of casting.
- To check the predictability of software by adding lab developed alloy to the database.

Addition of silicon to aluminium improves its fluidity and quality of cast component. Silicon expands during solidification and reduction in shrinkage defect is normally observed with aluminium silicon alloy. Aluminium alloy with silicon exhibits improved strength at room temperature compared to pure aluminium. The improved mechanical properties are due to distribution of second phase inside the primary matrix. Only addition of silicon to aluminium without other alloying elements is not preferred due to inability of heat treatment. Aluminium alloys which are known for strength improvement due to precipitation hardening are not possible with only silicon as alloying element. Silicon which has very low solid solubility in aluminium even at high temperature and therefore not suitable for precipitation strengthening without any other elements. Copper is added which forms Al_2Cu intermetallics known for strengthening due to precipitation hardening. The most commonly used Al-Si-Cu alloy for automotive application is not suitable for high temperature operations. When it comes to aluminium alloy with copper as only alloying element it is very good for improving strength at room as well as at high temperature operations. The main limitation for Al-Cu alloy is quality of cast component and reduced ductility.

So, objective of the present analysis is to keep copper wt% in aluminium such that the changes in microstructure due to copper addition can be studied for 4 wt % (which is slightly below max solubility level at 548°C) up to 12 wt%. Upper limit of copper addition chosen as 12wt% which is well above its solubility in aluminium at eutectic temperature. Tensile tests results also suggested beyond 8 wt% of copper addition the strength of the alloy reduces. The best microstructure and mechanical properties were obtained when copper added at 8 wt%.

Study of effect of heat treatment on tensile behaviour for different copper addition is also included in the objective. Due to variation of copper wt% in aluminium, microstructure of the cast component change which eventually affect the tensile behaviour before and after heat treatment.

Addition of copper as major alloying element with other minor alloying elements is good for applications at room as well as at high temperature. Therefore, analysis of Al-Cu alloy is gaining importance. Analysis of microstructure with varying copper and in the absence of any other alloying elements can predict the tensile properties of cast components which will

be very helpful in choosing different compositions.

In the recent work alloying elements and their percentage in aluminium alloy chosen for study are such that mechanical properties must be enhanced not only at room temperature but also at elevated temperature. Aluminium alloy commonly used are added with copper for improving strength and silicon for better fluidity, corrosion resistance and to some extent strength at ambient temperature. But addition of silicon affects the strength at elevated temperature.

Use of simulation software and predicting the defect formation virtually which is validated experimentally so that the software can be used to produce defect free casting is also an objective of the study. Comparison of the accuracy of defects formation are done by using existing casting process parameters such as riser dimension, sprue size ; which give defect free results for aluminium alloy containing silicon.

1.7.2 Abstract

Aluminium alloy with copper as major alloying element is known for their high strength. Al-Cu alloy exhibit high strength at room as well as high temperature applications. The most common alloying element added to aluminium and copper is silicon, which imparts good casting properties. Adding silicon to Al-Cu alloy improve their castability at the cost of strength at higher temperatures. The current analysis is aimed at assessing different mechanical and microstructural changes for alloys of aluminium with copper when silicon is not added. Different casting processes and their results are also analysed for the Al-Cu alloy system. Aluminium alloys containing 4wt%, 8wt% and 12wt% of copper developed in the laboratory for the study has been tested for their mechanical properties and microstructure changes. Green sand casting and gravity die casting process used to compare the casting qualities and properties of components developed from these alloys. Wear properties of developed alloy also has been studied. The alloy containing 8wt% copper found to be best among all the three alloys developed based on tensile strength and microstructure. All the developed alloys were heat treated and tensile strength improved for all the alloys after heat treatment. From microstructure study it has been established that finer grain sizes and Al₂Cu intermetallics found are suitable to retain strength at higher temperatures for the developed alloys. The present study conducted simulation analysis with validation to improve cast qualities which happened to be poor due to excess copper and in the absence of silicon. Present analysis is a balanced combination of conventional alloy and modern techniques which may help to optimize alloy development and castability.

1.8 Structure of thesis

Chapter-1 of the thesis contain introduction to Al-Cu cast alloy. This part includes briefly about “Casting simulation software” and applications.

Chapter-2 of the thesis includes the literature and researches related to Al-Cu alloy for high temperature applications based on their microstructure.

Chapter-3 contains the summary of experimental methods and alloy synthesis for the current study.

Chapter-4 is about the results obtained and discussions related to the study of Al-Cu alloy. It includes results of microstructure study, mechanical behaviour, tribology and simulations with validations.

Chapter-5 is the conclusions from the current analysis.

Chapter-6 is brief summary of future scope related to the study.

2. CHAPTER 2

LITERATURE REVIEW

2.1 Aluminium alloy

Aluminium alloys are considered as the future of automotive industry due to their light weight and high strength. But the main challenge is retaining strength at elevated temperature. Addition of copper improves strength whereas silicon improves cast quality. Physical and mechanical properties of any alloy are dependent on factors other than composition such as cooling rate during solidification, casting method, heat treatment etc. Current analysis has taken account of all the above factors. Variation in compositions and its effect when different casting methods are followed, at different cooling rate and after heat treatment has been analyzed for Al-Cu alloy in the present thesis.

This section is the summary of extensive research outcomes and literatures present relevant to Al-Cu cast alloy based on above said factors.

2.1.1 Aluminium-copper alloy for high temperature applications

Pure aluminium is too soft and hardly has any applications in engineering. Therefore, alloys of aluminium are preferred over pure aluminium. Alloys of aluminium are the second most used alloys after steel. Aluminium alloys gained their popularity due to qualities which can be summarized as light weight, good conductivity, adaptability to various manufacturing processes, nontoxic nature etc. It is well known that due to light weight property when compared to the ferrous counterpart, alloys of aluminium deliver greater efficiency, better fuel consumption and less pollution making component for automotive applications. Aluminium alloys used in automotive applications are exposed to high operating temperatures (above 200°C). With increase in uses of aluminium and its alloys continuous evolution and research are simultaneously taking place. Among alloys of aluminium those extensively being used and researched are its alloys with copper and silicon. Especially when it comes to use in automotive sectors many parameters are needed to be considered. Mechanical properties, choice of manufacturing processes, precision of dimensions and cost of production are some of them.

Alloys of aluminium with metals like copper, magnesium, silicon as major alloying elements improve its tensile behaviour and make it more useful for different applications. Aluminium alloys are gaining popularity in automotive and aviation industries recently due to various reasons. High strength to weight ratio, ease in choice of different manufacturing processes, nontoxic behaviour, corrosion resistances are few to be named. Alloys of aluminium with Cu and Mg can retain good mechanical properties even under high temperature applications. Most of the aluminium alloy response to heat treatment is also excellent [1-4]. Aluminium is also 100% recyclable which is another reason for its vast use in recent years. M.O.Adeoti et al in their study concluded that scrap aluminium can be reused without compromising on its mechanical properties [5]. Copper for example, is added to Al primarily to increase the strength. Increasing the Cu content causes a continuous increase in the hardness; however, the strength and especially the ductility depend on how the Cu is distributed [6]. In the paper [7] it is described that copper addition improves the mechanical properties of aluminium alloy. Strength of aluminium alloy both at room temperature and elevated temperature increases with increase in Cu (wt%) content. With increasing copper wt% in aluminium above its solid solubility limit at eutectic temperature increases super plastic behaviour at high temperature [8]. Adding alloying elements like copper (Cu), magnesium (Mg), nickel (Ni) combined enhance the tensile properties of Al-Si foundry alloy at 250°C [9]. Addition of copper as major alloying element with other minor alloying elements is good for applications at room as well

as at high temperature. Therefore, analysis of Al-Cu alloy is gaining importance. Analysis of microstructure with varying copper and in the absence of any other alloying elements can predict the tensile properties of cast components which will be very helpful in choosing different compositions. Like aluminium alloys with copper and nickel improve its creep resistance along with its elastic modulus at elevated temperatures when copper content is increased. The strength at elevated temperature is due to the age hardening effect [10]. Aluminium when combined with copper gives very good strength at room as well as high operating temperatures. The strength of Al-Cu alloy is due to the tetragonal structure of the θ' phase. Precipitate-hardened aluminium alloy A201 possesses the highest mechanical strength between room temperature and 200°C when compared to other casting aluminium alloys [11]. Therefore, improving aluminium foundry alloys for elevated temperature applications is topic of concern for lots of industries. Heat treatable alloys of aluminium exhibit very good strength for room temperature applications, but they usually lose strength when exposed to temperatures above their aging temperature (above 150°C) due to softening of the precipitate phase. The strength is dependent both on exposure time and temperature. Aluminium alloys with copper and nickel improve its creep resistance along with its elastic modulus at elevated temperature when copper content is increased due to age hardening effect. Volume fraction of precipitation hardened alloy plays key role in enhancing the strength of commercial alloys. Gladman discussed about the optimum size of these precipitated particles in his research [12]. But in the paper [13] it has been observed that after certain time of exposure to high temperatures the strength and hardness cease to deteriorate. It is also reported that mechanical behaviour of AlCu5 alloys at high temperature showed better results despite the reported worse casting properties compared to conventional Al-Si alloys [14-17].

2.1.2 Al-Cu alloy and castability

Among the methods of manufacturing processes used in automotive industries casting is one of the mostly preferred, due to its cost effectiveness and ease of producing complex shapes with precision. Taking all into account the main focuses in recent days are developing alloys of aluminium that can withstand high operating temperatures without losing its castability and vice versa. Developments in aluminium alloys and optimization of casting techniques have led to improved material properties and functional integration which enable aluminium castings to satisfy the new market requirements and have allowed replacing engine components made with heavy cast iron alloys [18]. Most of the researches on fluidity of Al-Cu alloy agreed upon presence of silicon are desirable to get better quality of cast products. Casting aluminium alloys based on those to which silicon is added as the main alloying element are probably the most important for engineering applications. This is because of the high fluidity provided by alloys with near eutectic composition [19]. The paper [20] gives a very detailed report on effect of copper and silicon concluding copper increases hot tear and decreases fluidity when added up to 5.5wt%. The spiral fluidity test done with addition of silicon established better fluidity. The paper also established that increasing solidification range with copper addition decreases the fluidity and hence the castability. Silicon due to its higher latent heat slows down the solidification rate and increase in fluidity. It is also reported in many literatures that tensile behaviour degrades with increase in silicon, especially when it comes to elevated temperature uses. Ravi et al in their paper discussed about the exceptional nature of silicon of increasing fluidity [21]. The paper reported Al-Si alloy are castable alloy suitable for ambient temperature use and not for elevated temperature applications [22].

Therefore, Al-Cu alloys are known to be of the most potential materials for research in today's context when considered for high temperature applications [150°C to 250°C] as compared with most commonly used Al-Si-Cu [A356] alloy groups. Though AlCu5 family exhibit good strength at room and high temperatures, still they are not very convenient for use in GSPM or LPDC [23]. Shabestari and Momeni in their paper observed porosity volume increase and

tensile properties improve with addition of copper to Al-Si-Mg alloy [24]. Addition of copper to aluminium in the range 4 to 8 wt% generally result in large freezing ranges which ultimately make these alloy vulnerable to hot tearing defects [25]. It is well established that [26] 2xx.x series of aluminium alloys are capable of giving cast alloy of highest strength among all cast alloys. The paper by Teng et al compared the tensile properties of Al-Cu alloy and Manganese (Mn) micro alloying at high temperatures and got good results [27]. It is established in the paper [28] due to brittle nature of Al₂Cu intermetallics in Al-Cu alloys adding copper beyond 10wt% is not recommended. The aluminium-copper alloys are single-phase alloys. Unlike the alloys with silicon, where highly fluid second phase are available during the late stages of solidification. When available, the second phase help in feeding the shrinkage areas and also compensate for solidification stresses [29]. Smart foundry techniques and designs should be implemented to get the best mechanical properties deliverable by these series of alloys. Careful techniques are usually needed to promote the progress of the metal solidification starting from the remote areas of the casting toward the hotter and more liquid casting areas, the risers, and then to the riser feeders. When these necessary and more accurate casting techniques are used, the aluminium copper alloys can be successfully used to produce high-strength and high-ductility castings [30]. Microalloying of Al-Cu alloy improves the thermal stability further. The optimum wt% of copper and carefully designed casting processes can help in developing high strength Al-Cu alloy which can retain strength at elevated temperatures. Al-Cu alloy with 7.3-8 wt% has been found to be most hot tear resistant alloy [31]. The paper [32] reported newly developed alloy of aluminium with copper having only 0.054% Si as the optimum performing aluminium alloy at room as well as high temperature conditions. It can be concluded from literatures compared to other aluminium alloys under experimental analysis alloys with minimum silicon responded better to heat treatment and high temperature operation conditions.

2.2 Microstructure and metallurgy

It is well known that mechanical properties of any alloy can be predicted from their metallographic features. It is very relevant to study microstructure of any alloy under different solidification and casting processes. Heat treatments alter microstructure and distribution of intermetallics which ultimately affect the strength both at room and elevated temperatures. Evolution of grain structures under different solidification rate for any particular composition is also responsible for its hardness. Many studies have been performed to analyse the microstructure under various parameters for Al-Cu alloy. This section includes literatures describing the microstructure evolution and change in Al-Cu alloy. Easton et al established in their research that secondary dendrite arm spacing (SDAS) are characteristic of an alloy at certain cooling rate for a particular composition [33].

2.2.1 Microstructure change due to copper addition

Microstructures developed during cooling processes affect the mechanical properties of an alloy. The phase equilibrium and analysis reveal the different types of phase formation which are ultimately responsible for mechanical behaviour of any alloy. Study at high temperatures of phase and analysis give an idea about the microstructure to be present after solidification [34, 35]. Grain sizes of Al-Cu alloy can be altered by varying the amount of copper added to aluminium while keeping other parameters such as casting process, rate of cooling etc unchanged. It has been reported that grain sizes of alloy decrease with increasing copper wt% within certain range. The change in grain sizes due to change in composition can be related to dependency upon parameters like super cooling parameters and growth restriction factors. The solidification interval variations as an effect of composition change are too responsible for grain size variation. Researches show that grain sizes of as cast Al-Cu alloy decrease with increasing solidification interval. However it is also reported that grain size refining may

deteriorate when copper exceed 5.7wt% [36, 37]. Adding copper to commercially pure aluminium transforms the columnar structure to equi-axial grains and also results in a linear increase of the micro hardness. Rawajfeh et al in their paper found that 6wt% copper with aluminium is the optimal composition based on corrosion resistance and mechanical behaviour [38]. Copper has greatest impact as compared to any other major alloying elements added to aluminium; both heat treated, and in as cast conditions, at room as well as at elevated temperature applications. Copper is preferred as an alloying element where strength is priority at room and at elevated temperatures [39]. Increasing copper content beyond maximum solid solubility limit at eutectic temperature in aluminium increases the precipitation strengthening. The intermetallics formed can withstand high temperature. On the other hand, increasing the copper content decreases the elongation [40]. The elongation however can be improved with different dendrite grain morphology which can be achieved by adjusting the casting parameters. As reported [41] compared to the equiaxed dendrite grains, the tortuous dendrite grains led to increased tensile elongation (from 10.4% to 16.8%) and work of fracture (from 11.2 J/mm² to 17.2 J/mm²) by more than 50%, respectively. Meanwhile, the high tensile strength (~540 MPa) and grain size (~80 µm) were unchanged. Microstructures of cast components also vary with change in casting processes. Many researchers reported varying grain morphology due to variation in casting processes. Gradient solidification methods implemented give better results both for sand cast and die cast components are reported in the paper [42]. Die casting impart finer grains compared to sand casting and centrifugal casting is reported in the paper [43]. Experimental evidences show that same aluminium alloy composition exhibit different mechanical properties when casting methods are altered. This happens due to different microstructure distribution associated with various methods [44]. Mechanical properties of any cast component greatly depend on the microstructure. Grain refinement is one of the best techniques to improve the mechanical properties. Besides adding grain refiner there are many process parameters which can deliver good results. In the paper by Guofang et al [45] relation between cooling rate and grain refinement has been established. Microstructure evolution of aluminium with 4.5 wt% copper alloy due to different casting methods and cooling rate variations are also reported in the paper [46]. It is established from many experiments that higher the cooling rate finer the grains and better the mechanical behaviour. The grain morphology and distribution are also responsible for sound and defect free cast components. Addition of copper extends the solidification range as compared to copper free aluminium alloy which result in developing micro porosity more likely [47]. The microstructure of aluminium alloy with copper exhibit finer grain size but tendency to developing porosity is associated with copper addition. Even slight variation of solidification rate due to copper addition affects mechanical behaviour [48].

2.2.2 Microstructure due to change in solidification rate

Solidification rate alters the microstructure formed even for the same composition. There are many literatures those conclude that higher rate of cooling can produce better microstructures and hence better mechanical properties. Formaro et al in their paper studied Al-Cu alloy having copper below its solid solubility limit and found the dendritic grains and eutectic formed with rapid cooling are absent with slow cooling process [49]. Detailed analysis of aluminium alloy in the paper [50] reported, change in microstructures and eutectic formation with sudden change in velocity of the molten metal. The changes in microstructures are the result of rate of change in solidification due to change in velocity. Researches reveal that change in solidification rate alter the dendrite arm spacing which consequently change the tensile behaviour of aluminium alloy.

2.2.3 Microstructure variation with casting processes

It is reported in many studies that altering the method of casting amicrostructure of components. The paper by Beroual et al studied extensively about microstructure of sand cast and dies cast aluminium alloy and reported smaller dendrite arm spacing for high pressure die casting compared to sand casting. It is also reported in the same paper components from die cast exhibit better hardness [51, 52].

2.2.4 Microstructure variation with dimension change

The dimensions of components to be cast play an important role in microstructure formation. Change in section size varies the solidification rate and also the formation of grains. It is well established that section with smaller dimension or thickness exhibit better and finer microstructure. The paper by Akhil et al reported important findings with section size change and micro structure variations [53].

2.2.5 Microstructure change after heat treatment

Aluminium-copper alloys are known for their improved mechanical properties due to heat treatment. It is also reported that prolong annealing affect adversely the mechanical properties due to coarsening [54] Different processes of heat treatment alters the microstructure. Controlled aging during heat treatment varies the morphology and size of precipitates which enhance the microstructure and consequently the mechanical properties [55]. Detailed study of heat treatment on microstructure of 356 and 319 aluminium alloys with microstructure has been reported in the paper [56].

Literature studies establish the relation between copper addition and elevated temperature strength for Al alloys.

2.3 Mechanical properties

The quantitative study of phase transformation can help in finding out the sequence of precipitation of Al-Cu alloy. In the paper [57] change of strengthening phase formation is reported which is responsible for improving mechanical behaviour of Al-Cu alloy. Lots of studies related to mechanical properties of Al-Cu alloy based on their metallographic features are present in literature. Analysis of mechanical behaviour based on microstructure should be validated with actual strength test. For polycrystalline materials the relation between grain sizes and tensile strength is given by “Hall-Petch” equation [Eq -2.1]. The equation suggests decrease in grain size increase the tensile strength [58].

$$\sigma = \sigma_0 + kd^{-1/2} \quad \text{[Equation -2.1]}$$

Where σ -Yield strength, d - Average grain size, σ_0 -internal back stress, k -HP slope

Aluminium alloys are preferred over ferrous alloy in automotive and aerospace industries due to their high strength and light weight combination. To balance between cost, strength and weight at high temperature applications such as automobile engine components is pushing researchers to experiment with alloy composition and manufacturing process. Though most of the aluminium alloy in recent automotive applications show high strength at room temperature but cannot retain the same at higher temperatures. Lots of literature suggest adding copper improve mechanical behaviour not only at room temperature but also at high temperature applications.

2.3.1 Copper addition and its effect on tensile behaviour

It is well established that mechanical behaviour is dependent on the microstructure developed during solidification. Mechanical properties of Aluminium and its alloys also depend upon microstructure developed. The microstructure developed depends on many factors such as composition of alloy, rate of cooling, casting process, dimension of components etc. Other factors which affect the mechanical properties are defects developed during solidification [59-61]. Studies show that decrease in DAS (dendrite arm spacing) of α -Aluminium phase achieved due to fast cooling rate, increases the strength and hardness of aluminium alloy [62]. Husain Mehdi et al in their paper concluded that ultimate tensile strength increases and %

elongation decreases with increase in copper wt% [63]. Jin et al from their analysis found that alloy of aluminium 2219 exhibit higher strength and better ductility with TiC [64]. Researchers found that addition of copper as the only alloying element beyond certain amount have drawbacks such as developing casting defects, like hot tears, porosities and difficulties in casting complex shapes [65]. Defects like hot tears, shrinkages, porosities in the final components consequently decrease the yield [66]. To overcome such difficulties and to get defect free components silicon (Si) is added along with copper in most of the aluminium alloys. But many researchers found that addition of silicon affect adversely the strength during high temperature applications [67, 68]. As discussed in [section 2.1] though addition of silicon improves the quality of cast components but intermetallics formed during solidification may not withstand high temperatures above 250°C. Most of the automobile components and aerospace industry are choosing aluminium alloy as alternative to ferrous alloy due to its high strength to weight ratio. But using Al-alloy at elevated temperatures is still a challenge for engineers. Unlike many other engineering materials, alloys of aluminium designated for high temperature applications actually operate between relatively low temperature i.e. between 200°C to 400°C. Though the absolute operating temperature is not very high but the homologous temperature is comparable to any other high temperature designated engineering materials [69]. Many recent studies with multicomponent aluminium alloys concluded adding copper improve performance at elevated temperature [70]. Addition of copper and heat treatment increases strength, hardness but decreases ductility in aluminium alloy [71,72]. Most of the aluminium alloy along with copper use silicon as a n alloying element to enhance the casting process and final yield. As discussed earlier [section 1.2] aluminium alloy using copper as major alloying elements has its pros and cons. Copper when added as only alloying element and beyond certain limits create defects during solidification process such as hot tears, micro porosity and shrinkage. This happens as in most of the cases addition of copper increases the solidification range. New requirements have pushed the casting supplier to develop new process solutions with the aim of increasing the quality of castings, minimizing defects (porosity, inclusions etc.) and improving the microstructure of the material (dendrite arm spacing), in order to achieve better mechanical properties [73,74]. The paper [75] reported copper is added to enhance the mechanical properties of aluminium alloy. Adding copper up to 4wt% increased the mechanical properties of Al-Si alloy.

2.3.2 Copper addition and its effect on hardness

Copper added to aluminium alter the microstructure and hence the hardness. Depending upon the intermetallics formed the secondary dendrite arm spacing (SDAS) changes. These factors affect the hardness. [76, 77]

2.3.3 Tensile strength and micro hardness as function of microstructure

The paper [78] reported quantitative relation between micro hardness and microstructure. The primary dendrite arm spacing decreases with increase in cooling rate and growth rate which consequently increase micro hardness. Variation in mold thickness and induced cooling rate which alters microstructure and changes micro hardness [79]. Presence of Fe in Al-Cu alloy affects the microstructure. The intermetallics formed with increase in Fe result in decrease of mechanical properties of Al-Cu alloy [80]. Elastic modulus too depends upon metallurgical properties of Al-Cu alloy [81].

2.3.4 Copper addition and high temperature strength

High temperature strength of aluminium alloy for variation in copper amount reported in paper [82-84] Tanaka et al mentioned the alloy named “KS2000” which is highly heat resistant alloy of aluminium. Al-Cu alloy used for developing components used in diesel engine have been reported [85, 86].

Literature study suggest copper addition to aluminium alloy in the absence of silicon improve its strength at elevated temperature. Microstructure of alloys also decide the elevated temperature strength of any alloy.

Mechanical properties at room and elevated temperature enhance due to copper addition has been found from different literatures.

2.4 Heat treatment

Mechanical properties of Al-Cu cast alloy can further be enhanced by heat treatment. The correct heat treatment process with optimised temperature and time can improve tensile behaviour and in some cases ductility too. Heat treatment improves the microstructure and hence the mechanical properties. Addition of copper and its effect on heat treatment for aluminium alloy has been the area of interest for many researchers. Most of the literature found T6 heat treatment to be best suited for Al-Cu alloy. Heat treatment consists of solution heat treatment, quenching and aging. These processes aid in precipitation strengthening of A- Cu alloy [87]. In their paper Li et al discussed about T6 heat treatment of aluminium-copper alloy the strengthening θ -phase improved further and enhanced the elongation without affecting the tensile strength [88].

2.4.1 Solution heat treatment of Al-Cu alloy

It is well established for aluminium-copper alloy that T6 heat treatment improves its mechanical properties remarkably [89-92]. Research suggests that increasing copper content in aluminium improve their age hardening characteristics. This is due to more solute atom present for diffusion [93]. Aluminium alloy with copper show good response to heat treatment as the distribution of θ -phase become more uniform at grain boundaries. Detailed analysis of microstructure and corresponding tensile behaviour for particular composition can help in developing good cast components. Optimising composition and heat treatment can give best combination of strength and microstructure [94]. Size and distribution of precipitates affects the solution heating temperature to be applied for best results after heat treatment [95]. Study of Al-Cu alloy show that in T6 heat treatment Al_2Cu precipitated around the edges of grains [96]. Precipitates near the grain edges enhance the mechanical properties which can be achieved from T6 heat treatment. For T6 heat treatment the first stage is solution heat treatment (SHT). The temperature and time for SHT is chosen such that complete dissolution of precipitates should be achieved. Quenching in water followed by artificial age hardening helps in enhancing the tensile property due to better distribution of Al_2Cu precipitates near the edge. Heat treatment not only improves tensile property but also enhance elongation in 2219Al alloys [97]. The paper is about the importance of heat treatment as a whole process and use of prediction model in casting to predict microstructure. Al-Si-Cu alloy solution temperature is kept about 495°C [98]. Decision of Solution temperature and time depends upon presence of strengthening phases. The temperature range is decided from the phase diagram and presence of elements in the alloy. In the paper [99]. It is established that rate of dissolution of second phase, onset temperature of melting peak is dependent on the elements present in the alloy. Presence of magnesium slow the dissolution of Al_2Cu in the alloy A205 whereas this is not the case for binary Al-Cu alloy. To achieve complete dissolution of the strengthening phase it is of great importance to choose the correct solutionising temperature and time. To limit the maximum temperature of solution heating incipient melting should be taken care of [100, 101].

2.4.2 Quenching process in heat treatment of Al-Cu alloy

It is reported for Al-Cu alloy having copper well below solid solubility limit at eutectic , liquid drops are formed during up quenching at eutectic temperature of 547°C. The study by Jinlong Chen et al showed that when copper percentage increased from 2 wt% to 7.5 wt% , strength of the alloy is enhanced in as cast as well as solutionized condition. During solidification process of Al-Cu alloy Al_2Cu precipitate near the grain boundaries [102].

Quench sensitivity is a very important criterion of heat treatment and especially in case of T6 heat treatment. Many research reported that Cu increases the quench sensitivity of aluminium alloy [103,104]. The process of quenching for age hardenable process not only affect its mechanical properties but also can develop heat inter granular corrosion (IGC) as reported in the paper. The paper reported the need of faster cooling rate during quench operation for aluminium alloys [105]. Quenching parameters that are important during heat treatment are transfer time and quench temperature. The paper [106] analyses the delay in transfer time and quench sensitivity of 6061 and 6069 alloy. The sensitivity is composition dependent.

2.4.3 Aging process in heat treatment of Al-Cu alloy

The third step of heat treatment after quenching is age hardening. The holding time and temperature are of equal importance in case of age hardening. As described in the section this step rearranges the precipitates. For aluminium alloy 6061 optimum temperature and time as reported in the paper [107] is 175°C to 195°C for 2-6 hrs. The paper [108] concluded that carefully chosen aging temperature and time enhance the tribological properties of Al-Cu alloy.

There are enough literatures and researches which support addition of copper improve heat treatment response of Al alloy.

2.5 Wear properties of Al-Cu alloy

Majority of the tribological applications for aluminium and its alloys are related to sliding wear behavior. Aluminium and its alloys are primarily affected by sliding wear or adhesive wear. The dry sliding wear behaviour of aluminium alloys are influenced by a number of factors including chemical compositions, microstructures and hardness. Copper with its maximum solid solubility limits 5.7 wt% add to the wear resistance of aluminium alloys [109]. It is reported [110] that copper beyond its solid solubility limit has adverse effect on wear behaviour due to formation of second phase. But not all the aluminium alloy has an inverse relationship of wear rate and Vickers hardness [111]. Copper rich and heat treatable aluminium alloy have good wear resistance properties and normally considered for metal matrix composites (MMC) [112]. Study of tribological behaviour of aluminium alloy with copper addition can help to develop different MMCs having improved wear resistance properties. Recent study reported that Al₂Cu present in Al-Cu alloy improve wear resistance properties while used in micro arc oxidation coatings [113]. Alloys of aluminium with increased copper also exhibit improved wear behaviour under different manufacturing process. As it is reported in paper [114] under equal channel angle processing (ECAP) method wear properties and improved co-efficient of friction with 5% of copper. It is well known that MMCs show better wear resistance when compared to alloys but study of wear properties of alloys is equally important which can help in developing important materials from tribological point of view. Aluminium alloy may show mild to severe wear depending upon many factors [115].

2.6 Casting simulation

The challenge to optimise casting parameters such as riser dimensions, gating systems, mold temperatures etc for alloys having poor castability has been eased with the use of “casting simulation software”. Uses of these software practically in foundries are largely dependent upon the validation of results through actual experiments. Studies have been carried out to fill the gap between practical and theoretical approach. Literature studies suggest use of “casting simulation software” help to increase yield by producing defect free casting. They are useful for casting components from alloys having better mechanical properties but poor castability. The current analysis of Al-Cu alloys having poor casting properties has been tested for its applications with “Z-cast casting simulation software” to achieve defect free castings virtually.

2.6.1 Use of simulation software

Use of simulation software in foundry is gaining popularity now days as this can be used to predict rejection rate thereby improving yield. Simulation analysis before actual shop floor casting also save time, material, money etc as all the trials are done virtually Solidification simulation helps to analyse both for existing and new alloy composition. Casting includes lots of complex physical and chemical changes which occur during solidification or cooling down process. To get simulation results close to experimental results input parameters should be carefully chosen. Simulation and experimental validation were in good agreement as reported in the book [116]. Results obtained from simulation and experiments decide the dependency on virtual process further. [117-120]. Research shows those computer aided cooling curves are useful in analysing grain morphology of casting by predicting thermo-physical properties of the alloy [121,122].

Incorporating cooling curve analysis to improve process parameters: Thermal Analysis (TA) has been widely applied in aluminium casting plants to control the quality of the melt. Use of modern data acquisition systems and computer processing thermal analysis becomes a powerful tool for casting process control. However, the data collected using cooling curve analysis should be applied in existing simulation software in order to improve the accuracy of simulation [123].

2.6.2 Validation

Validation of the solidification simulation is very important for the practical point of view. It will definitely indicate the accuracy of the prediction obtained from the simulation results. It also helps the floor shop people to work with more confidence and scientifically approved logics.

Studies show that replacing the trial and error with simulation software which involves a virtual process can make our resources to be used efficiently. Many researches established that simulation results are comparable with experimental results [124]

3. CHAPTER 3

MATERIALS AND METHODS

3.1 Alloys and components development in the laboratory

Al-Cu alloys containing varying wt% of copper were developed in the laboratory for the current analysis. Commercially available alloys of aluminium contain silicon more than the permissible amount required for the present study. Therefore the first step for the analysis is to develop alloys of aluminium and copper using 99.9% pure aluminium with electrolytic copper. The required Al-Cu alloys having different wt% of copper for the analysis were developed from the master alloy, which is mainly 50% of aluminium and 50% of copper. Al-Cu alloys thus developed were used both for gravity die castings and green sand castings. The whole process of alloy development and components casting are described in details below.

1. Development of alloys for analysis: This part deals with developing the master alloy by mixing 50% of electrolytic copper and 50% of aluminium and then diluting with pure aluminium to get required composition. Alloys developed for the current study mainly have variation in copper wt% and silicon as only impurities (as no extra silicon is added)
2. Casting components from the developed alloy: Alloys having varying wt% of copper and their behavior when subjected to different casting methods and shapes have been described in this section. For green sand casting step shape wooden pattern and for gravity die casting die of cast iron [step-shape] have been prepared. For spiral fluidity test a match-plate pattern has



WOODEN PATTERN



CAST IRON DIE



Figure 3.1 Patterns and die used for casting

been used, [Figure 3.1]. The step-shape is chosen for casting components so that the effect of

solidification behavior for different thickness can be studied. The components thus developed may throw light on the solidification pattern and defects formed when section thickness change. The component shapes used in the current research are such that section thickness decrease with distance from the riser. The thinnest part is farthest from the riser and pouring sprue. All the alloy compositions with varying wt% of copper tested under similar conditions to maintain the validity of comparison.

3. Computer aided virtual castings to help in quality improvement: After developing alloys and components it is necessary to find out ways so that the flaws in the whole processes can be restricted to minimum level. The major flaws for the current study have been fixed with virtual process of casting simulations. For this part computer aided casting simulation software “Z-cast simulation software” has been used. This software uses both finite element method (FEM) and finite differential method (FDM) for analysis. Therefore, the simulation software used here considers both fluid and solid aspect of the solidification process. The simulation software used here is specially procured and customized for the alloy compositions used in current research.

Metallurgical, mechanical and tribological tests were conducted with the developed alloys having varying copper wt% in aluminium. As it is discussed earlier alloys of aluminium developed for the analysis kept the presence of silicon only as unavoidable impurities. To achieve these criteria utmost care has been taken. The section describes both green sand casting and gravity die casting processes to cast components for each of the compositions developed. Each test was carried out for four numbers of samples. Averages of the results obtained from these four samples were documented.

3.1.1 Alloy development

Master alloy was developed by mixing 500gm of pure electrolytic copper and 500gm of 99.9% pure aluminium in an induction furnace. The mixing was done at temperature of 1100°C. Proper mixing of aluminium and copper is ensured by stirring the molten metal. Flux is added to separate the impurities. Compositions required for this experiment were developed from the master alloy by mixing the master alloy with calculated amount of 99.9% pure aluminium in the furnace. Mixing the master alloy with previously calculated and measured amount of pure (99.9%) aluminium resulted in different alloys with varying wt% of copper in aluminium. By this method three different compositions of Al-Cu alloy were prepared with different wt% of copper. Chemical composition test ASTM-E-1251-17 done for developed alloy and it was found that elements are within the required limits.



Figure 3.2Electrical Resistance Furnace

Final samples of Al-Cu alloy after spectro analysis were melted in an electrical resistance melting furnace (max temp 1050°C) for casting. The furnace has one stirrer attached for mixing and a tilting wheel for ease in pouring. The weighted quantity of aluminium alloy is melted to desired temperature of 760°C in graphite crucible 3-phase electric resistance furnace with temperature controlling device as shown in Fig 3.2. Same procedure has been repeated for all the compositions. 2-3 trials have been attempted before the final best one is chosen for analysis.

3.1.2 Step-shape gravity die casting

Al-Cu alloy ingots with different copper wt% prepared from above method were re-melted . The molten metal tapped from the furnace with ladle and poured in to the die at about a temperature of 720°C . The die was kept at an angle $3-4^{\circ}$ [Fig 3.3] with the floor to aid metal flow.

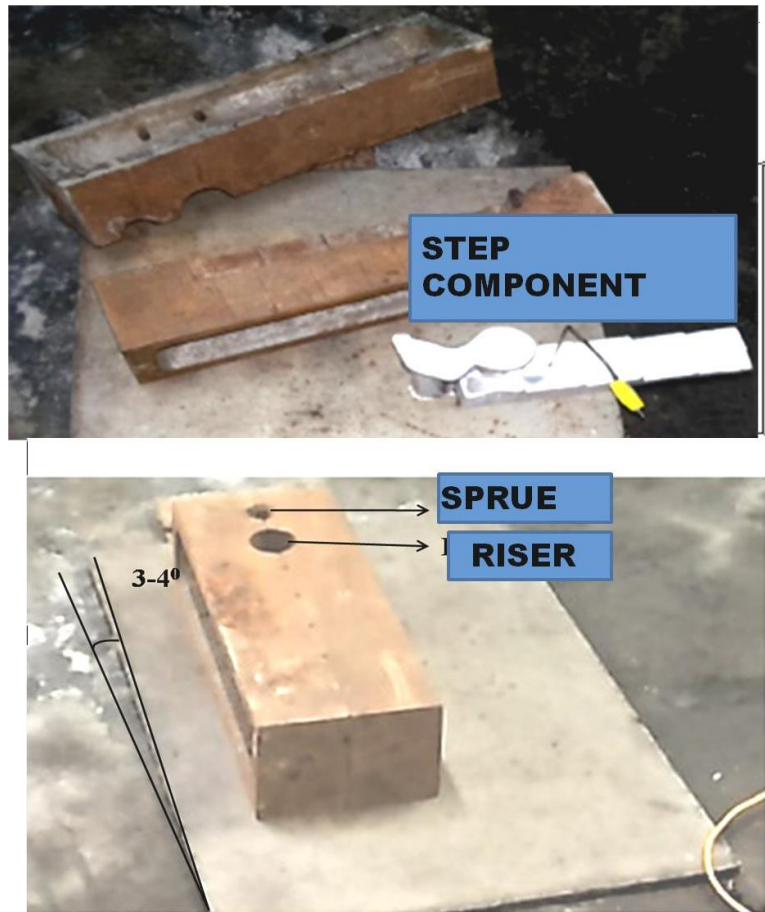


Figure 3.3 Gravity die casting set-up on the floor & Step casting developed from gravity die casting

The cast components were allowed to cool in the die. Schematic diagram and dimensions of step-shape casting is given in [Fig-3.4].

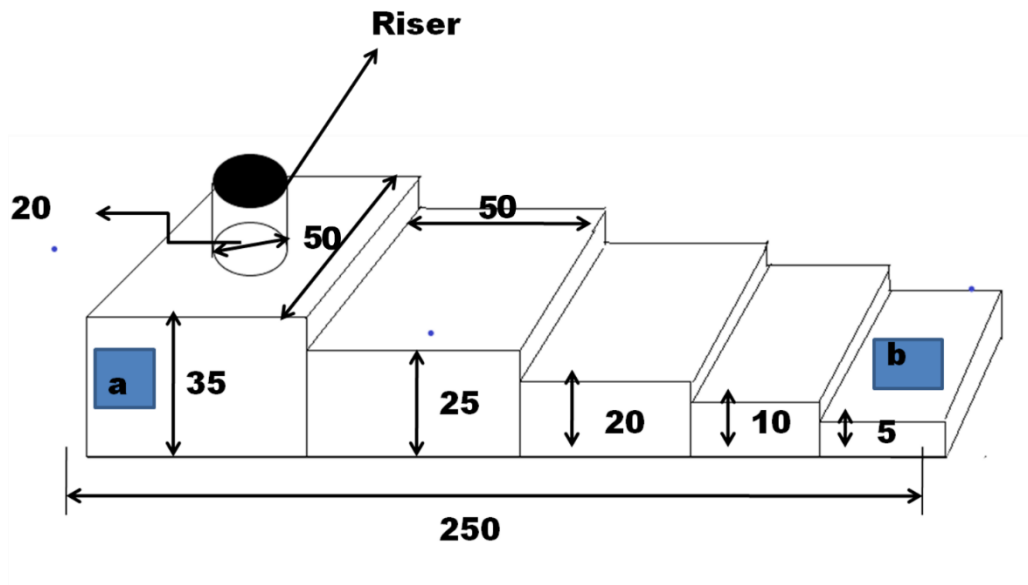


Figure 3.4 Schematic diagram of gravity die cast component (all dimensions are in mm)

3.1.3 Step-shape green-sand casting

Green sand mold was prepared by adding water, coal dust and bentonite as additives. Bentonite is used as the binder. The composition of the prepared mold is listed in the Table 3.1. After preparing the sand mixture mold was prepared. The mould was prepared with the help of 5-stepped wooden pattern [Fig 3.5] and its risering & gating system by ramming the sand mixture manually in the mould box. The alloy ingots of varying wt% of copper have been put in a graphite crucible. The crucible for melting placed in the electrical resistance furnace. The pouring from the furnace was done by tapping molten metal with the help of a ladle. Pouring temperature was maintained at 720°C with the help of k-type thermocouple.

Table 3.1 Green sand mold composition

Sand	High silica sand(sieved)
Coal dust(additive)	1 wt% of the sand
Bentonite(binder)	5 wt% of the sand
Water/Moisture	4 wt% of the sand

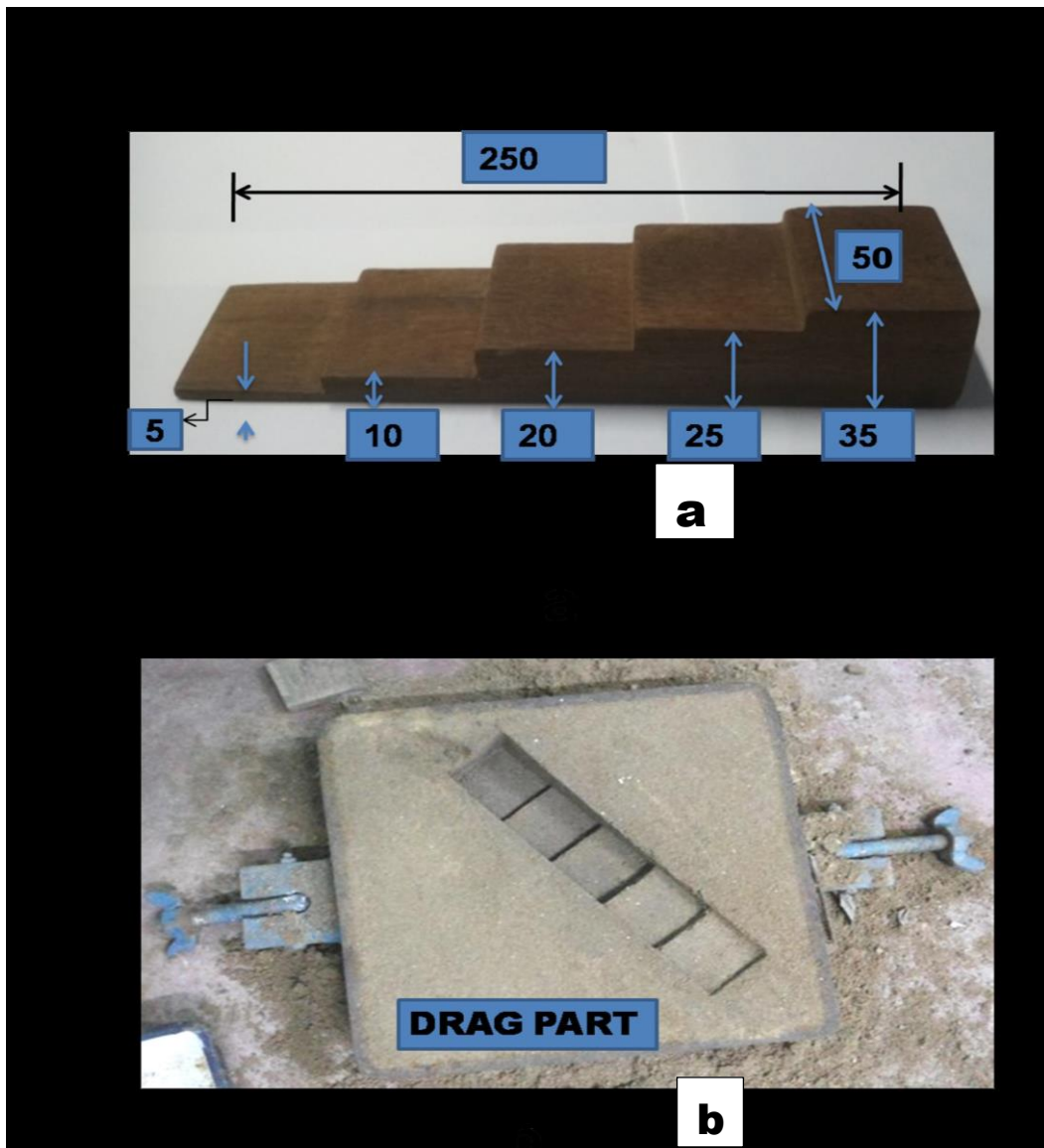


Figure 3.5 Sand casting step shape (a) pattern with dimension (mm) (b) green sand mold

3.1.4 Tensile test specimen preparation

Tensile test specimens were prepared by green sand cast and gravity die cast methods. For green sand cast specimen same method [3.1.3] of sand preparation was followed. Once the green sand was ready cylinder-shape sand mold of dimension approximately of diameter $\phi 20\text{mm}$ and length 150 mm has been prepared. Molten metal alloy from the furnace tapped and poured in to the mold at about 720°C . From these bars tensile test pieces were turned as per the dimension required.

Similarly for gravity die cast tensile test bars cast-iron die of approximately $\phi 20\text{mm}$ and length 150 mm prepared from cast iron die having two parts. Two semi-cylinder shape cast iron pipe clamped together and molten liquid poured at about 720°C .

Tensile specimens were prepared from these cylindrical bars by turning method and maintaining E8 standard.

3.1.5 Fluidity (spiral) test samples preparation:

The spiral sand mold was prepared with the help of match plate spiral pattern. The match

plate spiral pattern and mould cavity of spiral casting has shown in the [Fig 3.6]. For making the CO₂ mold, sand is initially mixed with sodium silicate and coal dust. The mixture is then loosely rammed in the mould around the spiral pattern. Carbon dioxide gas is blown into the mould. Carbon dioxide mixed with sodium silicate forming silica gel. [Eq 3.1]



The molten metal has poured into the skin dried CO₂ sand mould at the centre of the spiral and the pouring temperature of molten metal maintained at 720°C, to measure the fluidity of aluminium copper alloy with varying copper.

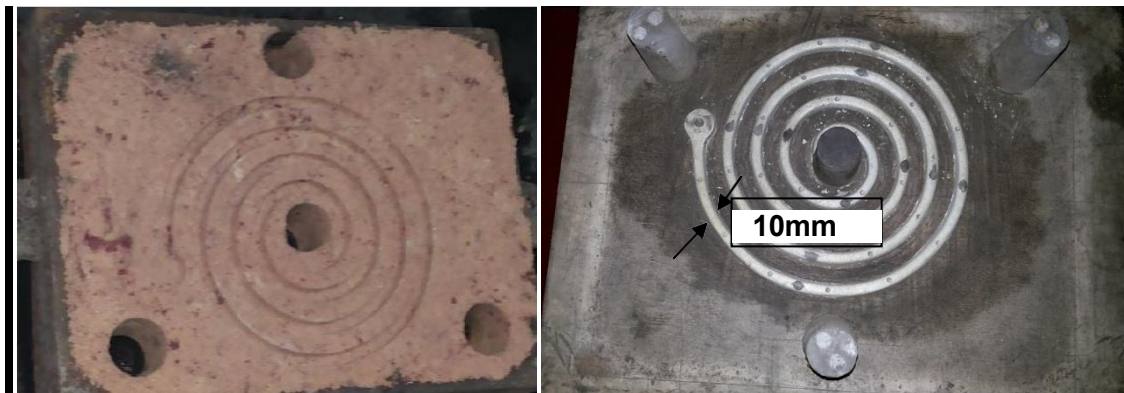


Figure 3.6 Spiral-shape pattern and CO₂ sand mold

3.1.6 Shrinkage volume calculation by water displacement method

The shrinkage defect volume was calculated by water displacement method. Volume of water displaced = Volume of the component

Volume of mold cavity - Volume of actual component = Shrinkage volume

V_m = Volume of mold cavity

W_s = Water displaced by sand cast

W_d = Water displaced by die cast

SV_s = Shrinkage volume sand cast = V_m - W_s

SV_d = Shrinkage volume die cast = V_m - W_d

3.2 Metallurgy and microstructure

To study the alloy properties different metallurgical test methods has been followed. It is well known that with variation in composition, casting process, cooling rate etc microstructure change occurs. Various test carried out for the analysis has been discussed below.

3.2.1 Sample preparation for Optical micrograph (OM) and SEM

Metallographic samples have been prepared by cutting 5x5x2 mm piece from the sand cast and die cast components. Fig 3.4 is showing the position of the step component (marked 'a' & 'b') from where the samples collected. For each composition of alloy similar procedures were followed. For metallographic analysis standard techniques were followed as polishing and etching. The samples of dimensions (5x5x2) mm were collected from different parts of the component. To maintain uniformity metallographic sample were cut for each composition considering the distance from the mold wall. Each sample thus collected was examined under optical microscope (Leica DM2700M) and scanning electron microscope (JSM 6360). For testing on optical microscope samples were grinded with SiC abrasive paper of grit size 180 followed by mechanical polishing to remove scratches. Samples were ready after both rough and fine polishing to be tested under light microscope. For scanning electron microscope (SEM) samples were further etched with Keller's reagent so that to reveal the grain boundaries

and orientations. Keller's reagent used consists of 1ml HF (48%) in 200ml of H₂O.

3.2.2 Grain morphology and grain size calculation

For analysis of grain sizes and secondary dendrite arm spacing (SDAS) linear intercept method applied with the help of "Image J" software. Area fraction covered by second phase was analyzed by adjusting threshold with the help of "Image J" image analysis software. After setting the scale to convert pixel into linear distance individual grain size was determined by taking the mean of several measured data. Finally, the mean of separately measured grains was calculated to determine the grain size. For each image mean of at least 50 readings were calculated. This method was followed for all the compositions to calculate the grain size. Similarly, % area fraction covered by second-phase for each composition was calculated by adjusting the image threshold with the help of the software. SDAS was calculated by dividing number of dendrites with length of the primary arm. Fig 3.7. The paper [125] investigated and established that such image analysis techniques for grain size measurements are trust worthy.

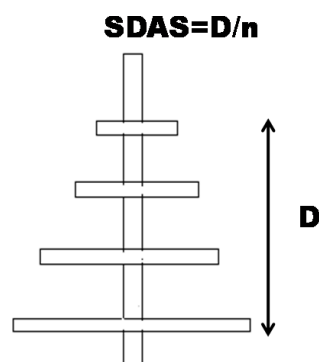


Figure 3.7 Secondary dendrite arm spacing [SDAS]

3.2.3 X-ray Diffraction (XRD) to study phase

Phase identification of the synthesised Al-Cu alloy was made by X-ray diffractometric analysis. The "Rigaku Ultimal III" diffractometer with monochromatic Cu-K α radiation (1.54059Å) was used for the current study. Unfiltered copper radiation was used to reveal peaks of secondary phases on an X-ray pattern.

3.2.4 Fractured surface microscopic test

Carefully cut fractured pieces after tensile test were mounted and SEM image has been prepared for analysis. The image reveals type of fracture occurred for different compositions. The metallographic tests for fractured surface conducted for as-cast, heat treated samples. The wear surface test too done by the help of SEM images to study the behaviour of wear.

3.3 Mechanical properties testing

3.3.1 Tensile strength test

Tensile test specimens were tested on universal tensile tester at room temperature in the laboratory as per ASTM E8 standard. (ASTM,1992) Test pieces of gauge diameter 12 mm and gauge length 50 mm were prepared from the cylindrical cast bars through machining. For each alloy composition 4 test pieces (as cast) prepared. Universal Testing Machine and schematic diagram of samples are shown in [Fig 3.8, 3.9]. Test was carried out at room temperature and the cross-head speed was maintained at 1mm/min. Load-displacement plot obtained from the digital universal testing machine on the X-Y recorder was used to calculate the ultimate tensile strength (UTS) and yield strength (YS). Percentage elongation (%EL) was calculated as shown [Equation-3.2]. The tensile test was conducted on Universal tensile machine (UTM-Q-4100).

$$\%EL = \frac{(\Delta l/L) \times 100}{L} \quad \text{[Equation-3.2] Where, } \Delta l = \text{Change in gauge length}$$

The load-displacement plot obtained from machine is used to calculate the yield strength (YS), ultimate tensile strength (UTS) and percent elongation for each tested sample. To calculate YS 0.2% proof stress method was used. UTS calculated by dividing applied load with the cross-sectional area of the test specimen. From stress-strain plot young's modulus was calculated. Similar procedure was followed to perform tensile tests for heat treated samples. Tensile tests performed for green sand cast and gravity die cast specimens. Values obtained are tabulated in results and discussion section.



Figure 3.8 Universal Tensile Testing Machine

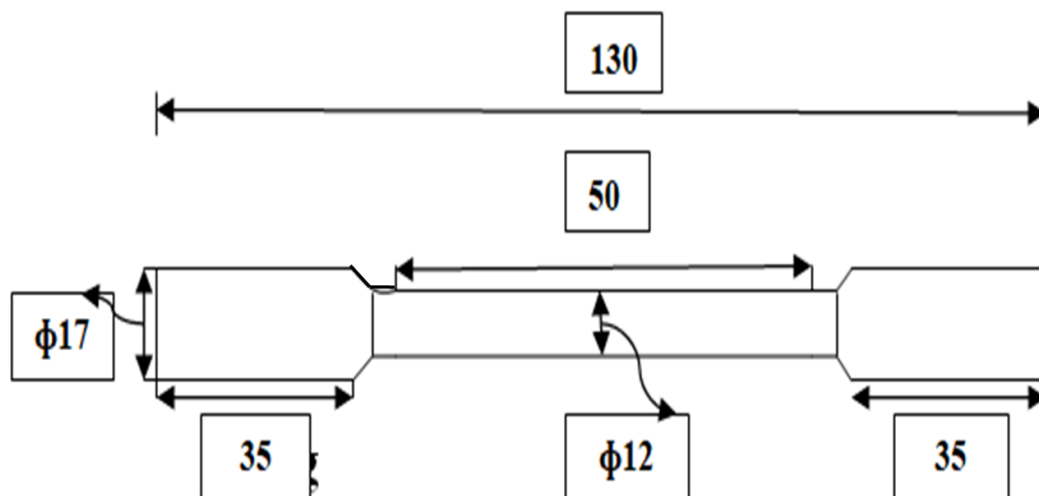


Figure 3.9 Schematic diagram of tensile test piece

3.3.2 Hardness test

Both macro hardness and micro hardness tests were conducted to find out the localised plastic deformation strength of the developed alloy. Hardness tests of green sand cast and gravity die cast components were conducted to study the plastic deformation behaviour. For

gravity die casting standard method defined by ASTM E10[Brinell hardness test] and for green sand-casting ASTM E 18[Rockwell hardness test] were done.

Micro hardness test conducted on ground and polished samples cut from thinnest part of the step-shape cast component. Vickers test performed (i) the sample was placed on an anvil and fastened with screw with the base (ii). The indenter was pressed into the specimen with controlled test force (iii) The force was maintained for 10seconds (iv) After the dwell time is complete, the indenter is removed leaving an indent in the sample that appears square shaped on the surface. The size of the indent is determined optically by measuring the two diagonals of the square indent (v) The Vickers hardness number is a function of the test force divided by the surface area of the indent. The average of the two diagonals is used in the following formula [Eq 3.3] to calculate the Vicker's hardness.

$$HV=1.854 [F/d^2] \quad \text{[Equation 3.3]}$$

Where HV is Vicker's hardness number 'F' is the test force [F=0.1kgf]

'd' is the average of diagonals of the indented square

3.3.3SEM of fractured tensile and wear surface

To study the nature of failure it is important to study microscopic images of the fractured surface. The scanning electron microscopy for the tensile fractured surface was carried out with 'ZEISS' scanning electron microscope [Fig 3.10]

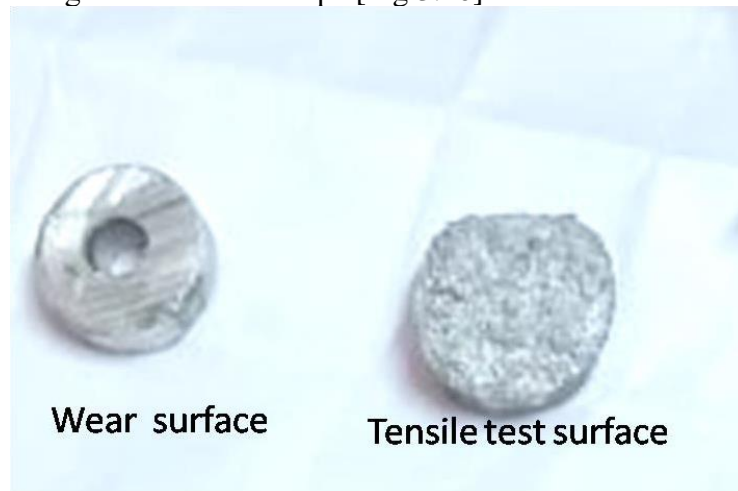


Figure 3.10 Test pieces for SEM

3.4Heat treatment

Aluminium alloys respond well to heat treatment process. Heat treatment of the alloys under consideration has been described in this section. The process mainly consists of three steps as shown in the schematic diagram [Fig 3.11]

3.4.1Solution heat treatment (SHT)

This is the first step in T6 heat treatment where the test bars were heated gradually to a temperature of 535°C in a muffle furnace [Fig 3.12]. For complete dissolution of the second phase the bars were kept inside the furnace for 6hrs. It is important during solutionizing not to exceed the temperature which may lead to incipient melting. The process was repeated for die cast and sand cast tensile bars. For each composition same procedures were followed.

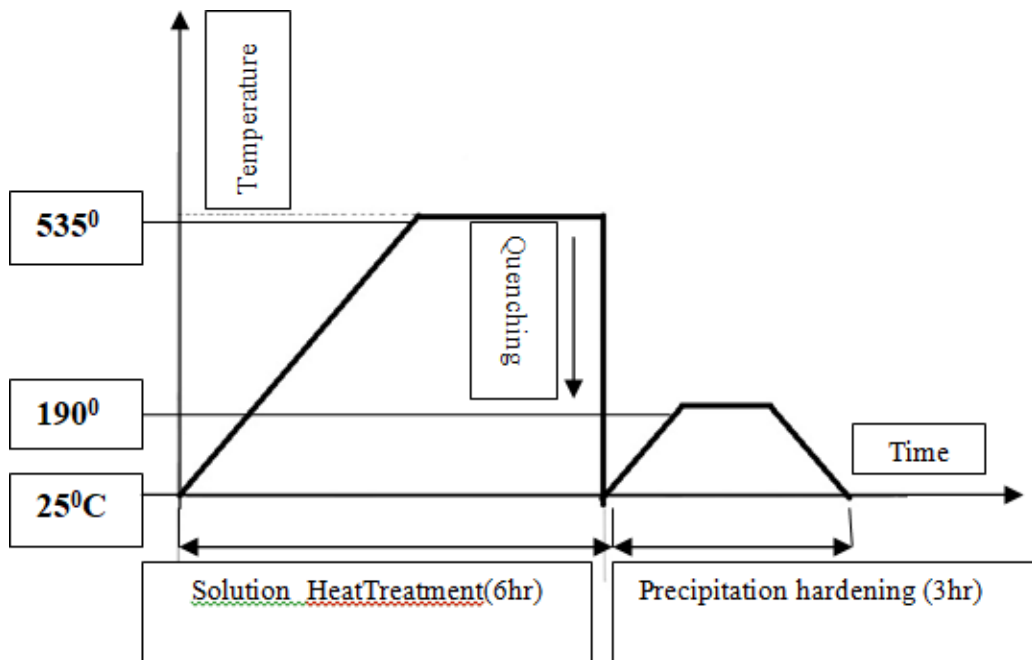


Figure 3.11 Schematic diagram of the heat treatment process

3.4.2 Quenching

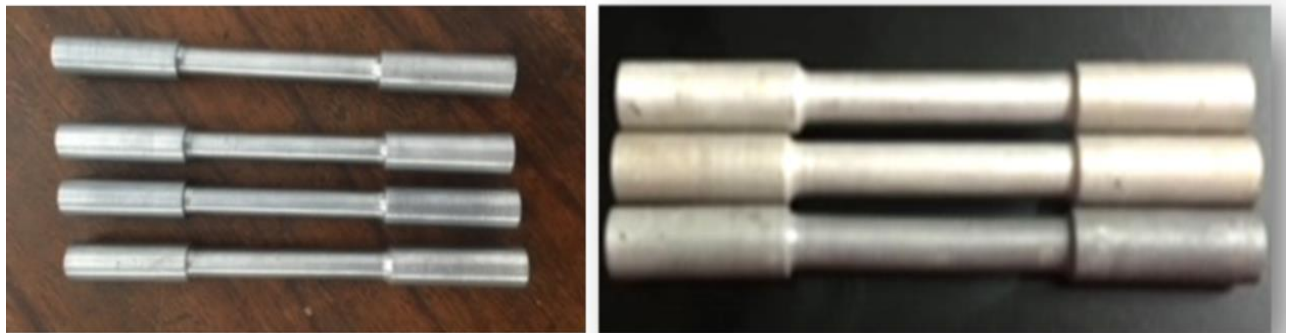
After the first step of solution heat treatment the test bars were quenched in water maintained at 25°C. Quenching in water is done to get super saturated solid solution which will eventually facilitate precipitation of the strengthening phase during aging process. The amount of Al_2Cu precipitated is crucial for improving the mechanical properties of the given composition. The alloy having finer grain structure exhibit better precipitation as more amounts of second phase particles dissolve during SHT. Quenching is an important step as most of the time stress developed during quenching may affect the mechanical behaviour of castings.



Figure 3.12 Muffle Furnace

3.4.3 Aging

For the current work aging temperature was chosen as 150°C. The quenched samples were heated again in the muffle furnace gradually to the aging temperature. For complete precipitation the temperature maintained for 3hrs. Then the samples cooled gradually in the furnace to room temperature [Fig 3.13].



a **b**
Figure 3.13 Test pieces (a) before and (b) after heat treatment

3.5 Pin-on-disc dry-sliding wear test

3.5.1 Dry-sliding pin-on-disc wear test

Samples were machined according to ASTM G99-95 (10 mm diameter x 30 mm length) standards. Pin-on-Disc was used to carry out a wear test at room temperature, as shown in Figures 3.14 (a) and (b). The disc is made of EN-32 steel with a track diameter of 120 mm & thickness 8 mm. All the test specimens were ground using a series of abrasive (800-1000 grade) papers. Before conducting the wear test, the samples were weighed with an accuracy of 0.0001g using an electronic weighing scale. Acetone was used to clean the disc's surface and the samples to remove oil, grease, and other debris before and after performing the test. Micro hardness test was carried out for all the samples. Brinell hardness measurements were carried out on samples according to ASTM B647-10. An average of six readings was recorded. Wear test conditions are illustrated in Table 3.2. By applying the weight-loss method, the sample's weight loss was determined as an average of three runs. The wear rate was calculated with the formula.

Wear rate = Average weight loss/ sliding distance [mg/m]

Table 3.2 Wear test variables for dry-sliding wear test

Control factor	Symbols	Level-1	Level-2	Level-3
Composition	A	A1	A2	A3
Load(N)	B	20	30	40
Speed(rpm)	C	300	400	500



a



b

Figure 3.14(a) Pin-On-Disc tribometer arrangements (b) monitor for readings [Courtesy: Tribology, AMU]

3.5.2 Taguchi method

Taguchi method was used to design the experiment and optimise the parameters. Genichi Taguchi developed a method using loss function to optimise results. Using Taguchi method reduces the experimental cost by using orthogonal array. Dry sliding wear of any alloy depends upon many parameters such as composition, load, casting process, speed, heat treatment, the temperature etc. for the current analysis mainly 3 control factors at 3 levels are chosen and the Taguchi method is used to optimize these variables. L9 orthogonal array and statistical tool “Minitab 17 software” has been used for the current study. Using orthogonal array in Taguchi method reduces the number of actual experiments needed. The present method used L9 orthogonal array which can determine the most effective combination of control factors and their levels which may result in least wear. The method is mainly difference between experimental and target value. The difference is converted to S/N ratio or signal/noise ratio. For the S/N ratio “smaller the better “option has been chosen so that minimum wear can be

reported. Confirmation test with analysis of variance (ANOVA) also conducted for the above variables.

3.5.3 SEM analysis of wear surface

The worn surfaces after the wear test were examined to find out types of wear for each composition. Careful analyses of images reveal the types of wear for different alloy composition. The worn surface tested with the help of a scanning electron microscope.

3.6 Casting simulation with “Z-cast simulation software”

3.6.1 Use of simulation software

The casting process for the recent study was simulated using “Z-cast simulation software”. This software uses both Finite difference method (FDM) and Finite element method (FEM) to simulate the whole process. For simulation of the die casting process initially 3D model of the component to be cast was imported followed by choosing the mold material. The Al-Cu alloy compositions to be simulated were selected from the database of the software. The database was specially modified according to the requirement as the alloys under analysis are not commercially available and developed in the lab. To obtain the computer aided cooling curves at different section thickness virtual thermocouples were positioned in the middle of respective sections. The whole simulation process can be represented with following steps:

I. Pre-processing

1. Importing the 3D model of the component in the required format (.stl file) from CAD system.

In this process accurate dimension and model of the part to be casted is prepared using solid modelling software. For the current analysis the step –cast component for (die cast and sand cast) using “solid work” software has been prepared as per the existing dimensions. For fluidity test too 3D model has been prepared. The drawings were saved in the required (.stl) format.

2. Meshing of the imported model into small elements with required ratio.

The model to be cast is imported and meshing of the model is done. Meshing is the process of dividing the whole model to number of small elements. Old material is chosen depending upon type of casting.

3. Selecting the required composition to be simulated from the data base.

The software database consists of different alloy composition. For the current analysis the composition of Al-Cu alloy needed has been added. The database has been customised to include aluminium copper alloy of required wt% without having silicon.

4. Input parameters setting.

Theoretical input parameters such as solidus and liquidus temperature, heat transfer coefficient for the mold materials, volumetric shrinkage of the alloy is to be given before starting the analysis.

5. Positioning the thermocouples at desired locations to get cooling curve.

To obtain the cooling curve thermocouple has to be positioned at the chosen point of the component. Type of thermocouple must be chosen from the data base.

II. Processing

1. Solidification analysis.

Once the preprocessing phase is over the solidification analysis can be started.

III. Post-processing

1. Obtaining cooling curves.

2. Detecting hot spot from solidification simulation.

3. Study of solidification temperature patterns.

4. Analysis and iterations to get defect free casting.

3.6.2 Solidification analysis

The solidification analysis results provide the virtual solidification of the component. This

includes the temperature pattern and time taken for the total solidification. The analysis also includes the instant temperature at any position of the component. After 100% solidification from the temperature pattern, it can be analysed at which part shrinkage can occur.

3.6.3 Cooling curve analysis

Position of thermocouples in the virtual casting process records the cooling curve of that point. The simulation software provides both in table form and graphical cooling curves. The data can be used to analyse the cooling pattern at any point of the cast components. For the recent analysis thermocouples positioned at the S-1 and S-5 of the step-die cast components.

3.6.4 Iterations and defect free castings

Simulation as a tool helps to optimise process parameters of casting to get defect free casting . Iterations to optimise riser dimensions, gating positions, sprue design etc can be carried out virtually and without wasting materials with every trial. This process helps to get better yield even for alloys having poor castability.

4. CHAPTER 4

RESULTS AND DISCUSSIONS

4.1 Alloy and Cast-Components

Al-Cu alloy developed with varying wt% of copper and in the absence of silicon [Sec- 3.1] have been tested to verify the exact composition and results were documented. It is important to verify the presence of other elements and their limits for which spectro analysis test has been conducted for each sample. The casting methods and alloy compositions used to prepare components impacted the quality of casting. From careful external examination of each cast component and analysis of the observations it can be said that increase in copper wt% affect the quality of casting adversely. This characteristic is same for green sand casting and gravity die casting. It is also noteworthy that externally the shrinkage defects are larger in case of gravity die casting as compared to sand casting.

4.1.1 Composition analysis

Results of composition analysis for the alloy developed [Sec 3.1] are reported in Table-4.1 . The impurities present such as Fe and Si are found to be well below (0.1%<) the desired level for this experiment. The aluminium alloys developed are represented according to the wt% of copper present. (i) Alloy containing 4wt% of copper as ‘A1’ (ii) Alloy containing 8wt% of copper ‘A2’ and (iii) Alloy containing 12wt% of copper as ‘A3’. For alloy A1 [Sec 1.5] amount of copper is below its maximum solid solubility limit in aluminium (at eutectic temperature). For A2 and A3 amount of copper present are well above the solubility limit of copper in aluminium (at eutectic temperature). The results presented in Table-4.1 are average value of samples randomly collected from four places of the ingots developed from master alloys.

Table 4.1 Al-Cu alloy composition for varying wt% of copper

Alloy	Alloy1 [A1]	Alloy2 [A2]	Alloy3 [A3]
Cu (wt %)	4%	8%	12%
Al (wt %)	96%	92%	88%

4.1.2 Macroscopic analysis results of gravity die cast step-shape component (varying copper wt%)

The step-shape components prepared by gravity die casting method [Sec-3.1.2] have been carefully examined externally for each composition. It has been observed that [Fig 4.1] with increase in wt% of copper in aluminium the shrinkage size at the base of the riser increases. The defect extends up to the 3rd step i.e. S-3 for alloy A3 having maximum amount of copper. It can be observed that both length and depth of shrinkage increases with increase in copper wt% in aluminium. With increasing distance from the riser the shrinkage size reduces. This is due to the smaller thickness of the farthest section. At thickest part of the casting maximum shrinkage has been observed. The shrinkage defect thus located at thick sections can be

attributed to insufficient feeding from the existing riser during solidification and increase in solidification time for thicker sections. It has been discussed [Sec- 2.1.2] that presence of silicon helps in preventing this type of defect as during cooling silicon expands. Silicon also provides better fluidity when present in aluminium alloy. Absence of silicon and excess copper increases the probability of defect formation. Variation in freezing range due to composition change is one of the reasons for these types of defects.

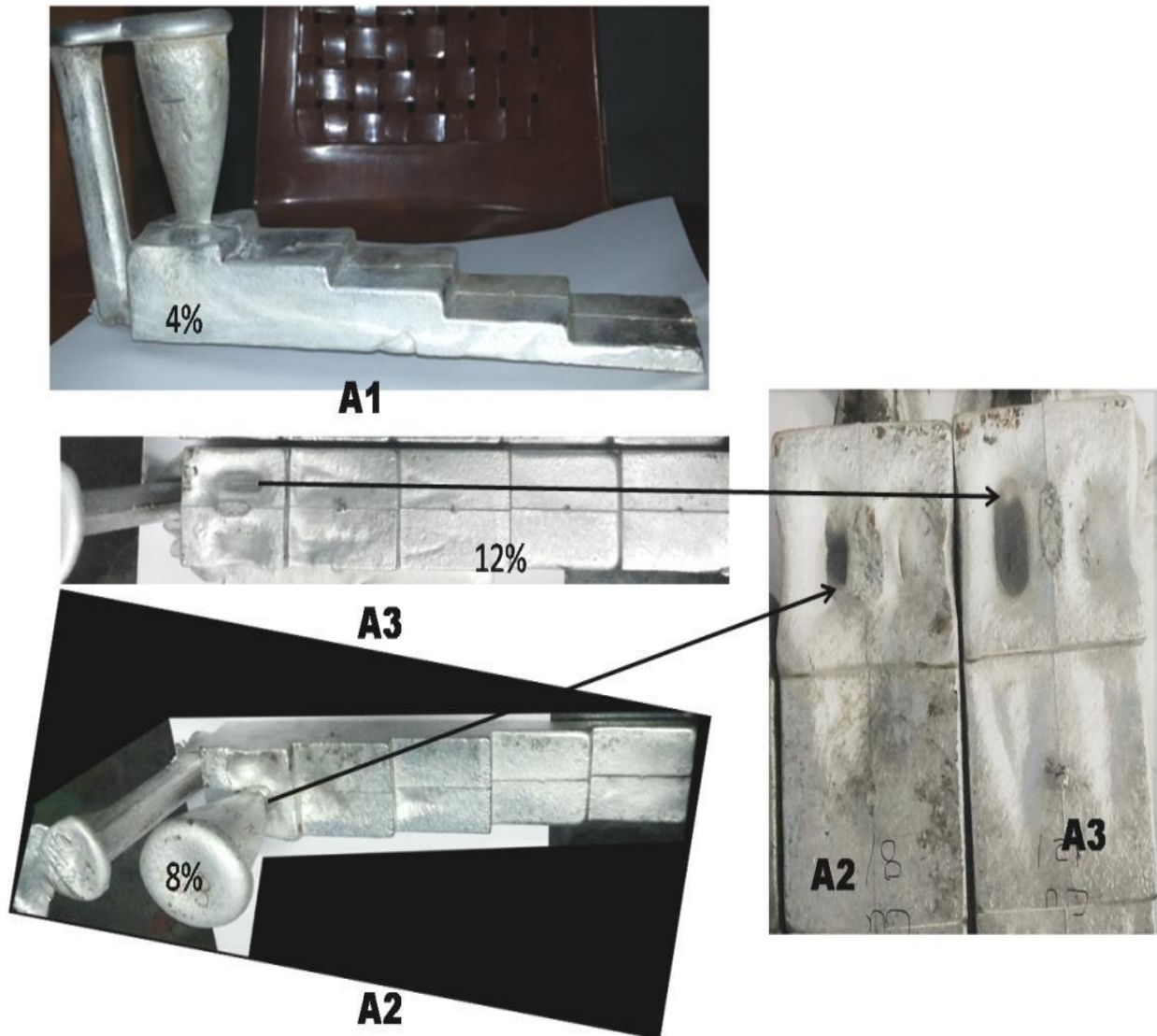
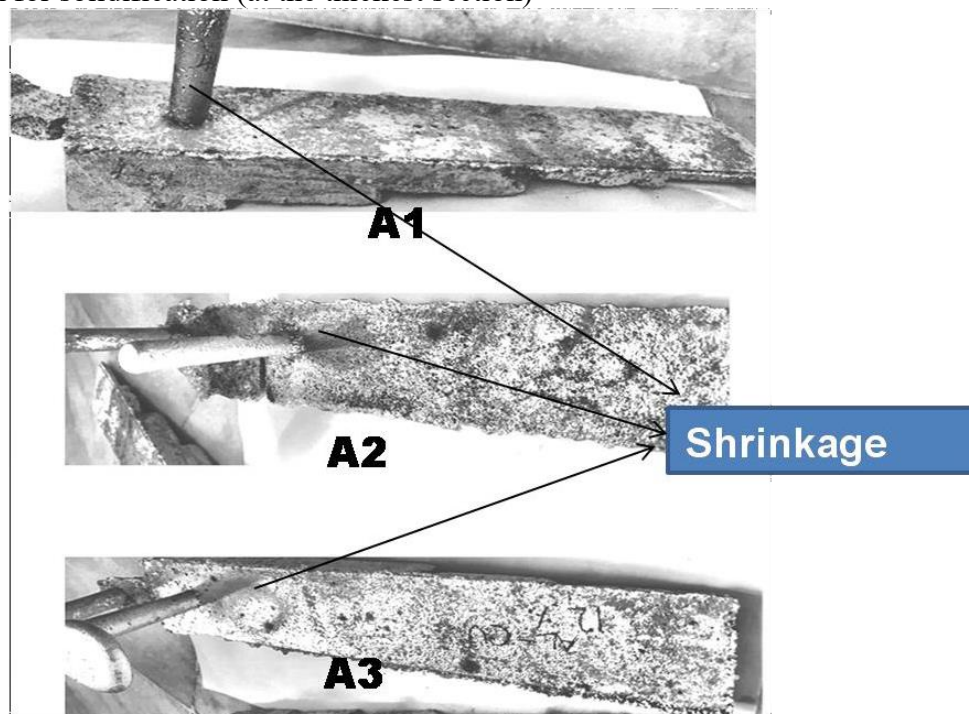


Figure 4.1 Step components for gravity die casting

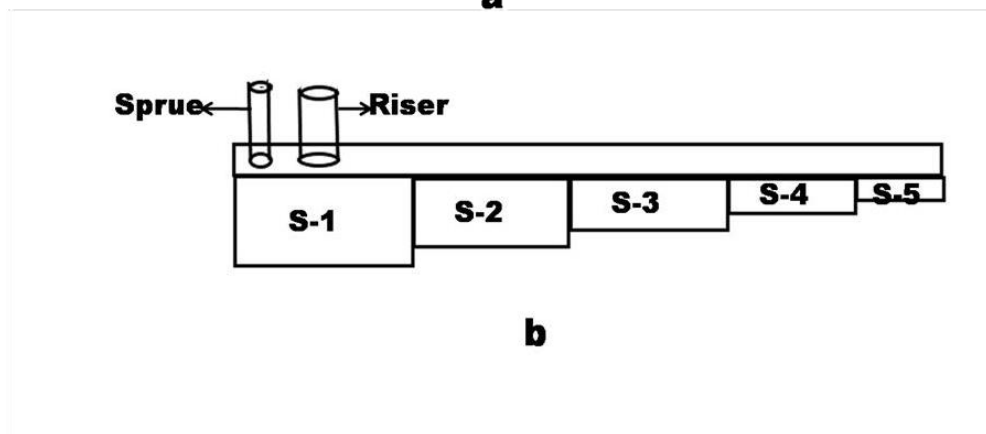
4.1.3 Macroscopic analysis results of sand cast step-shape component (varying copper wt%)

The ‘step-shape’ sand cast components casted from aluminium-copper alloy [Sec-3.1.3] have shrinkage defects at the base of the riser. Position of shrinkage at the riser base is same for gravity die casting and green sand casting. For increase in copper wt% the shrinkage defect size (external) keeps increasing. For alloy with 4wt% of copper i.e. A1, the shrinkage dimension is very less. Figure 4.2(a) is showing shrinkage dimensions for different composition. Maximum shrinkage was noticed alloy having 12wt% of copper i. e. A3. The similar nature of shrinkage cavity formation at the base of the riser for both gravity die-

cast and green sand-cast components are due to
 (i) excess amount of solute present in the alloy
 (ii) excess time taken for solidification (at the thickest section)



a



b

**Figure 4.2 Green sand cast step-shape components (b)
 Schematic diagram showing S-1 to S-5**

(iii) Longer period of mushy zone. Sand casting when compared to die casting have slower cooling rate. In the current analysis dimensions of step component casted are approximately the same, but due to difference in cooling rate defects formed are of different nature. Therefore, the cavities formed at the riser base are wider and larger for die casting when compared to sand casting. The location of defects is similar in nature for sand and gravity die casting when composition is kept constant.

4.1.4 Comparison (quantitative) of shrinkage defects for green sand-cast and gravity die-cast 'step-shape' components

Comparing the die-cast and sand-cast components it is observed that [Table 4.2] shrinkage dimensions are smaller for green sand-cast components when compared to die-cast

components keeping the composition constant. The shrinkage volume calculated by water displacement method [section3.1.6]

This is due the slower cooling rate for sand casting due to which molten metal are available for longer period to compensate the shrinkage. In case of gravity die casting metals solidify faster near the walls (high cooling rate) and at thicker section away from wall it takes longer period to solidify. So, at the middle part of thicker section liquid metal cannot enter resulting in shrinkage. The riser solidifies faster too for gravity die casting, which make it difficult to compensate for the required amount of liquid metal to minimise shrinkage. It can be noticed that for sand cast components shrinkage dimensions are less as compared to die-cast components when composition is kept constant for same geometrical shapes. [Fig 4.3].

Table 4.2 Comparison of shrinkage volume

Alloy	V_m mm ³	W_s mm ³	SV_s mm ³	W_d mm ³	SV_d mm ³
A1	2375	2164	211.75	2063	312
A2	2375	2013	362	1984.5	390.5
A3	2375	1906.9	468.1	1859.8	515.2

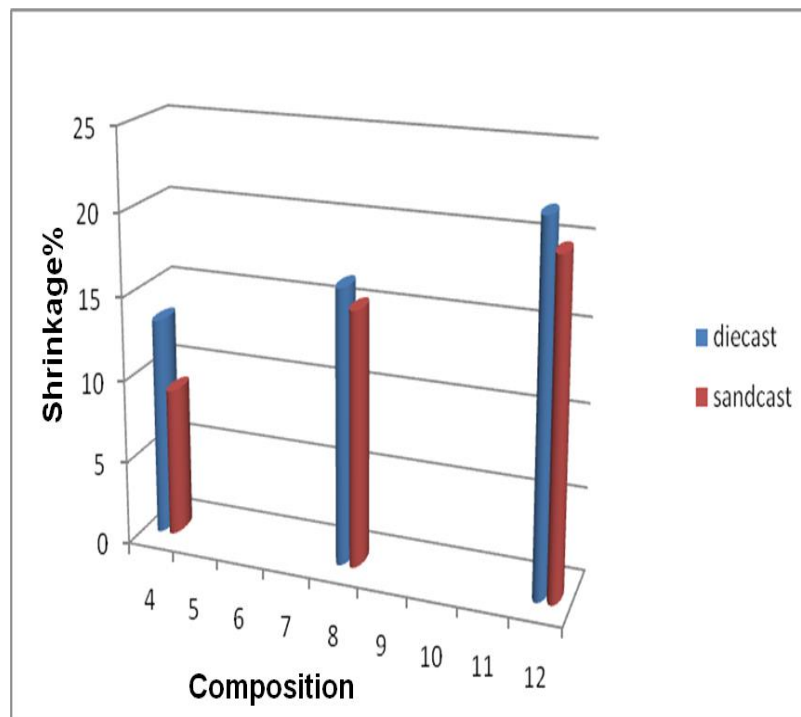


Figure 4.3 Shrinkage % comparisons for same copper wt%

4.1.5 External features of ‘step-shape’ cast components (varying section dimensions)

Study of ‘step-shape’ cast component revealed that smaller the section dimension better the quality with lesser defects. Figure 4.2(b) is showing schematic diagram of step-shape

component and their position from riser. Moving from thickest section i.e.S-1 near the riser to thinnest section S-5 which is farthest from riser; size of the shrinkage decreases. For the thinnest section, both in case of gravity die cast and green sand cast method there are no defects at all. The defect free thinnest sections can be seen for each composition irrespective of the castability and composition. It can be observed that even for poor castability alloy section having thinner dimension exhibit better cast quality. So such type of alloy can be used for thin sections without developing defects. It is also evident that with excess copper [absence of silicon] sand casting process is preferable over die casting when cast quality is priority.

4.1.6 Spiral /Fluidity test analysis

The fluidity of alloy can be interpreted in terms of spiral (Archimedes spiral) length the liquid metal travelled before solidifying. Aluminium alloy with different wt% of copper exhibit different fluidity. The highest fluidity is often associated with short freezing range alloy. It is also well established that fluidity is a complex phenomenon and depend upon many factors other than the freezing range.

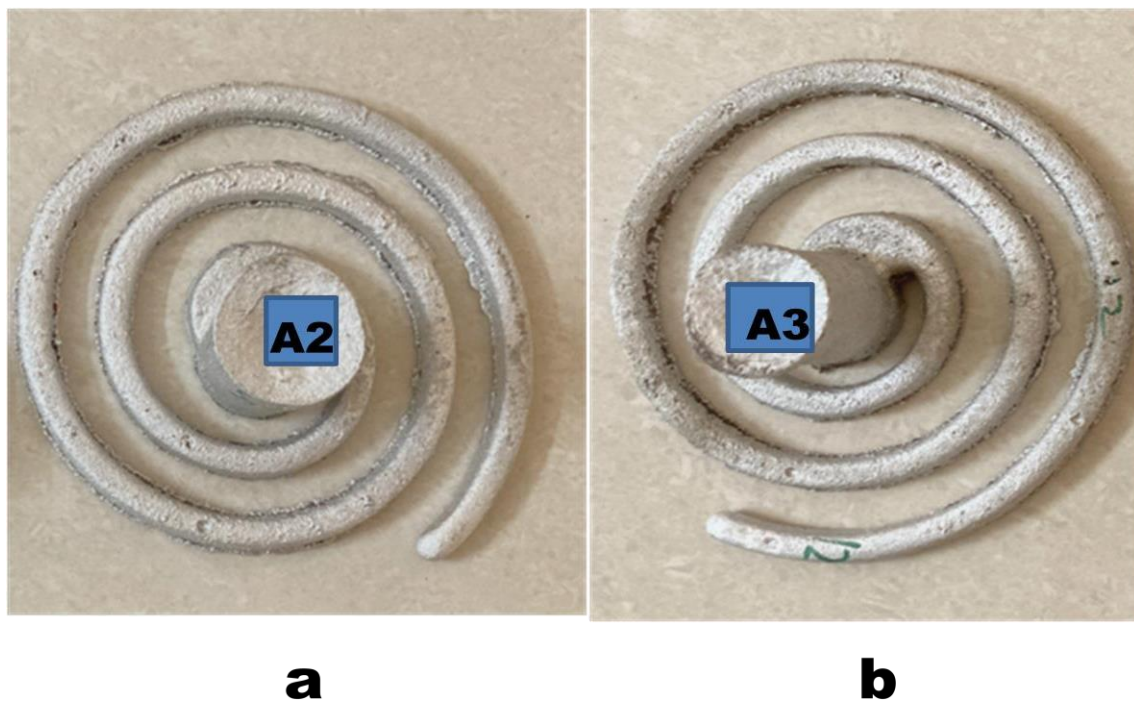


Figure 4.4 Spiral-shape casting for fluidity analysis (a) A2 (b) A3

The spiral length measured for alloy A2 is smaller as compared to alloy A3 [Fig. 4.4]. Mao et al in the paper reported about resin bonded spiral fluidity of A357 alloy. They observed that with decrease in solidification range fluidity increases [126]. The phase diagram of Al-Cu alloy [Sec 1.5] indicates that solidification range of A3 is less than alloy A2. The spiral test conducted for alloy A2 and A3 under similar condition resulted with longer length for alloy A3. The spiral length for alloy A2 measured to be 100 cm and for A3 it was 104 cm. Table 4.3 is showing spiral length comparison obtained from actual casting and virtual simulation results. Behera et al [127] conducted similar type of spiral tests and found length of the spiral for aluminium alloy with silicon (LM6) to be 126 cm, while the pouring temperature was 720°C.

Table 4.3 Simulation and actual spiral length comparison (in cm)

Alloy	length(simulation)	length(actual)
A2	77	100
A3	82.4	104

4.2 Metallographic results and analysis

Change in microscopic features such as grain size, distribution etc affect mechanical properties of any alloy. Study of results obtained from metallographic analysis and microscopic features can predict strength and hardness of alloys under consideration. The current study reveal microstructure depends on composition of alloy, casting process and the dimensions of cast components. The results are in accordance with literature presented in section 2.2.1.

4.2.1 Microstructure change for gravity die-cast components (variation of copper wt%)

Optical micrograph (OM) and scanning electron microscopy (SEM) were conducted for gravity die cast components [section 3.2.1]. The microstructure consists of primary α -phase and eutectic Al_2Cu as can be seen from [Fig 4.5]. The OM images mainly consist of α -aluminium matrix which is the primary phase for alloy A1. The images for alloy A2 and A3 can be marked with presence of θ -phase at grain boundaries even at lower magnification (OM). The presence of second phase in case of alloy A1 which is mostly eutectic of Al_2Cu can be observed in highly magnified image (SEM) as shown in Fig 4.6(a). During solidification after primary phase which is mainly α -Al solidify, it pushes the remaining liquid towards eutectic composition. Therefore, Al_2Cu eutectics are seen along with primary phase. When wt% of copper exceeds the solid solubility limits as in case of alloy A2 and A3 the intermetallics are formed at grain boundaries. These intermetallics of Al_2Cu form the second phase are responsible for improving the mechanical behaviour. So, comparing the images it was found that with change in copper from 4wt% to 8 wt% the grain distribution become finer but further increase in copper up to 12wt% make the grain distribution coarser. Keeping all other factors unchanged only the variation in copper wt% changes the grain morphology.

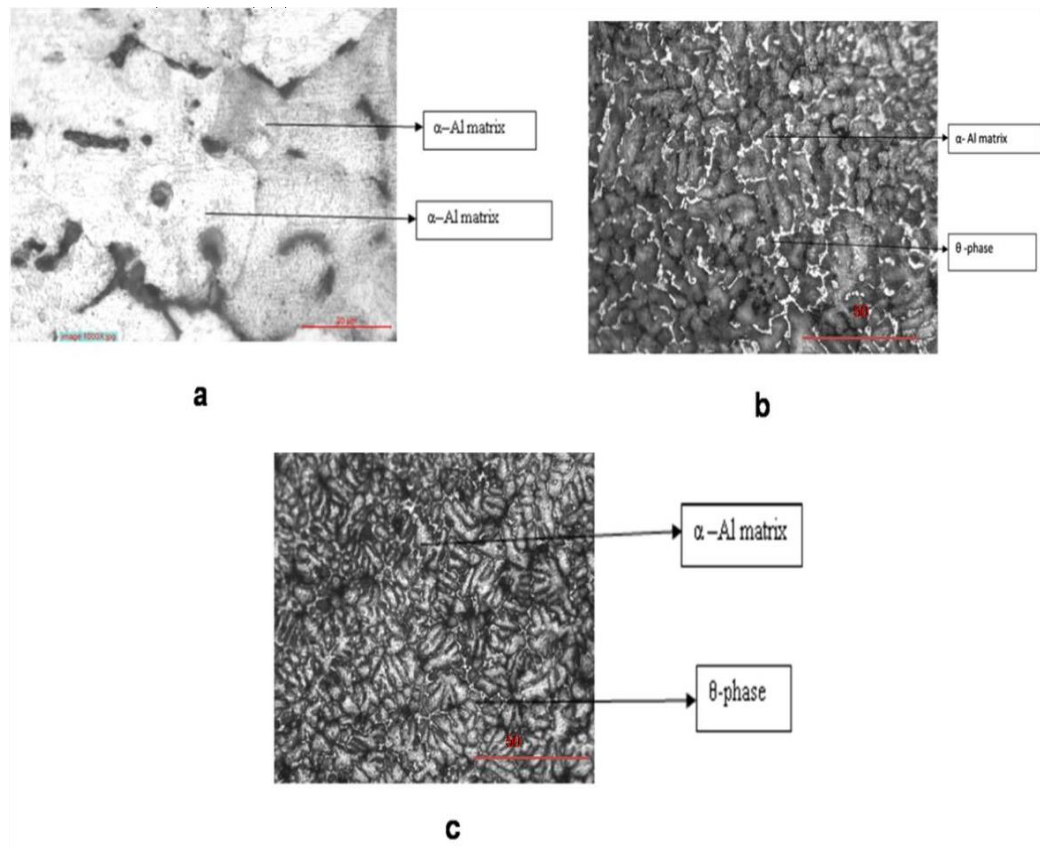


Figure 4.5 Optical Micrograph for (a) alloy A1 (b) alloy A2(c) alloy A3

The SEM images in Fig 4.6(b) and (c) can be seen with presence of θ -phase at the grain boundaries which is known as the strengthening phase. Comparing the grain sizes and percentage area covered [Table 4.4] by θ - phase it can be said that alloy A2 is having finer grains and maximum area percentage covered by the strength improving Al_2Cu phase.

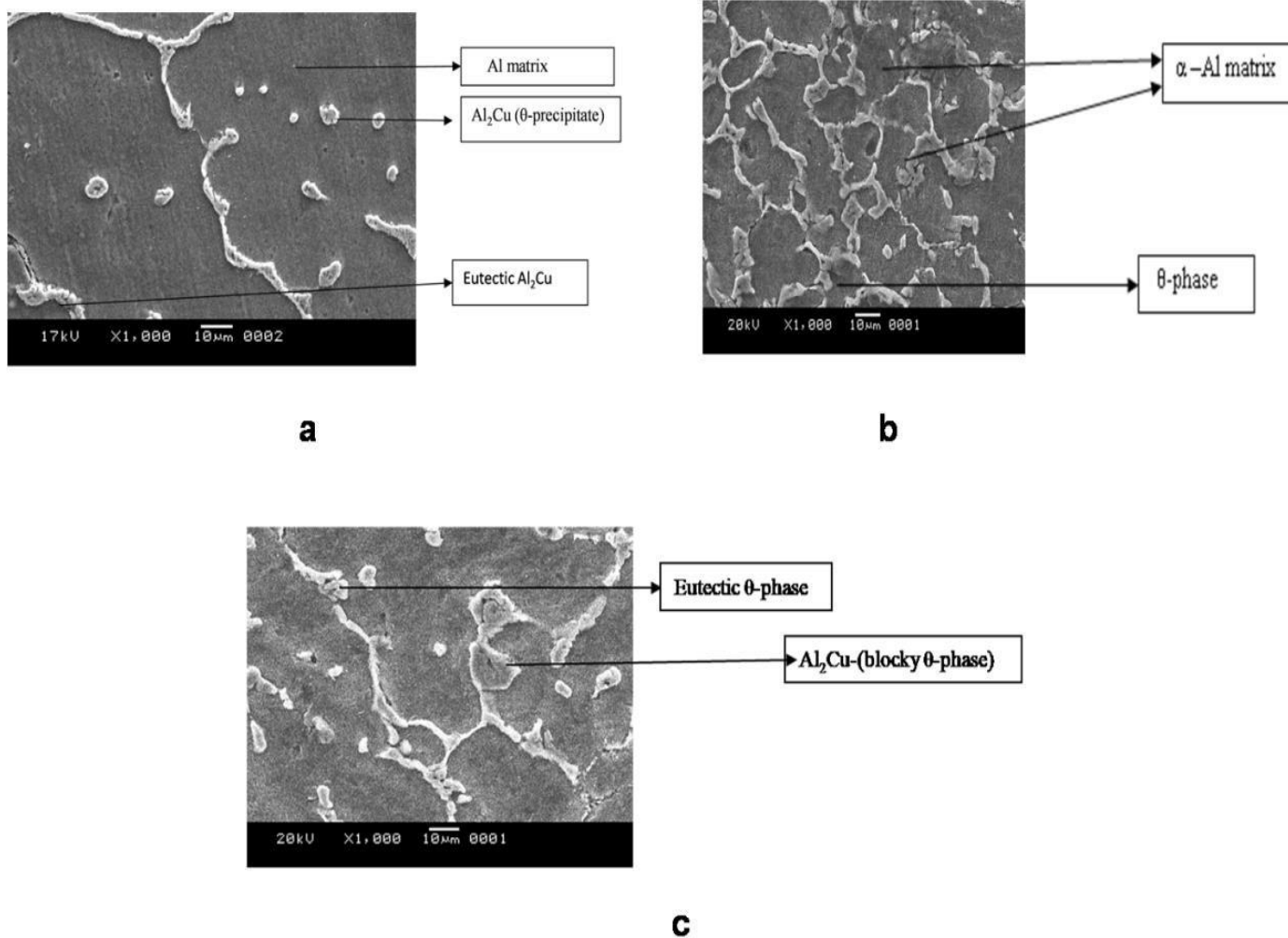
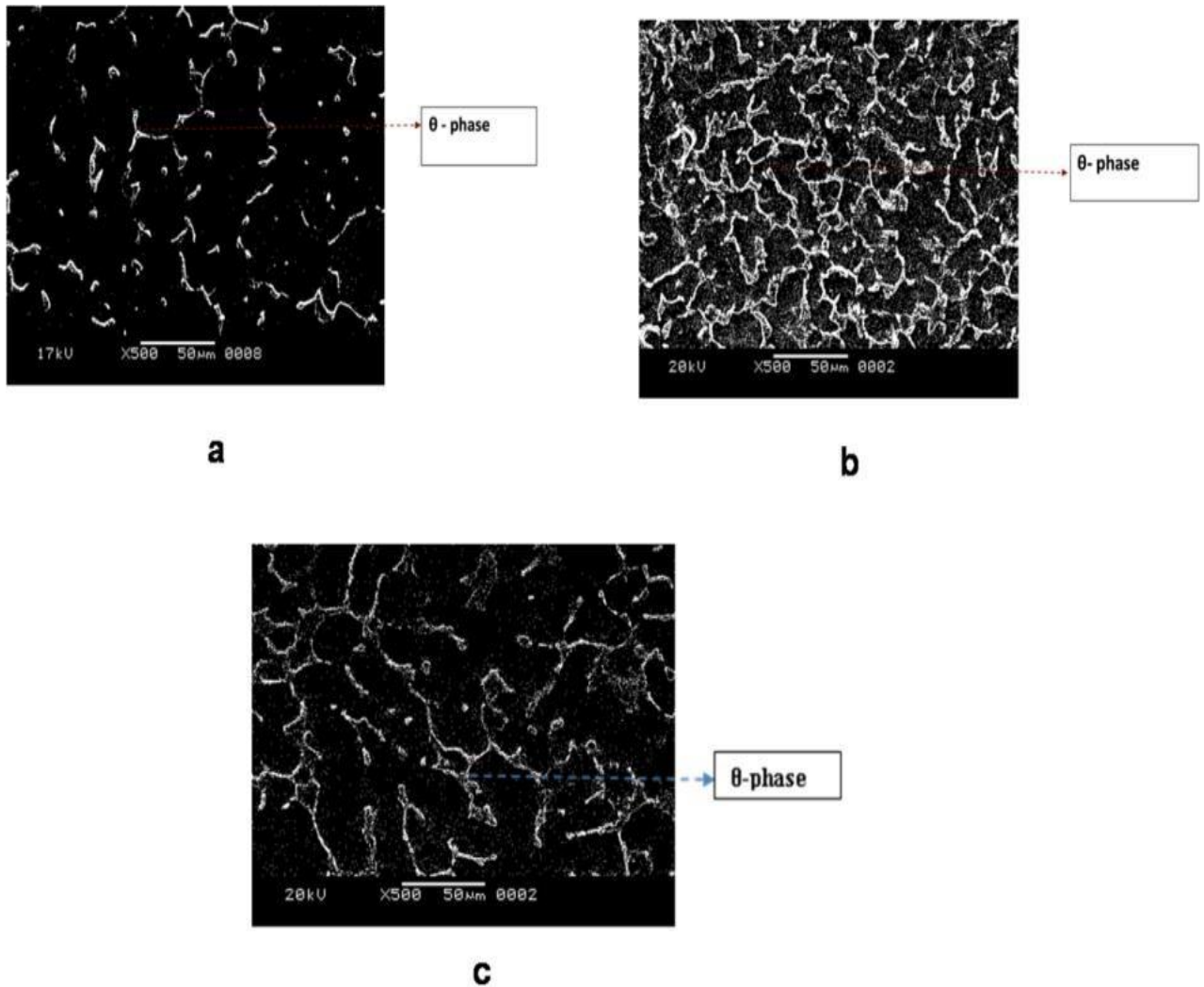


Figure 4.6 SEM images of (a) Alloy A1 (b) Alloy A2 (c) Alloy A3

Comparing the size of θ-phase for A2 and A3 it can be noted that A3 is having blocky θ-phase. This may be due to the availability of excess copper which increases the latent heat and the solidification becomes slower. It is also clear from the images that alloy A3 is having more eutectic Al₂Cu as compared to alloy A2. This characteristic affects the heat treatment process by making less intermetallics available during solution treatment.

The area percent (% area) covered by second phase plays an important role in mechanical behaviour too. The more area percent covered by θ-phase means better strength [Fig 4.7]. It can be seen that the strengthening phase or Al₂Cu (light colored) is in abundance for alloy A2 when compared to other two alloys. The presence of these intermetallics not only improves the mechanical behaviour in as-cast condition but also after heat treatment.



**Figure 4.7 %Area fraction covered by θ -phase (light colour in the image)
(a) A1 (b) A2(c) A3**

4.2.2 Microstructure change for green sand cast component (varying copper wt%)

The metallographic features of green sand cast component reveal that with increase in copper wt% both the grain size and distribution change. Similar nature of variation observed for sand cast and gravity die cast components. But in case of green sand casting the grain sizes are larger [Fig 4.8] as compared to the gravity die cast component having same wt% of copper. In green sand casting. The optical micrograph image reveals that alloy A2 and A3 having second phase or θ -phase distributed along the grain boundaries.

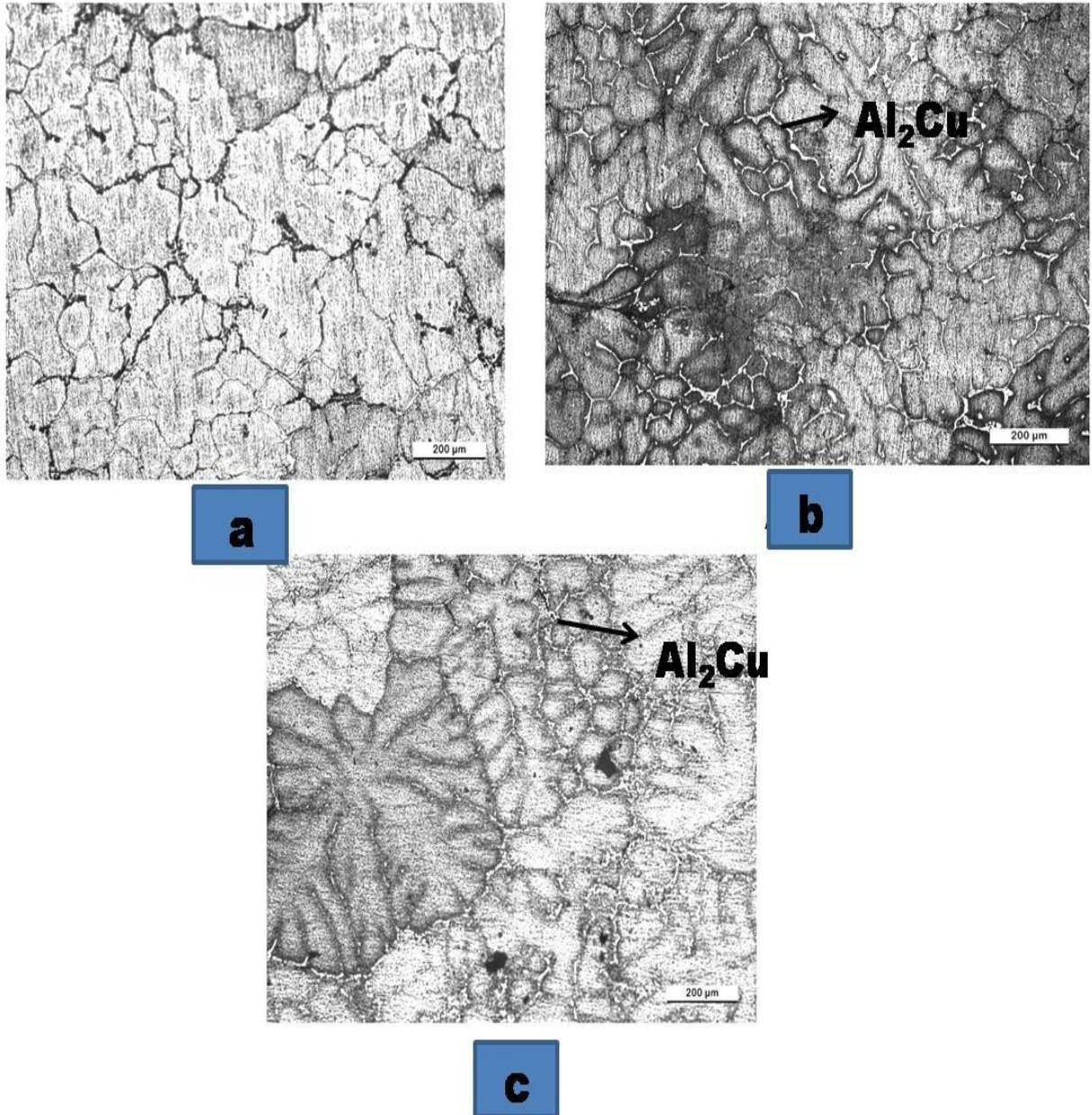


Figure 4.8 Optical microscopy [200X] images (a) A1 (b) A2(c) A3

Grain sizes for various compositions have been listed in [Table 4.4]. Green sand casting compared to gravity die casting have lower cooling rate which resulted in coarser grains when compared; having same copper wt%. For gravity die casting and green sand-casting alloy A2 observed to have the lowest grain size. Alloy A2 having 133 μm and 268 μm average grain size for gravity die casting and green sand casting respectively. The smaller grains for die casting can be attributed to faster cooling rate as compared to green sand casting. It can also be noted that for die casting second phase at grain boundaries are finer and fibrous whereas for green sand casting they are coarse and plates like. This is due to difference in solidification rate.

The SEM images also reveal that for sand cast component porosity formation is more compared to gravity die cast components. This is due to insufficient feeding between dendrites. With increase in solute particles and slower solidification rate liquid metal could not enter the inter dendritic regions resulting in more pore formation for green sand casting.

Table 4.4 Grain size variation with change in casting process for same copper wt%

Alloy	Grain size (μm) Sand cast	Grain Size (μm) Die cast
A1	356	198
A2	268	133
A3	391	180

4.2.3 XRD of alloy A1, A2, A3

The XRD profiles of all three alloy compositions reveal characteristics sharp peaks of α -Al. XRD results reveal addition of copper affect peak positions and shape [128]. The peaks for 2θ at 38.6, 44.8, 65.206 and 78.1 correspond to α -Al. The highest at 38.6. The lattice indices are (111), (200), (220) and (311) respectively. Other than these distinguished high intensity peaks which can be seen at angles 29.54, 42.72, 47.89 correspond to Al_2Cu . The second phase Al_2Cu peak

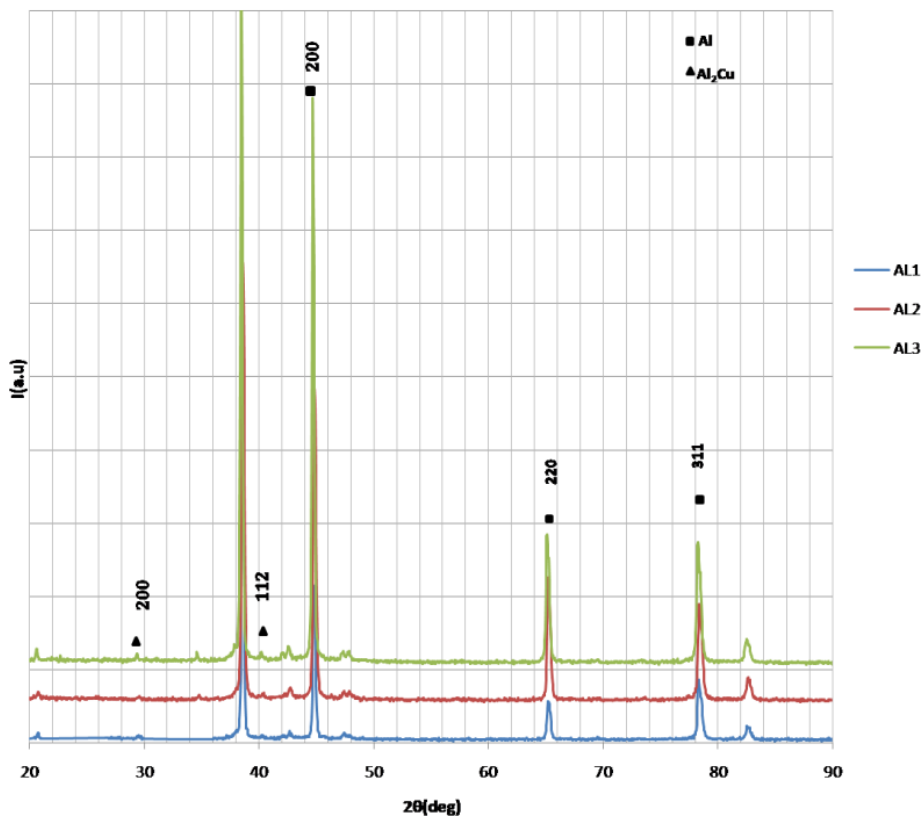


Figure 4.9 XRD of alloy A1, A2, A3

intensities increases with increase in copper wt% [Fig 4.9]. Addition of copper beyond 4wt% introduces higher intensity Al_2Cu peak and it can be confirmed from the XRD analysis. For alloys with 8wt% and 12wt% copper more peaks with Al_2Cu phase can be traced as compared to A1 alloy having 4wt% copper. Aluminium alloy having 8wt% copper also exhibit broader peak [Fig 4.10] compared to other two alloy compositions. This may be attributed to smaller grain sizes of A2 alloy which is in agreement with the microstructure analysis results.

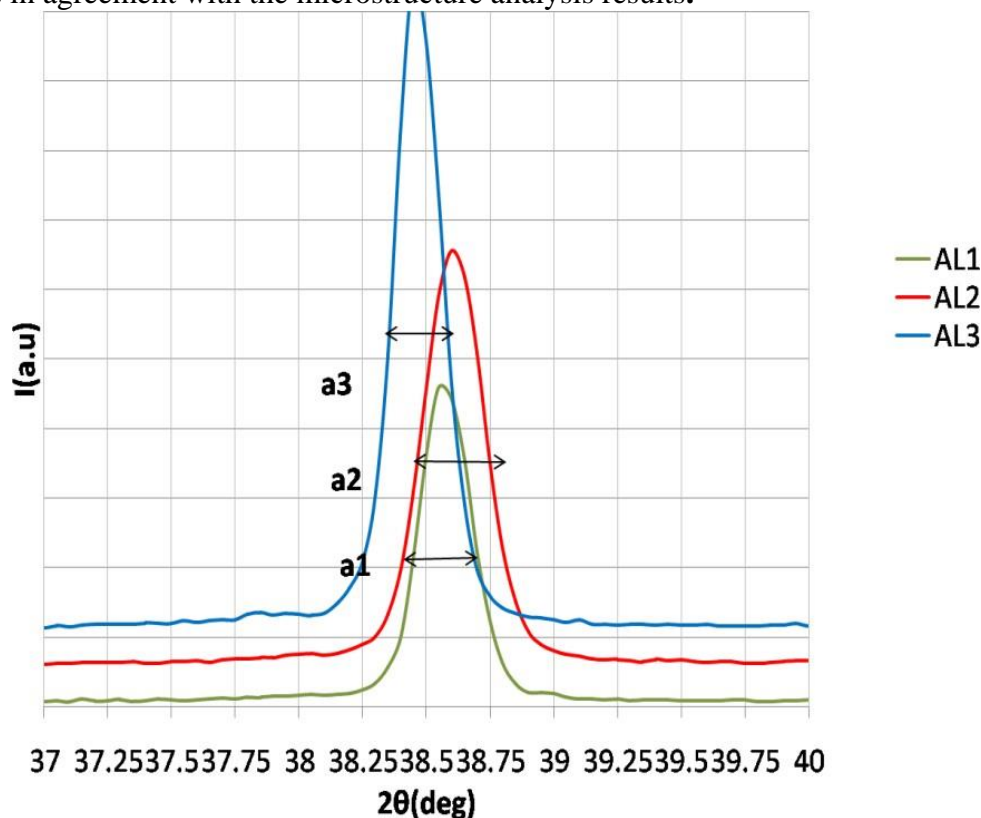


Figure 4.10 Peak shift of alloy with varying copper wt %

4.2.4 Comparison of grain size and change in copper wt%

Microstructure study of samples collected and the secondary dendrite arm spacing (SDAS) Measurement for alloy A1, A2 and A3 is listed in table 4.5. The smallest SDAS was for alloy A2 which is 20.571 μm . The percent area covered by theta phase is maximum for alloy A2. Both of the results indicate towards better mechanical properties of alloy A2 when compared to other two alloys. Fig 4.11 is showing the area covered by θ -phase with increase in wt% of copper. It can be noted that the variation is not linear.

Table 4.5 Grain size and % area covered by θ -phase (die cast)

Alloy	SDAS (μm)	%Area fraction(θ -phase)
A1	47.684	11.46
A2	20.571	27.48
A3	33.691	7.37

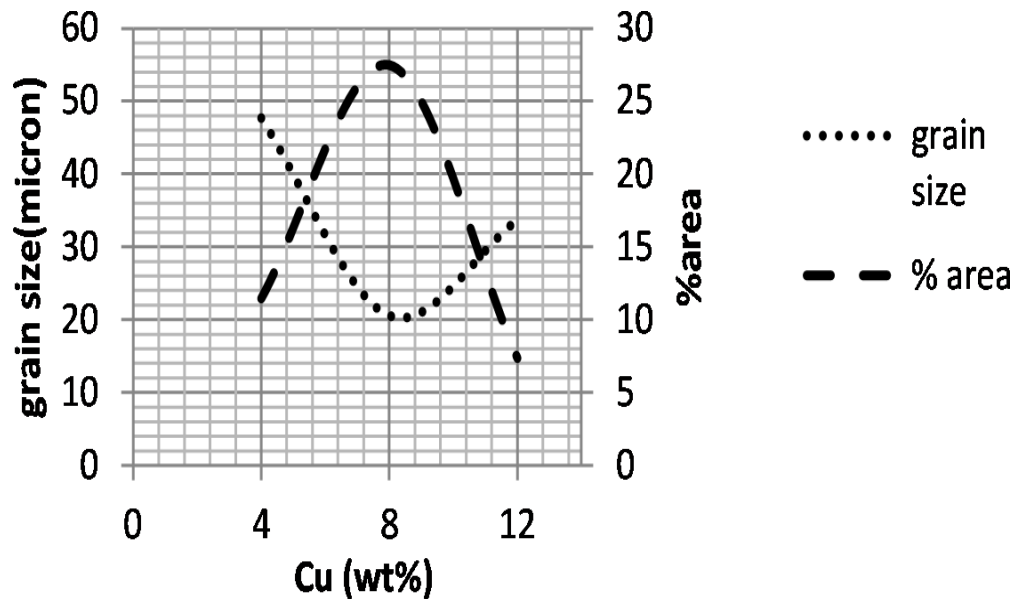


Figure 4.11 Comparison of grain sizes and % area covered by θ -phase

4.2.5 Grain size variation with change in casting process

Change in casting process alters the grain size (section 2.2.3). The results from sand casting and die casting process go with the literature very well. In Table 4.5 for sand casting and die casting the grain size measurement from microscopic sample collected from thickest part (marked 'a' in Fig 3.4) for each composition is listed. The bigger size grains for slow solidification rate sand casting compared to die casting are clearly comparable [Fig 4.12]

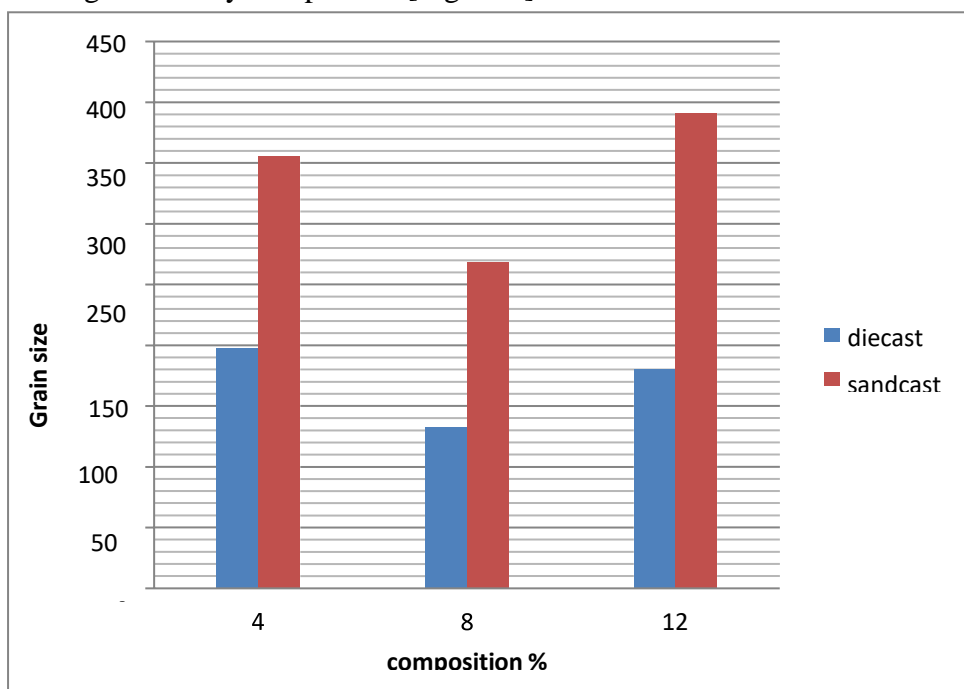
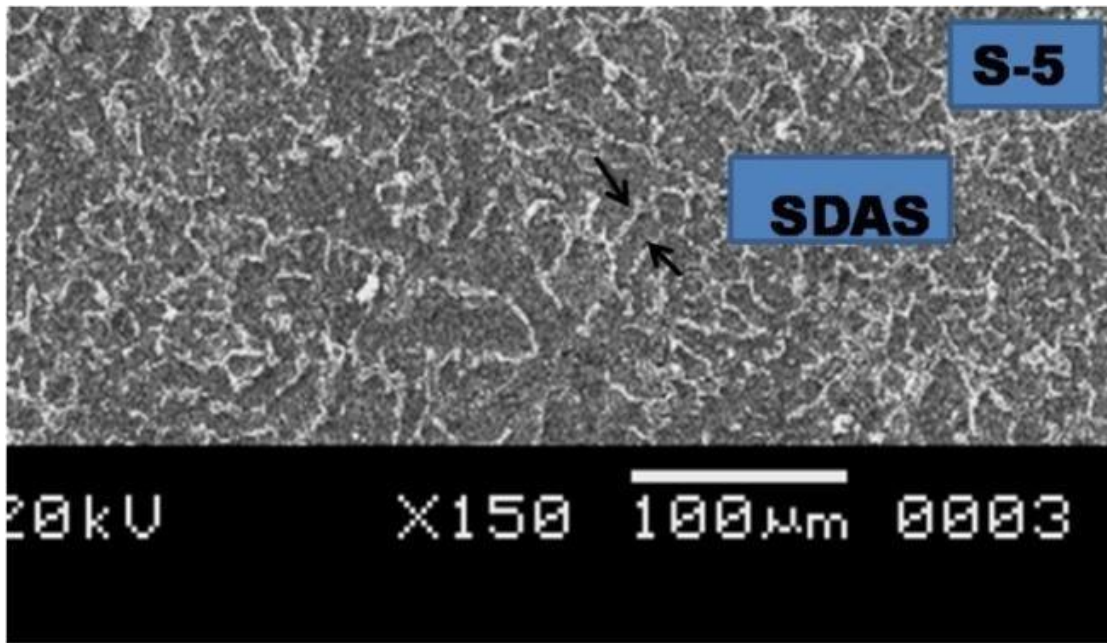


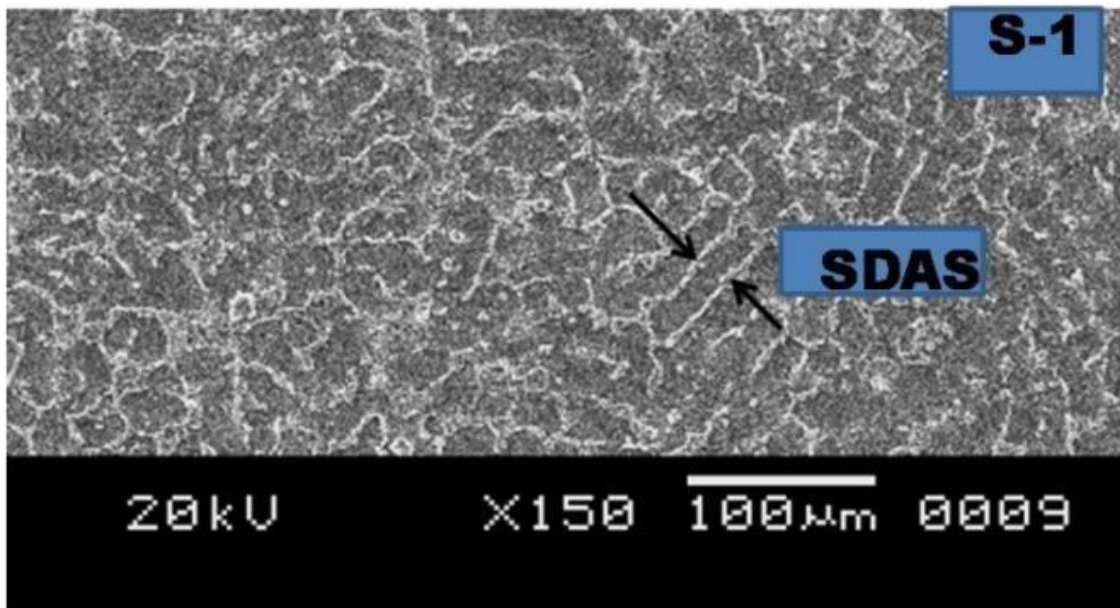
Figure 4.12 Comparison of grain size for sand cast and die cast

4.2.6 Grain size variation with change in thickness [Thickest S-1 & thinnest S-5]

Effect of change in composition and casting process has their effect on grain structure and size. The dimension of cast component too impacts the grain size, which is studied in the current analysis. The step-shape components vary in thickness. The section thickness decreases as we move away from sprue and riser. It can be seen from Fig 4.13 and 4.14 that with decrease in section thickness grains become finer. The secondary dendrite arm spacing (SDAS) for alloy A2 are finer compared to alloy A3. The SDAS further reduces in size for the thinnest S-5 section.

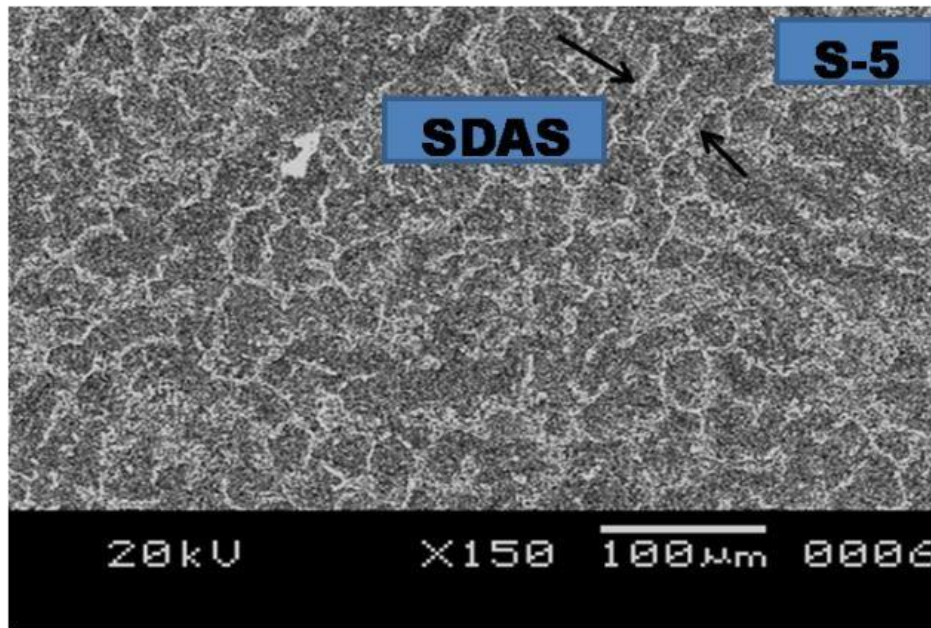


a

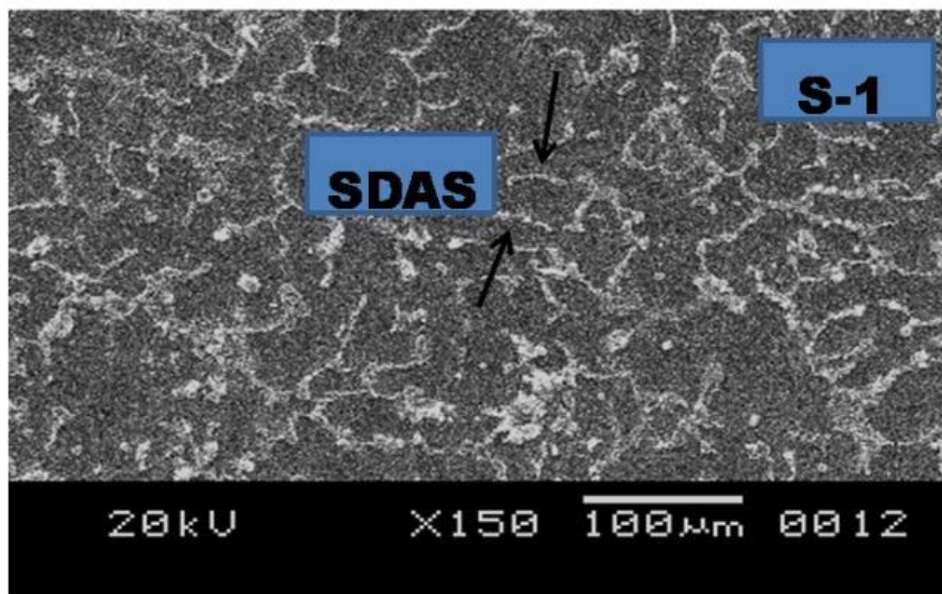


b

Figure 4.13 Grain size variation for S-1 and S-5 for A2



a



b

Figure 4.14 Grain size variation for S-1 and S-5 for A3

The Al_2Cu at interdendrite regions for alloy A3 are blocky in shape even for the thin section S-5.

4.3 Mechanical properties analysis

Mechanical properties of any cast component is dependent upon its microstructure besides other factors such as temperature, presence of defects, composition etc. Mostly from analysis of metallographic features and microstructure can predict the mechanical properties of castings. The current analysis found that variation in copper wt% as well as for different casting methods mechanical behaviour especially tensile properties are affected. The composition with finer grains exhibits better tensile properties.

4.3.1 Tensile test analysis of ‘step-shape’ component [gravity die casting]

Tensile test results obtained from testing method discussed in 3.3.1. for gravity die casting listed in Table 4.6 for as cast condition. Test results of tensile behaviour conducted for each composition and from gravity die cast method were compared for varying copper wt%. The ultimate tensile stress (UTS) and yield stress (YS) for alloy having 8wt% i.e.A2 has been found to be 136MPa and 124MPa respectively.

Microstructure pattern and solute distribution affect the mechanical behaviour of any material. Load-displacement plot obtained from the X-Y recorder used to calculate the stress and strain values. [Fig 4.15-4.17] showing the stress-strain curve for alloy containing different wt% of copper. The stress-strain curve within elastic limit is as shown in [Fig 4.18- 4.20]. Young’s modulus of elasticity as can be seen from stress-strain curve within elastic limit is between 63.4-63.8GPa for all the three compositions. It can be noted that for alloy A2 the ultimate tensile strength recorded is maximum when compared with other two compositions. It can be seen that [Fig 4.21] increase in copper wt% elongation decreases. This is due to the presence of harder second phase particles in these alloys. It is also observed that UTS and YS do not have linear relation with variation of copper wt%. Maximum UTS and YS for alloy A2 can be explained from the microstructure analysis. As grain size for alloy A2 is the tensile strength is maximum. It is well known that finer grains show better tensile properties. The % area fraction covered by θ -phase is also highest for alloy A2 (section 4.2.4) which further contributes towards the better tensile properties. Elongation is least for alloy A2 among all three compositions. This behaviour is due to presence of more Al_2Cu precipitates which affects the ductility of A2 compared to other two alloy compositions. For alloy A3 ultimate tensile strength is least among all the three compositions tested. This can be explained from coarse grain distribution for this composition. For alloy A3 the microstructure consist mostly eutectic θ -phase distributed in primary α -Aluminium and blocky Al_2Cu intermetallics at grain boundaries. Such type of microstructure with large grain structure are responsible for lower tensile strength of alloy A3 as compared to A2.

Table 4.6 UTS, YS, %EL for alloy composition A1, A2, A3

Alloy	UTS N/mm ²	YS N/mm ²	%elongation (%EL)
A1	126	112	2.5
A2	136	124	1.0
A3	112	106	1.2

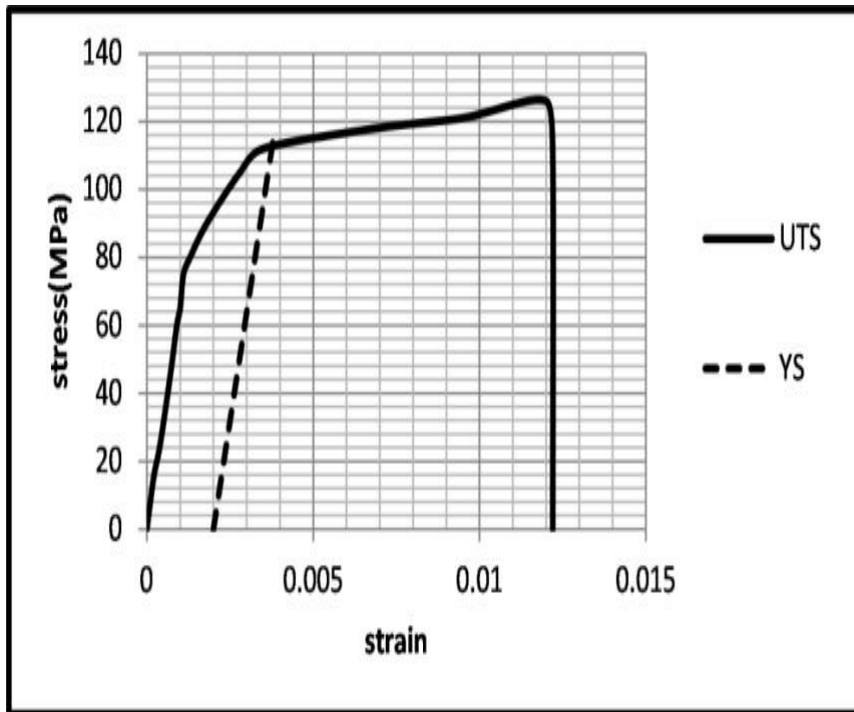


Figure 4.15 Alloy A1 UTS & YS

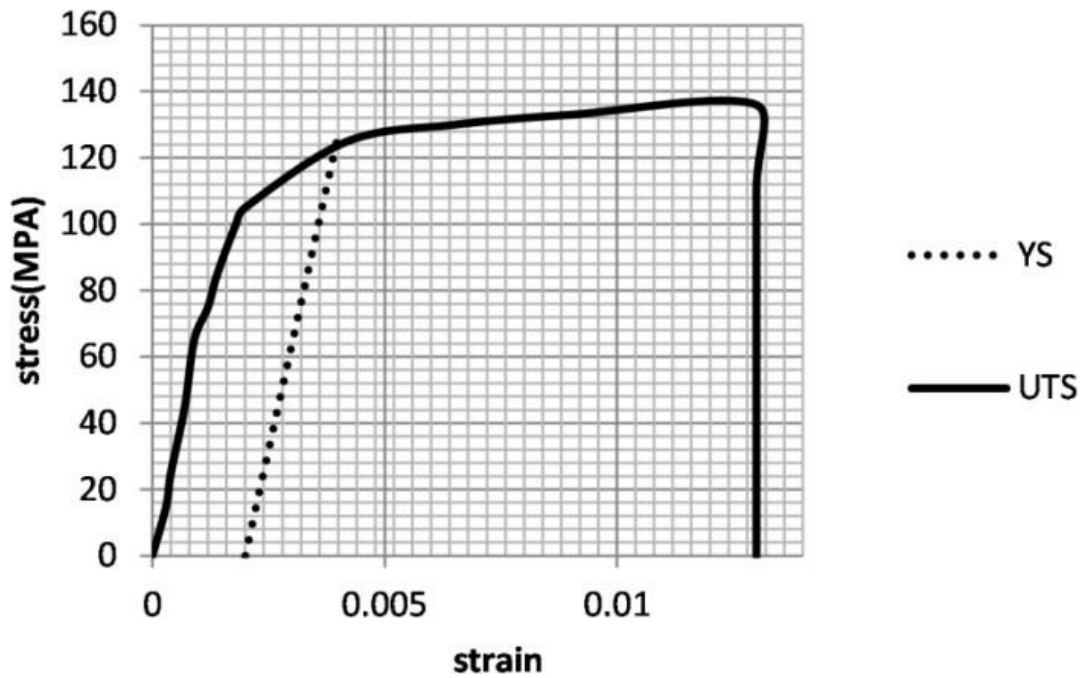


Figure 4.16 Alloy A2 UTS & YS

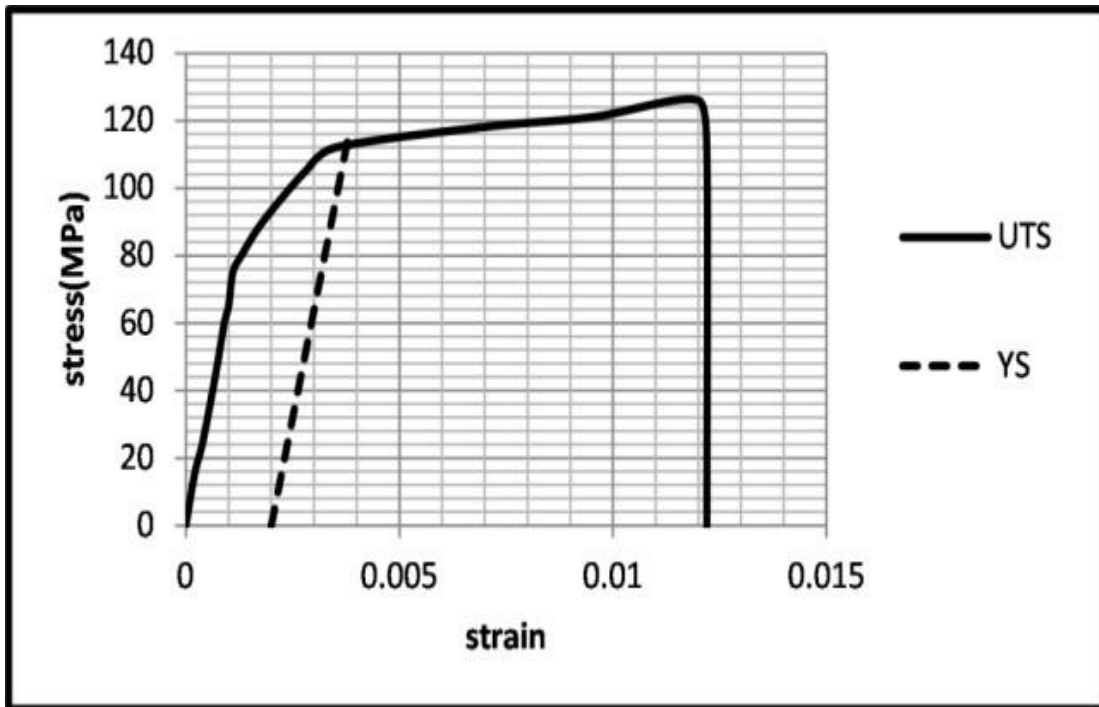


Figure 4.17 Alloy A3 UTS & YS

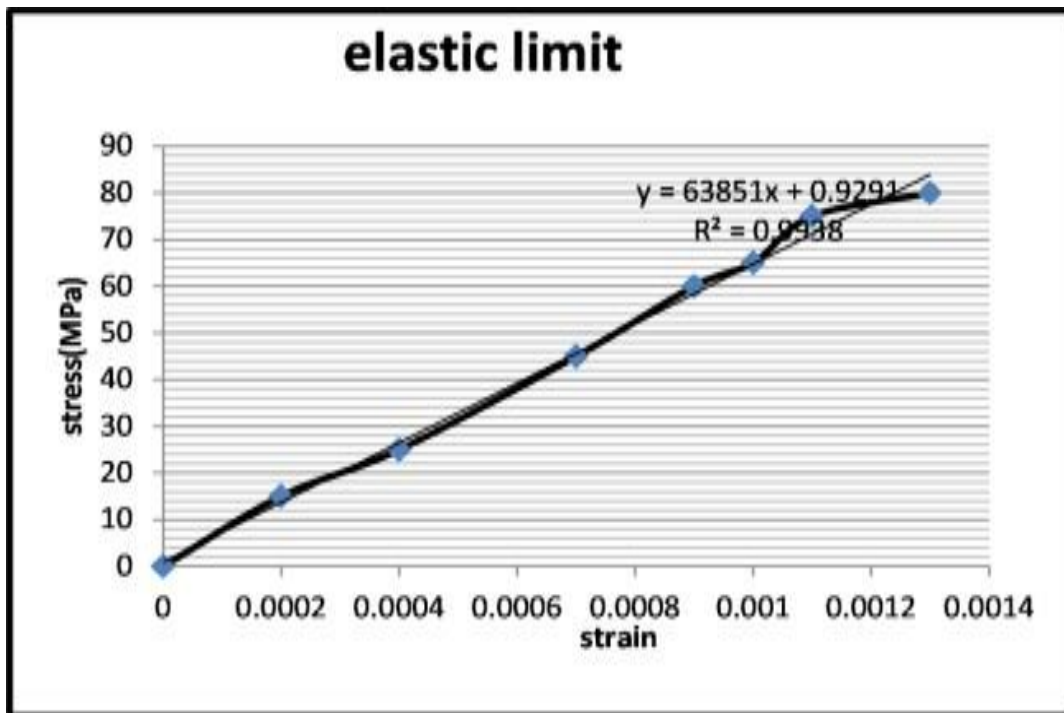


Figure 4.18 Young's modulus of elasticity for A1

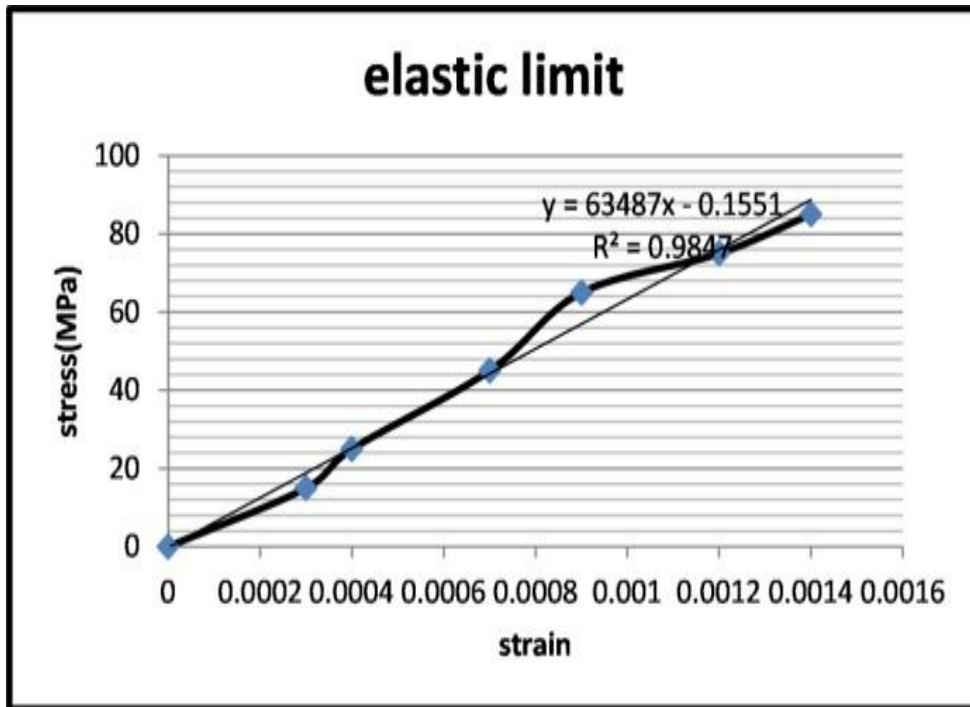


Figure 4.19 Young's modulus of elasticity for A2

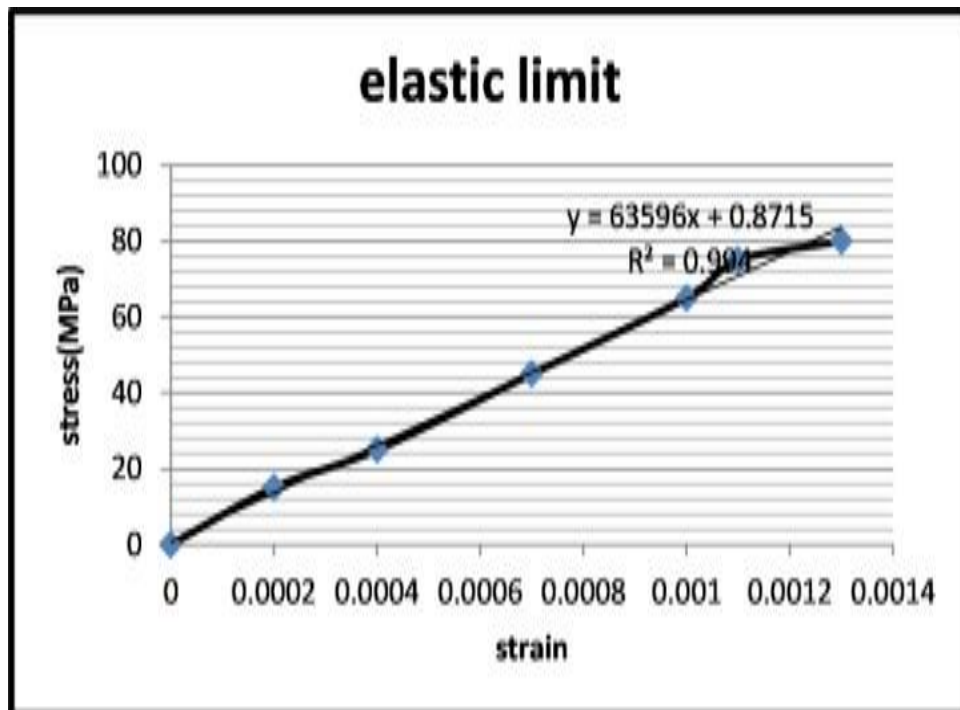


Figure 4.20 Young's modulus of elasticity for A3

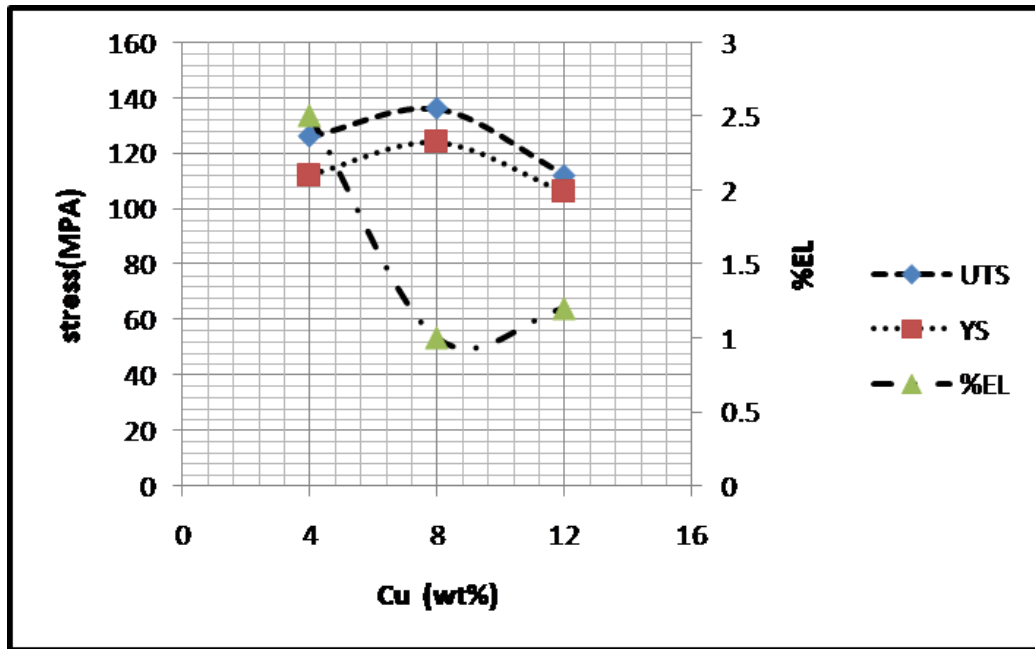


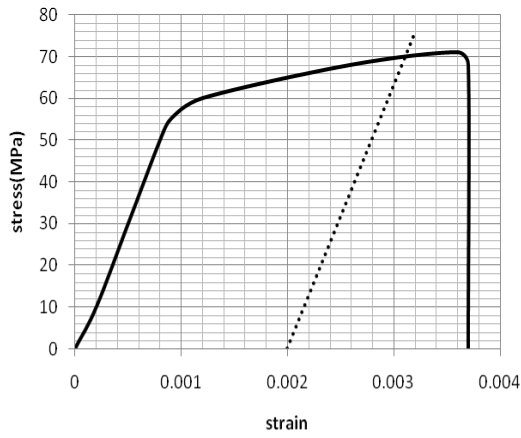
Figure 4.21 Comparison of UTS, YS and %EL of A1, A2, and A3

4.3.2 Tensile test analysis of ‘step-shape’ component [green sand casting]

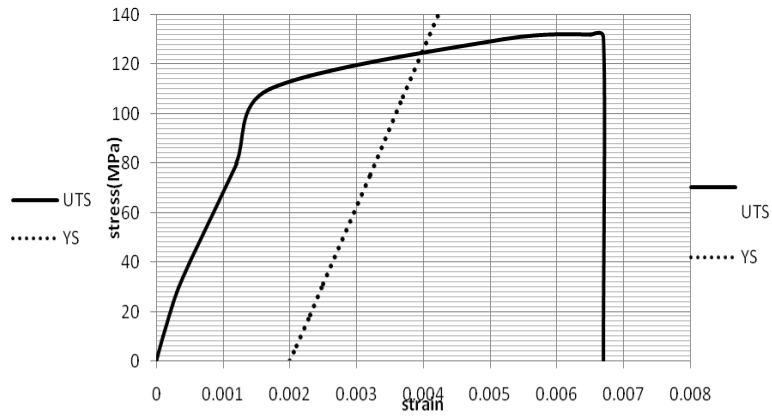
The tensile specimen prepared from green sand method were tested and results listed in Table 4.7. For varying wt% of copper the UTS and YS varies too. The maximum value of UTS and YS are 132MPa and 125MPa respectively reported for alloy A2. Similar to the gravity die casting the tensile strength can be explained from the microstructure analysis. Smallest grains impart best tensile properties. Fig 4.22 is showing the stress-strain plot for alloy A1, A2, A3. Stress-strain curve calculated from the load-displacement plot.

Table 4.7 Sand cast UTS, YS

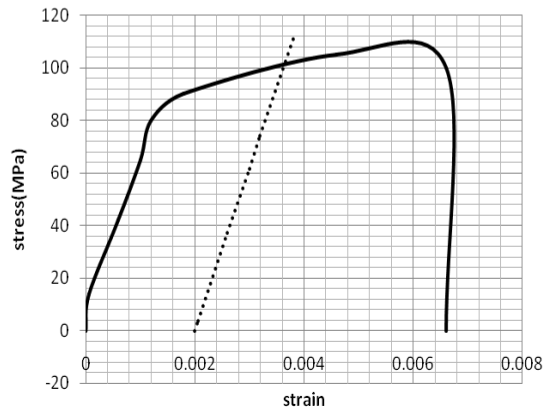
Alloy	UTS(MPa)	YS(MPa)
A1	71	69
A2	132	125
A3	105	100



a



b



c

Figure 4.22 UTS, YS for step-shape component (a) A1 (b) A2(c) A3

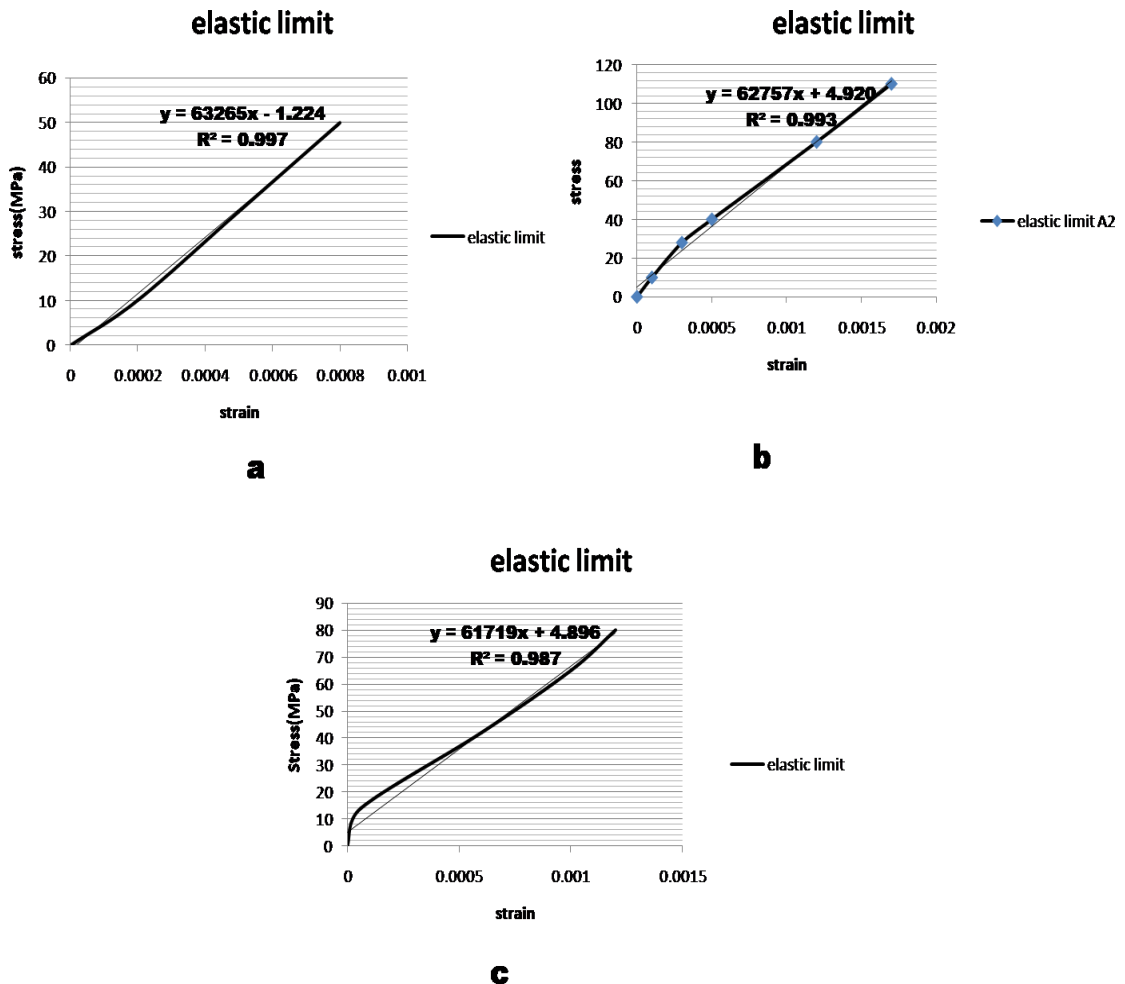


Figure 4.23 Elastic modulus of sand cast alloy

4.3.3 Hardness of green sand cast and gravity die cast component [varying copper wt%]

Hardness test results of both sand cast and gravity die cast component is listed in [Table 4.8]. It was observed with increase in copper hardness keep on increasing. For gravity die cast standard method defined by ASTM E 10 [Brinell hardness test] and for green sand casting ASTM E 18 [Rockwell hardness test] was followed. The unit of hardness test conducted for green sand cast component is HRB and for gravity die casting is HBW respectively.

Table 4.8 Hardness of sand cast and gravity die cast alloy

Alloy	Hardness (HRB)	Hardness (HBW)
A1	10	97
A2	25	110
A3	30	114

4.3.4 Comparison of gravity die cast and green sand cast tensile results

The Fig 4.24 is the plot showing comparison of tensile strength for variation in copper wt% for sand casting and gravity die casting. It is observed that keeping composition constant gravity die cast exhibit better tensile results compared to sand casting.

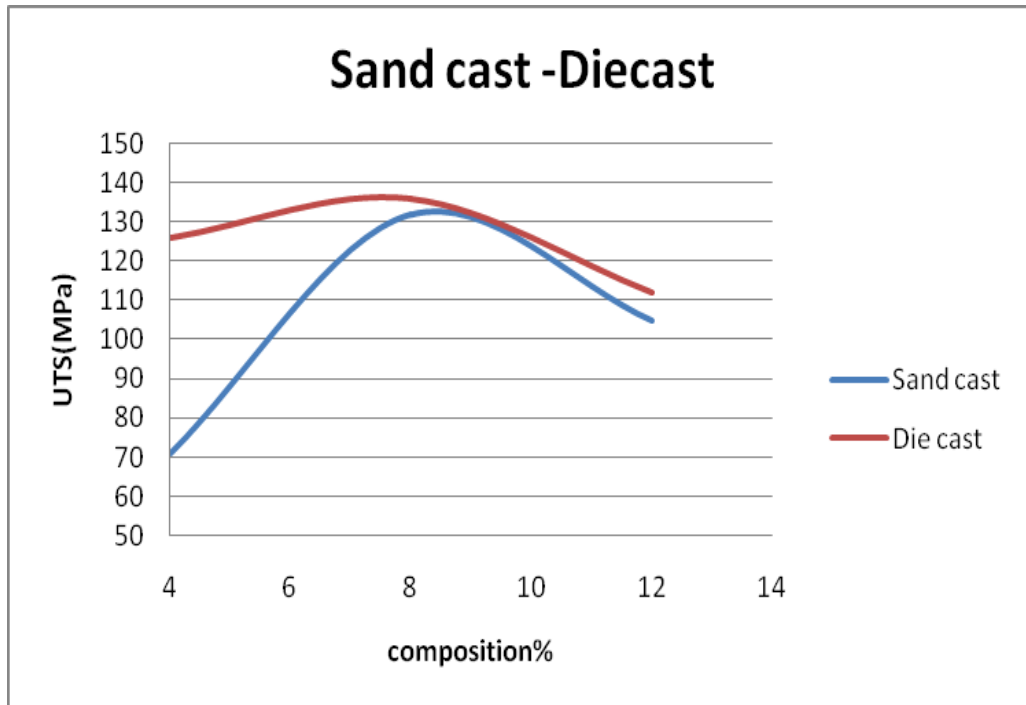


Figure 4.24 Sand cast and gravity die cast tensile strength (varying copper wt%)

4.3.5 Comparison of Die cast and Sand cast hardness results

Both gravity die cast and green sand cast components reveal higher hardness with increase in copper wt%. This increase in hardness reported is due to the presence of more strengthening Al_2Cu phase with excess copper addition [Fig 4.25]. The gravity die casting hardness are Brinell hardness number (HBW) and for green sand casting it is Rockwell hardness number (HRB).

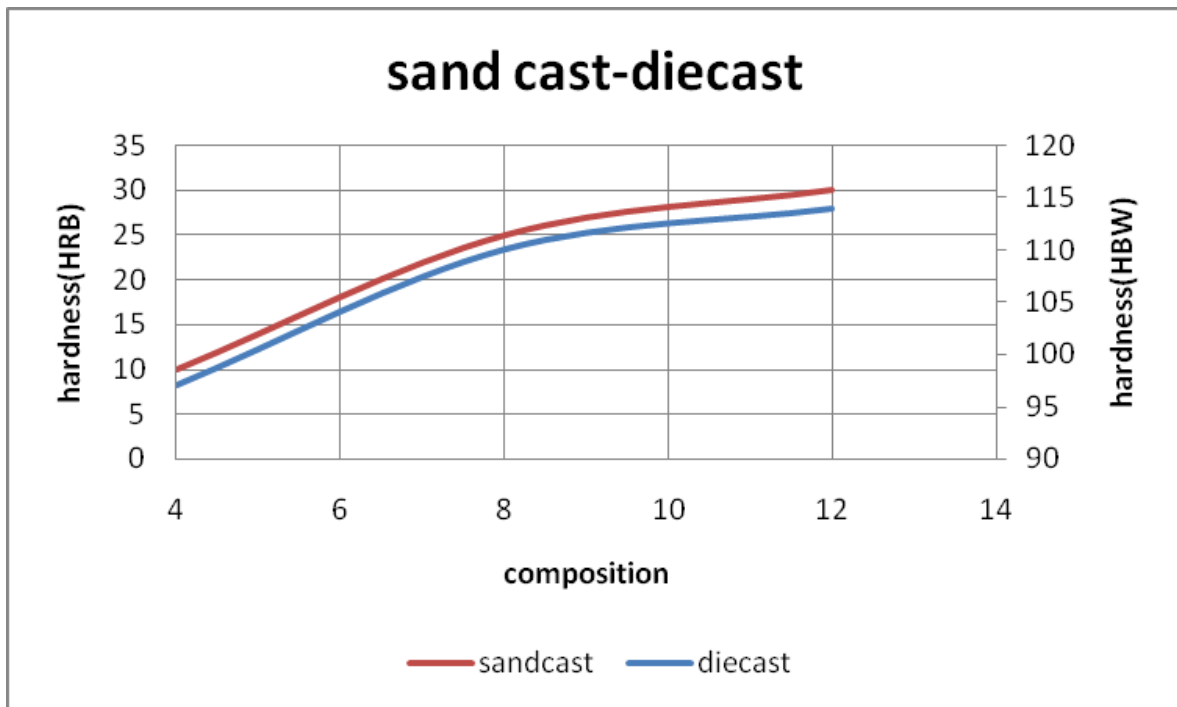
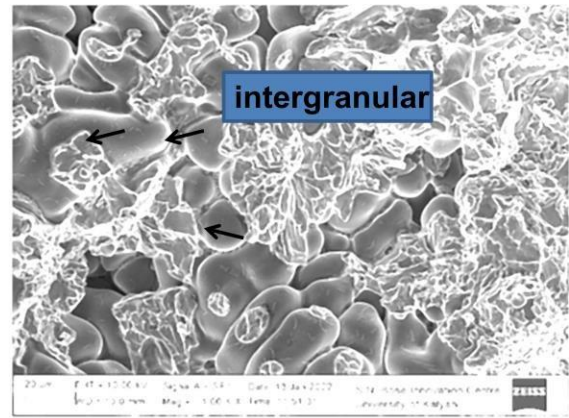
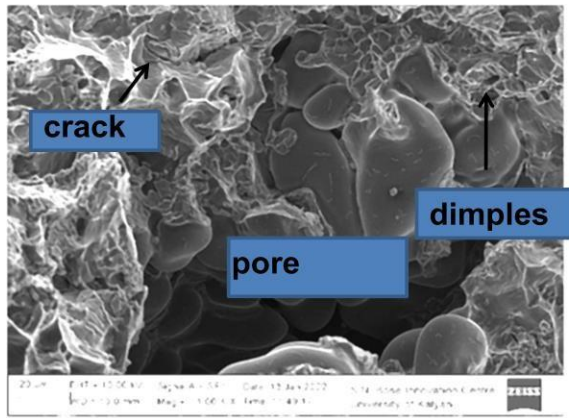


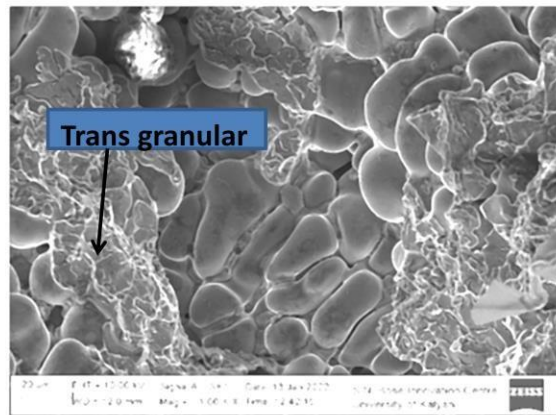
Figure 4.25 Hardness of sand casting and gravity die casting (varying copper wt%)

4.3.6 SEM images of fractured surface (Die cast)

Fracture images for alloy A1 exhibit ductile fracture Fig 4.26(a). For alloy A2 the fracture mainly consists of inter granular fracture Fig 4.26(b). For this alloy mixed nature of fracture can be observed. For alloy A3 the fracture Fig 4.26(c) mainly trans granular and most of the pattern are of brittle type. Shallow dimples are found for alloy A2 and A3. This is due the presence of harder Al_2Cu at grain boundaries.



a



b

c

Figure 4.26 Fracture surface SEM die cast (a) A1 (b) A2 (c) A3

4.3.7 Micro hardness of sand cast and die cast alloys

Micro hardness of alloy was conducted with standard procedure defined by ASTM E384 standard. The test conducted on thin samples with load 0.1kgf and the value calculated as discussed in [Sec 3.3.2]. The result obtained is listed in Table 4.9 for each alloy composition and both gravity die casting and green sand casting. For both the casting method alloy A2 having highest hardness. Alloy A2 having 125HV and 173.4 HV for green sand and gravity die casting respectively

Table 4.9 Micro hardness of sand cast and die cast alloys A1, A2, A3

Alloy	Micro hardness(sand)HV	Micro hardness(die)HV
A1	102.5	107
A2	125.5	173.4
A3	123.6	122.5

4.4 Heat treatment of Al-Cu alloy

Mechanical properties of Al-Cu alloy can be enhanced with heat treatment. Improvement in mechanical properties after heat treatment is due to redistribution of θ -phase at the grain boundaries and interdendrite regions. Alloy having 8wt% of copper i.e. A2 show the optimum improvement in yield strength, ultimate strength and hardness.

Heat treatment (T6) for all the alloy compositions were conducted by steps discussed in (section 3.4) and the results of heat treated tensile samples are listed in **Table 4.9**.

4.4.1 Tensile results of heat treated gravity die-casting [varying copper]

Heat treated tensile samples for die casting show excellent tensile strength improvement. The alloy A2 response is the best among the entire alloy for heat treatment as compared to other two.

Table 4.10 UTS, YS, %EL for heat treated die cast samples

Alloy	UTS (MPa)	YS (MPa)	%elongation (%EL)
A1	161	158	3.0
A2	210	207	1.0
A3	165	163	1.5

4.4.2 Tensile results of heat treated green sand casting [varying copper]

Green sand cast and heat treated tensile specimen test results are listed in Table 4.10. The UTS and YS for alloy A2 is 169MPa and 142MPa respectively. Whereas alloy A1 results show UTS and YS as 74MPa and 72MPa respectively. The alloy A2 exhibit best tensile results for sand casting in heat treated condition. The response to heat treatment for alloy A2 is highest as compared to other two alloys. This is due the availability of finer intermetallics during solution treatment.

Table 4.11 UTS &YS of heat treated sand casting

Alloy	UTS(MPa)	YS(MPa)
A1	74	72.5
A2	169	142
A3	125	119

4.4.3 SEM images of fractured tensile surface heat treated [green sand cast]

The heat treated green sand casting fractured surface [Fig 4.27 & 4.28] show presence of both aluminium and copper. The EDS of the cross marked spot for A2 and A3 have copper 24.65 and 34.53% respectively. It can be observed that alloy A2 is mostly having inter granular fracture whereas A3 is having brittle trans-granular fracture.

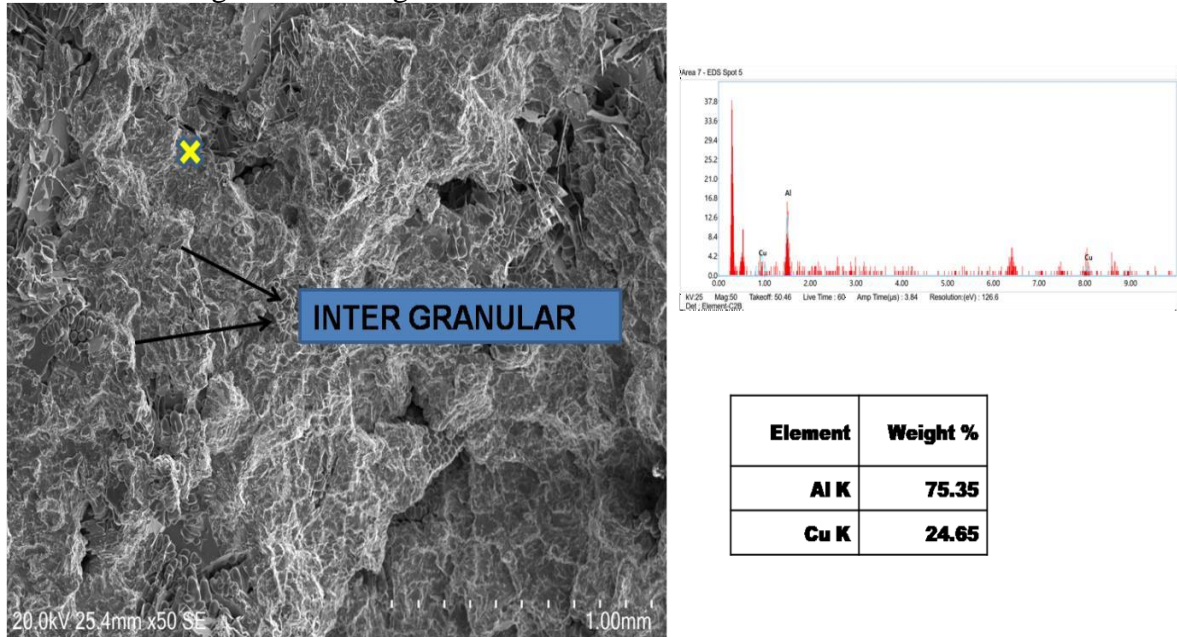


Figure 4.28 SEM-EDS of A2

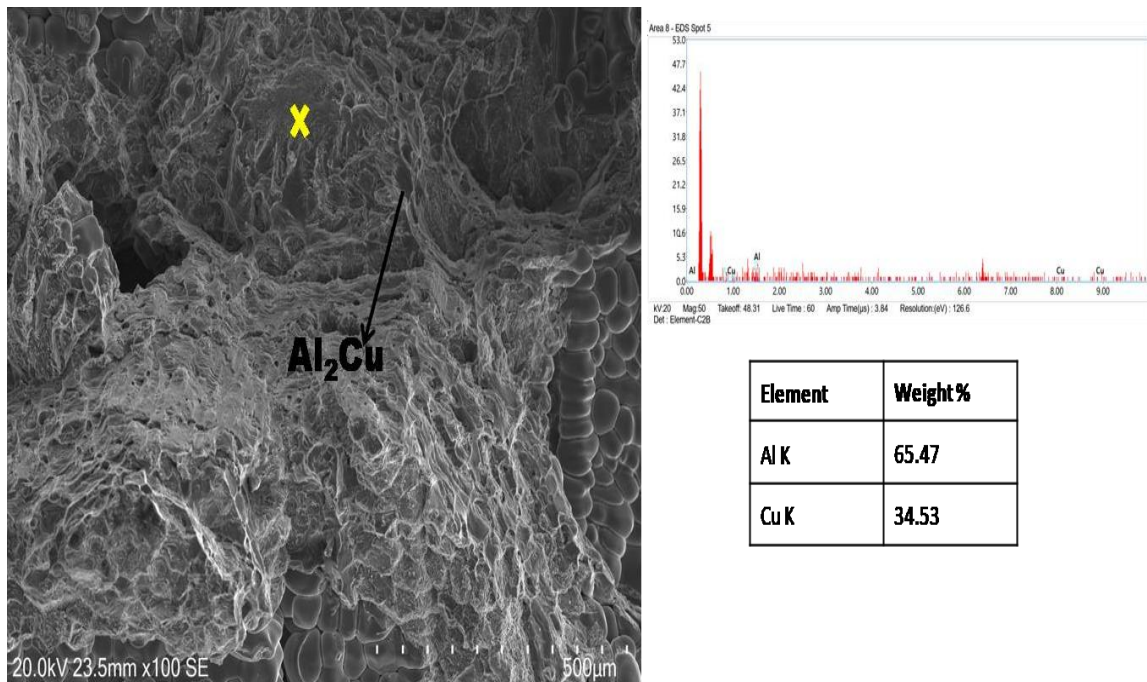


Figure 4.27 SEM-EDS of A3

4.4.4 SEM images of fractured tensile surface heat treated [gravity die cast]

Heat treatment redistributes the strengthening Al_2Cu and enhances the tensile strength. It can be noted that heat treatment facilitates brittle failure for alloy when compared with as cast condition.

Alloy A3 after heat treatment exhibit tensile failure of brittle nature (river pattern) [Fig 4.29 (c)]. In case of alloy A2 the fracture mostly found to be inter granular [Fig 4.29(b)]. This may be due to the presence of harder Al_2Cu at the intergranular spaces which initiate crack leading to failure. Alloy A2 exhibit mixed ductile and brittle failure after heat treatment.

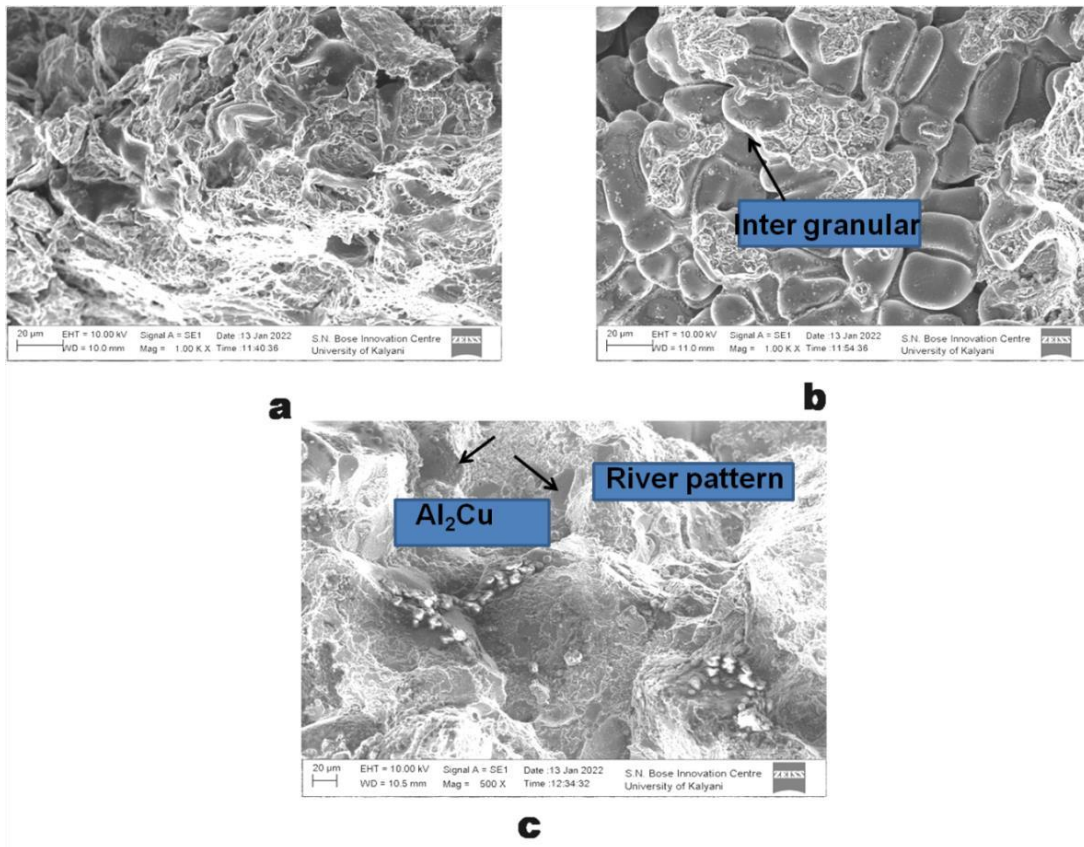


Figure 4.29 Fractured surface SEM of heat treated alloy (a) A1 (b) A2(c) A3

4.4.5 Gravity die cast and green sand components [heat treated]

Heat treatment enhances the tensile strength of both green sand and gravity die cast components. From Fig 4.30 it can be observed that with varying copper wt% the heat treatment response for the alloy A2 is highest for both gravity die casting and sand casting. So irrespective of the casting method heat treatment can enhance alloy properties remarkably for the alloy A2.

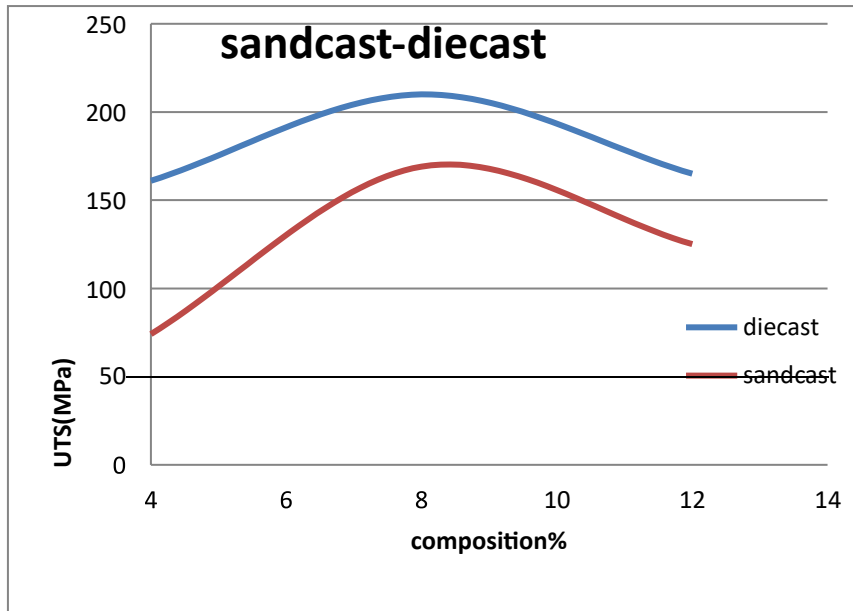


Figure 4.30 UTS of Gravity die casting & sand casting (heat treated)

4.4.6 Comparison of as cast & heat-treated tensile results [gravity die cast]

Figure 4.31 is showing tensile strength comparison based on varying copper, casting methods and heat treatment. It is observed that heat treated alloy A2 with die casting is having excellent tensile strength of 210MPa.

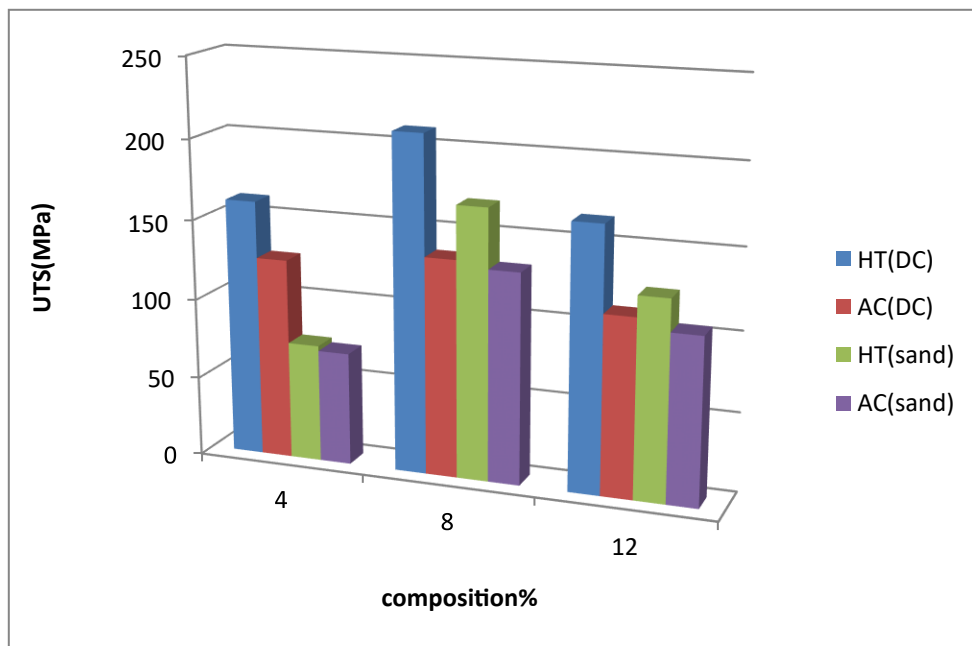


Figure 4.31 Comparison of as cast & heat treated tensile results

4.4.7 Comparison of grain size and tensile test results

The tensile tests carried out for different alloy under different casting methods. The test results and comparison with the grain size measured reveal the relation between microstructure and tensile properties. In the Fig 4.32 grain size and tensile strength relations are shown graphically. The graph clearly indicates for minimum grain size tensile strength is highest. It can be noted from the

graph that % area fraction covered also play an important role in mechanical properties. Both as cast and heat treated samples show maximum UTS for minimum grain size.

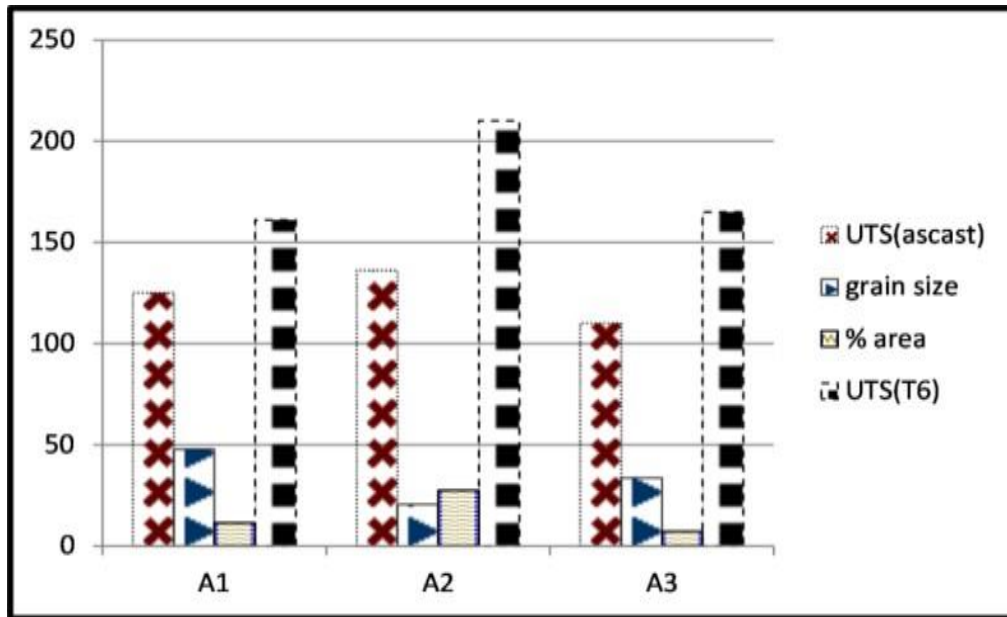


Figure 4.32 Comparison of UTS (as cast and heat treated) & grain size

4.5 Tribo-mechanical analysis

4.5.1 Results for dry-sliding wear properties with addition of copper

The pin-on-disc tribometer used to measure dry sliding wear behaviour of given alloy based on the weight loss of the test specimen under varying load and speed condition. The results of wear tests as mass loss are listed in the Table 4.12 & 4.13.

Table 4.12 Mass loss with varying load for alloy A1, A2, A3[300rpm]

Load(N)	A1 mass loss(gm)	A2 mass loss(gm)	A3 mass loss(gm)
20	0.008	0.008	0.012
30	0.009	0.011	0.011
40	0.005	0.005	0.011

Table 4.13 Mass loss with varying speed for alloy A1, A2, A3[40N]

Speed(rpm)	A1 mass loss(gm)	A2 mass loss(gm)	A3 mass loss(gm)
300	0.005	0.005	0.011
400	0.013	0.014	0.013
500	0.006	0.012	0.011

4.5.2 Design of experiments

For the current analysis L9 orthogonal array has been chosen which has 9 rows and 3 columns. A total of 9 experiments were tabulated [Table 4.14] based on the run order generated by the Taguchi model. The response for the model is wear rate. The wear rate as mentioned in Sec 3.5.2 is mean of weight loss/sliding distance and the unit is mg/m. In Orthogonal array, first column is assigned to alloy composition, second column is assigned to load applied and third column is assigned to sliding speed. The objective of model is to optimise the variables for minimizing wear rate. The responses were tabulated [SNRA] and results were subjected to Analysis of Variance (ANOVA). The Signal to Noise ratio (S/N), which determines the dominant variable mainly condenses multiple data points within a trial. The S/N ratio for wear rate is applied ‘smaller the better’ characteristic. The experimental observations are further transformed into Signal to Noise ratio.

To find out the optimum wear properties help of “Minitab software” has been taken and the process described in section 3.5.2. The following table are the results of the design of experiments by ‘Taguchi’ method.

Table 4.14 L9 Orthogonal array and S/N

Run Order	A	B	C	Alloy	Load(N)	Speed	Wear	SNRA
1	1	1	1	4	20	300	0.042	27.5350
2	1	2	2	4	30	400	0.047	26.5580
3	1	3	3	4	40	500	0.019	34.4249
4	2	1	2	8	20	400	0.042	27.5350
5	2	2	3	8	30	500	0.006	44.4370
6	2	3	1	8	40	300	0.026	31.7005
7	3	1	3	12	20	500	0.063	24.0132
8	3	2	1	12	30	300	0.058	24.7314
9	3	3	2	12	40	400	0.051	25.8486

The signal to noise ratio from design of experiment showing though all the variables are responsible for wear rate change but composition of alloy is the most effective and dominant for the wear properties. In the present analysis speed and load are second and third effective variables respectively. Fig 4.33 is indicating optimum combination for minimum wear is alloy A2 at load 30N and 500rpm. The micro hardness results goes very well with the wear characteristic as for composition A2 the micro hardness is found to be maximum.

Response Table for Signal to Noise Ratios

Smaller is better

Level	Alloy(%)	Load(N)	Speed(r.p.m)
1	29.51	26.36	27.99
2	34.56	31.91	26.65
3	24.86	30.66	34.29
Delta	9.69	5.55	7.64
Rank	1	3	2

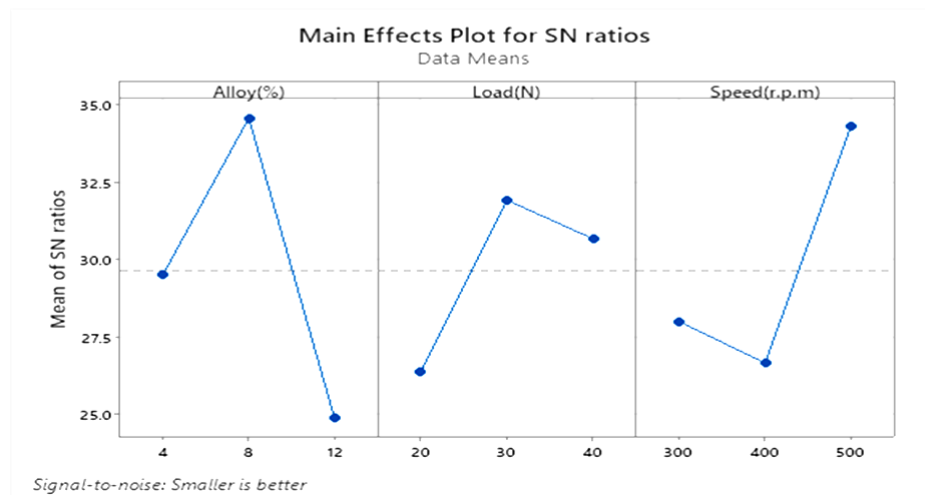


Figure 4.33 S/N response table and graph

Analysis of variance of means table obtained from “Minitab” software and % contribution of the variables is as shown in Table 4.15. The last column shows the % contribution of control factors chosen. Interaction effects of the control factors found to be non-significant from the analysis. The experimental results were analyzed by ANOVA, which is used to examine the influence of the wear parameters, namely, applied load, sliding speed and composition of alloy that extensively affects the performance measures. By performing ANOVA, the independent factor which dominates over the other can be determined and the percentage contribution of that particular independent variable can be found out. Model summary is given in Table 4.16. The co-efficient of determination or R^2 is 87.21% which states that the model fits well to the assumptions. The ANOVA test confirms that percentage of contribution for wear is 58.14% by alloy composition. The load and speed contribute 16.24 and 17.12 % respectively towards wear. The percent contribution calculated by dividing individual Seq SS value by the total Seq SS value.

Table 4.15 ANOVA response results and % contribution

Source	DF	Seq SS	Adj SS	Adj MS	% contribution
Alloy%	2	0.001651	0.001651	0.000825	58.54
Load	2	0.000458	0.000458	0.000229	16.24
Speed	2	0.000483	0.000483	0.000241	17.12
Residual error	2	0.000229	0.000229	0.000114	8.1
Total	8	0.002820			100

Table 4.16 ANOVA model summary

S	R-Sq	R-Sq (adj)
4.6258	87.21%	48.84%

4.5.3 Analysis of SEM images for wear properties [varying copper wt%]

Alloy A1 is showing adhesive wear [Fig 4.34] and fine continuous grooves in the direction of sliding. This type of wear is the result of less presence of harder θ -phase in alloy A1. With increase in load the wear become severe. At 40N load the alloy with 4 wt% of copper show poor resistance to wear.

For alloy A2 wear characterised by abrasive wear from Fig 4.35(a). This may be due to presence of harder Al_2Cu intermetallic. These intermetallic resists the wear and ultimately plastic deformation takes place at higher loading condition. For alloy A3 the deformation [Fig 4.35(b)] is in the form of deep groove and delamination. The worn surface study and Taguchianalysis both indicate toward less wear for alloy A2. Presence of finer Al_2Cu is the reason for better wear properties of alloy A2 compared to alloy A1 and A3. Though A3 possess Al_2Cu but blocky and bigger size help to de-bond easily.

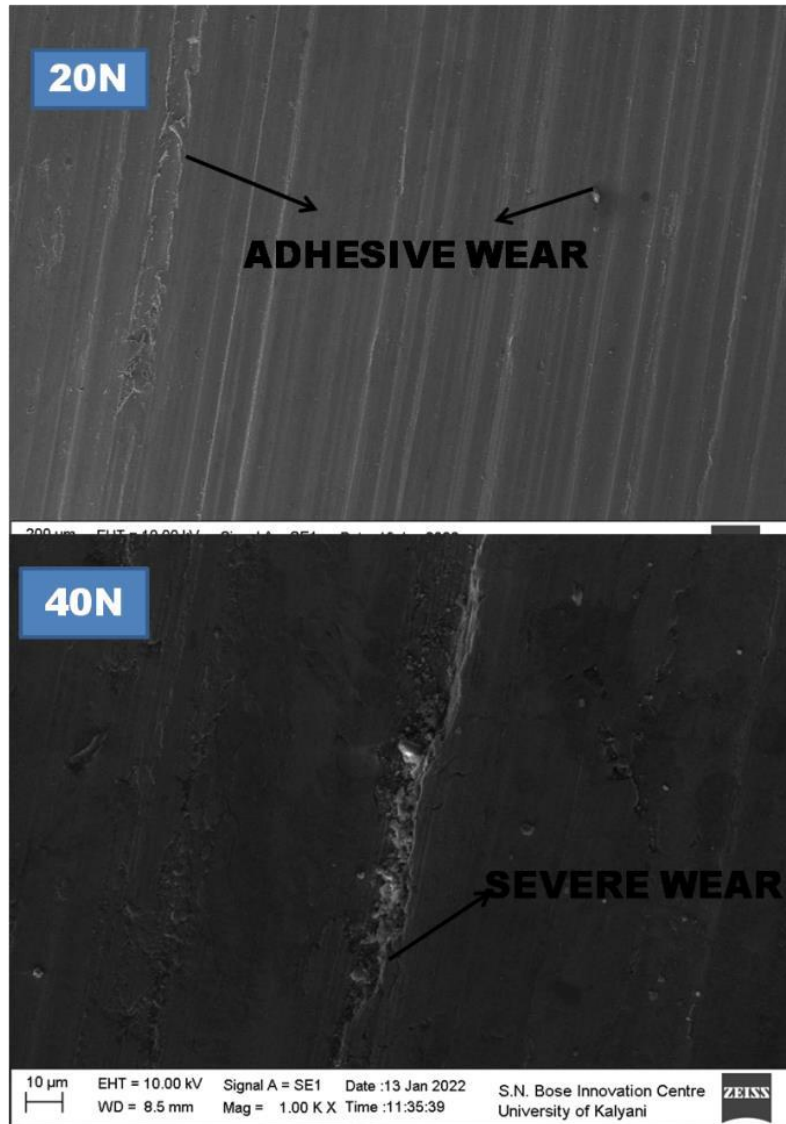


Figure 4.34 SEM of wear surface (1000X) for A1[load 20 N]

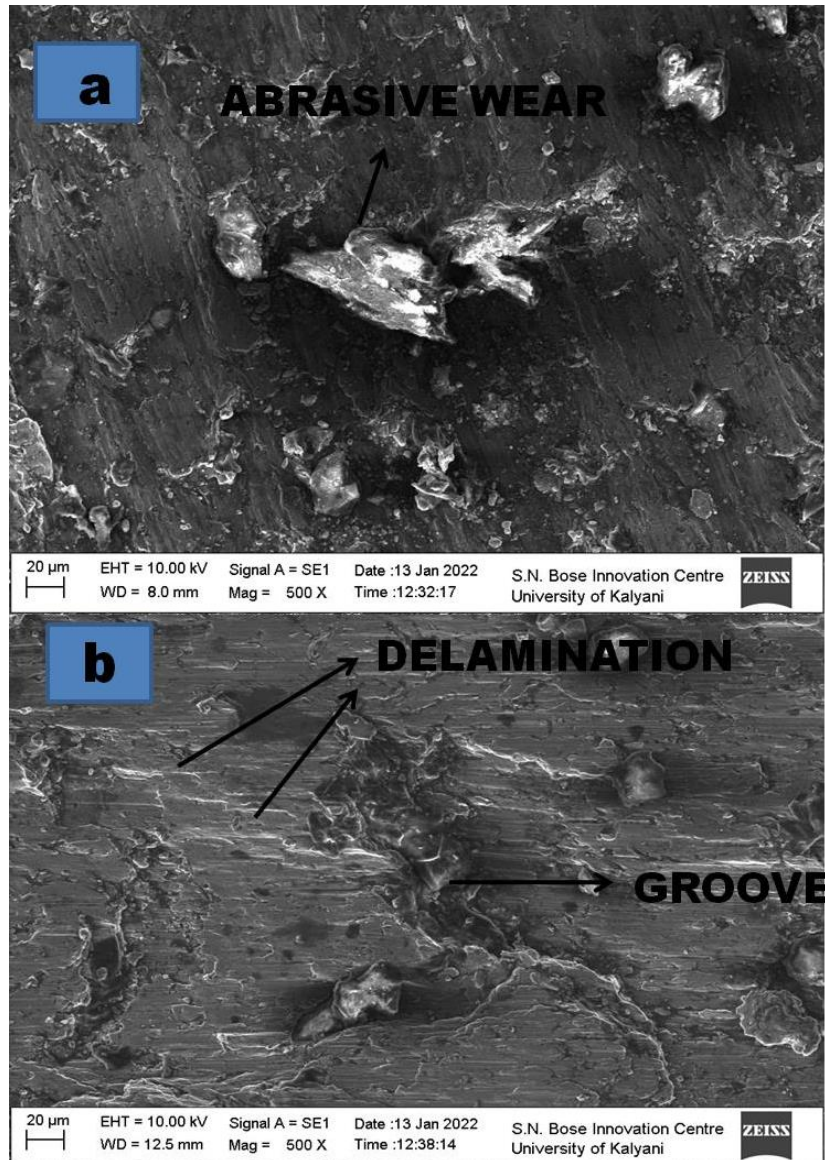


Figure 4.35 SEM for wear (500X) of (a) A2 (b) A3

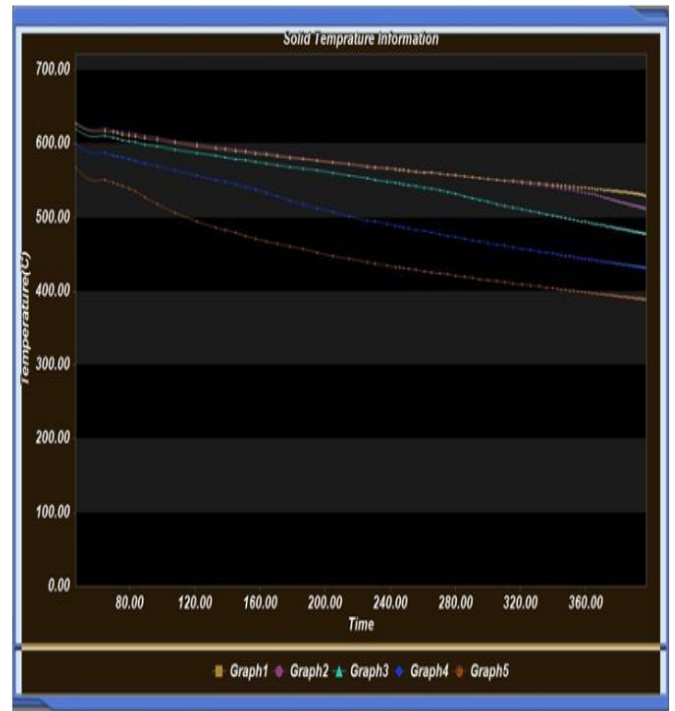
4.6 Casting Simulation Results

4.6.1 Simulation results of green sand casting:

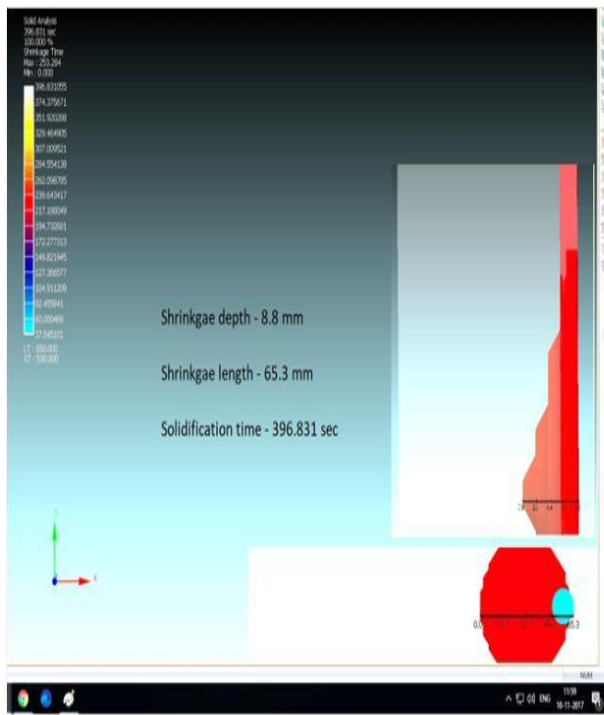
Solidification simulation results of sand casting (step-shape) for all the three compositions have shrinkage cavities near the base of the riser. The cooling curves obtained from simulation indicated higher cooling rate towards thinner section. The rate of cooling affects the grain morphology which is discussed in the section (section 4.2.4). [Fig 4.36-4.38] showing simulation results for green sand casting and their time temperature relationship. Figure[4.36 a-4.38 a] showing time temperature relationship obtained from thermocouple and [Fig 4.36-4.38(b)] showing the graph. Sand casting defects are shown in Fig 4.36 (c) &(d) - Fig 4.36(c) &(d) for alloy A1, A2 and A3 .

720.00	625.50	616.40	614.14	613.00	611.69	610.02	608.45	606.25	603.80	609.95	599.55	596.77	592.21	590.51	590.67	590.96	595.24	591.62	579.57	577.51
720.00	628.90	620.50	618.37	617.32	616.11	614.54	613.05	610.88	608.11	604.24	599.95	596.16	594.30	592.47	590.80	590.80	590.99	595.00	592.30	580.75
720.00	619.71	609.96	607.53	606.34	604.97	603.20	601.54	599.12	596.06	591.79	586.95	582.06	580.00	578.76	576.70	574.77	572.64	570.47	567.96	565.44
720.00	600.84	597.78	594.56	592.99	591.18	578.87	576.71	573.59	569.85	564.10	557.49	551.54	548.00	545.21	541.76	537.96	533.55	528.65	523.27	518.00
720.00	566.75	549.82	545.70	543.82	541.48	537.91	533.45	525.26	516.59	503.70	492.31	484.17	480.55	476.71	473.18	469.69	466.00	462.50	459.50	454.72
238.09	243.25	245.79	248.06	251.28	255.75	260.76	266.21	270.53	275.41	279.95	285.38	290.32	294.91	300.05	305.32	310.32	315.30	320.72	325.94	331.24
594.75	593.50	593.01	592.51	591.79	590.81	589.74	587.59	585.53	583.56	581.41	579.36	577.07	575.07	573.66	571.91	570.80	569.70	568.63	567.40	566.27
567.36	566.22	565.66	565.15	564.41	563.37	562.18	561.13	559.89	558.89	557.59	556.26	555.04	553.90	552.59	551.21	549.80	548.53	547.02	545.53	543.96
547.80	546.93	545.03	544.20	542.99	541.24	539.16	537.25	534.70	532.39	530.04	527.66	524.49	522.13	519.52	516.92	514.50	512.14	509.61	507.25	504.89
491.02	488.83	487.76	486.80	485.45	483.57	481.47	479.62	477.42	475.42	473.60	471.39	469.43	467.82	465.63	463.60	461.70	459.84	457.83	455.93	454.02
433.16	431.35	430.48	429.71	428.63	427.15	425.53	424.11	422.44	420.93	419.55	417.91	416.44	415.00	413.58	412.05	410.82	409.21	407.69	406.24	404.70
552.48	555.01	557.46	559.68	561.83	563.92	565.66	567.40	569.24	570.84	572.17	573.55	574.77	575.87	576.96	577.91	578.80	579.70	580.63	581.40	582.37
540.41	539.80	539.36	539.90	538.44	538.00	537.63	537.26	536.66	536.52	536.22	535.50	535.65	535.40	535.15	534.90	534.71	534.51	534.29	534.00	533.86
536.99	536.99	534.97	533.99	532.96	531.88	530.91	529.87	528.77	527.76	526.94	526.12	525.35	524.70	524.02	523.45	522.86	522.37	521.80	521.29	520.76
496.83	494.75	493.70	492.74	491.81	490.91	489.16	488.41	487.92	487.34	486.74	486.20	485.04	485.72	485.25	484.84	484.41	484.06	483.65	483.02	482.39
446.66	445.81	444.99	444.26	443.54	442.85	442.27	441.70	441.10	440.57	440.13	439.68	439.20	438.92	438.56	438.25	437.93	437.66	437.00	437.00	436.70
399.09	398.43	397.79	397.19	396.66	396.13	395.67	395.23	394.76	394.36	394.02	393.67	393.36	393.00	392.81	392.57	392.33	392.12	391.89	391.61	391.46

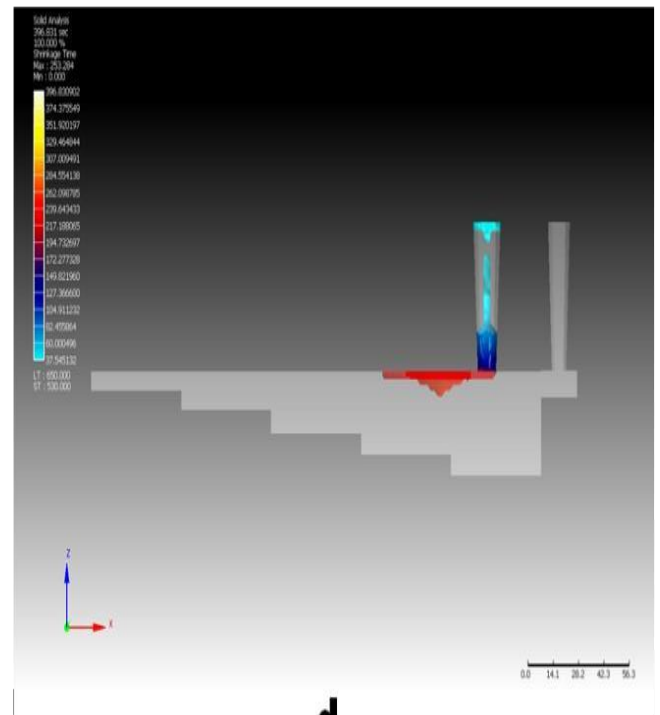
a



b



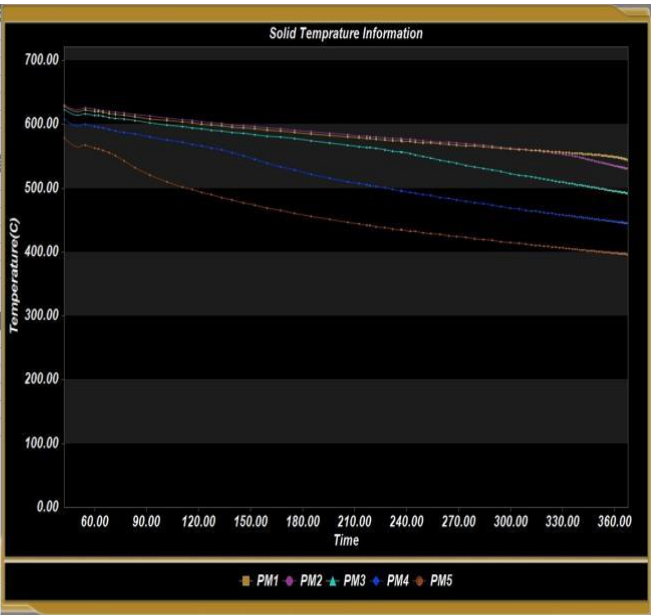
c



d

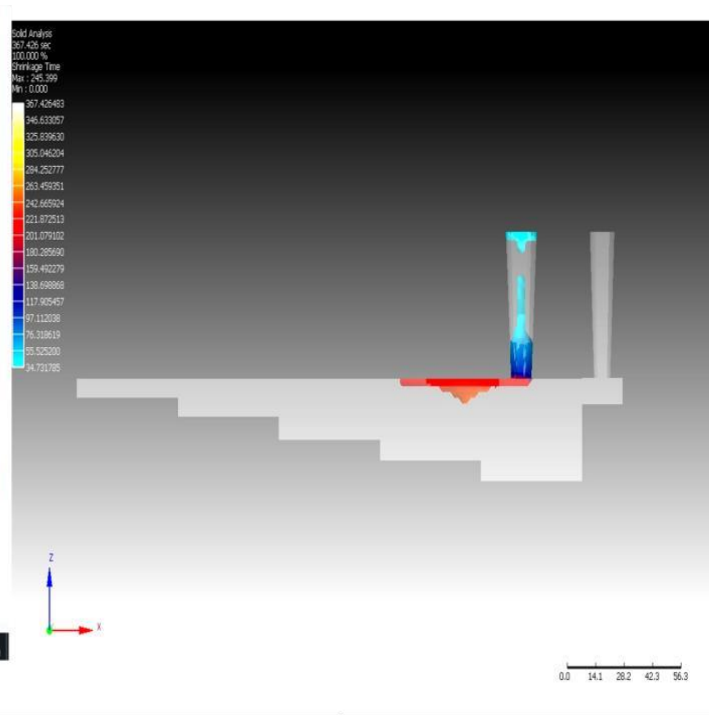
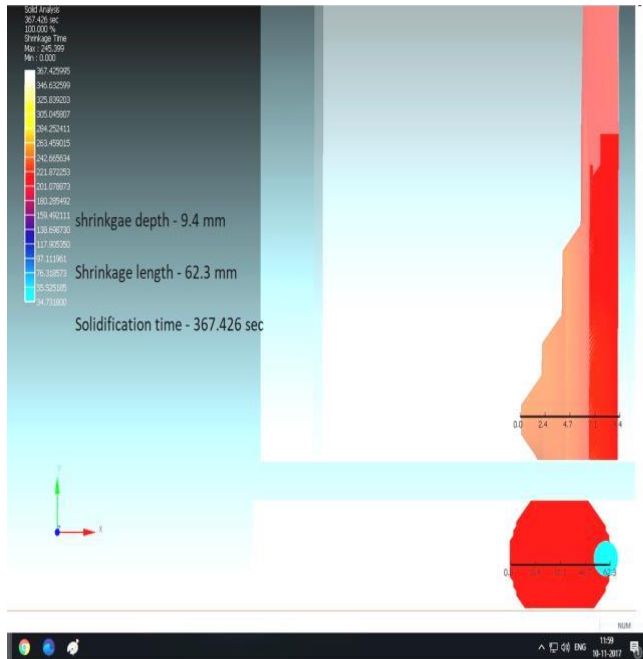
Figure 4.36 Sand casting simulation for A1

	0.00	42.50	84.75	127.00	169.25	211.50	253.75	296.00	338.25	380.50	422.75	465.00	507.25	549.50	591.75	634.00	676.25	718.50	760.75	803.00	845.25	887.50	929.75	972.00	1014.25	1056.50	1098.75	1141.00	1183.25	1225.50	1267.75	1310.00	1352.25	1394.50	1436.75	1479.00	1521.25	1563.50	1605.75	1648.00	1690.25	1732.50	1774.75	1817.00	1859.25	1901.50	1943.75	1986.00	2028.25	2070.50	2112.75	2155.00	2197.25	2239.50	2281.75	2324.00	2366.25	2408.50	2450.75	2493.00	2535.25	2577.50	2619.75	2662.00	2704.25	2746.50	2788.75	2831.00	2873.25	2915.50	2957.75	3000.00	3042.25	3084.50	3126.75	3169.00	3211.25	3253.50	3295.75	3338.00	3380.25	3422.50	3464.75	3507.00	3549.25	3591.50	3633.75	3676.00	3718.25	3760.50	3802.75	3845.00	3887.25	3929.50	3971.75	4014.00	4056.25	4098.50	4140.75	4183.00	4225.25	4267.50	4309.75	4352.00	4394.25	4436.50	4478.75	4521.00	4563.25	4605.50	4647.75	4690.00	4732.25	4774.50	4816.75	4859.00	4901.25	4943.50	4985.75	5028.00	5070.25	5112.50	5154.75	5197.00	5239.25	5281.50	5323.75	5366.00	5408.25	5450.50	5492.75	5535.00	5577.25	5619.50	5661.75	5704.00	5746.25	5788.50	5830.75	5873.00	5915.25	5957.50	5999.75	6042.00	6084.25	6126.50	6168.75	6211.00	6253.25	6295.50	6337.75	6380.00	6422.25	6464.50	6506.75	6549.00	6591.25	6633.50	6675.75	6718.00	6760.25	6802.50	6844.75	6887.00	6929.25	6971.50	7013.75	7056.00	7098.25	7140.50	7182.75	7225.00	7267.25	7309.50	7351.75	7394.00	7436.25	7478.50	7520.75	7563.00	7605.25	7647.50	7689.75	7732.00	7774.25	7816.50	7858.75	7901.00	7943.25	7985.50	8027.75	8070.00	8112.25	8154.50	8196.75	8239.00	8281.25	8323.50	8365.75	8408.00	8450.25	8492.50	8534.75	8577.00	8619.25	8661.50	8703.75	8746.00	8788.25	8830.50	8872.75	8915.00	8957.25	8999.50	9041.75	9084.00	9126.25	9168.50	9210.75	9253.00	9295.25	9337.50	9379.75	9422.00	9464.25	9506.50	9548.75	9591.00	9633.25	9675.50	9717.75	9760.00	9802.25	9844.50	9886.75	9929.00	9971.25	10013.50	10055.75	10098.00	10140.25	10182.50	10224.75	10267.00	10309.25	10351.50	10393.75	10436.00	10478.25	10520.50	10562.75	10605.00	10647.25	10689.50	10731.75	10774.00	10816.25	10858.50	10900.75	10943.00	10985.25	11027.50	11069.75	11112.00	11154.25	11196.50	11238.75	11281.00	11323.25	11365.50	11407.75	11450.00	11492.25	11534.50	11576.75	11619.00	11661.25	11703.50	11745.75	11788.00	11830.25	11872.50	11914.75	11957.00	12000.00
--	------	-------	-------	--------	--------	--------	--------	--------	--------	--------	--------	--------	--------	--------	--------	--------	--------	--------	--------	--------	--------	--------	--------	--------	---------	---------	---------	---------	---------	---------	---------	---------	---------	---------	---------	---------	---------	---------	---------	---------	---------	---------	---------	---------	---------	---------	---------	---------	---------	---------	---------	---------	---------	---------	---------	---------	---------	---------	---------	---------	---------	---------	---------	---------	---------	---------	---------	---------	---------	---------	---------	---------	---------	---------	---------	---------	---------	---------	---------	---------	---------	---------	---------	---------	---------	---------	---------	---------	---------	---------	---------	---------	---------	---------	---------	---------	---------	---------	---------	---------	---------	---------	---------	---------	---------	---------	---------	---------	---------	---------	---------	---------	---------	---------	---------	---------	---------	---------	---------	---------	---------	---------	---------	---------	---------	---------	---------	---------	---------	---------	---------	---------	---------	---------	---------	---------	---------	---------	---------	---------	---------	---------	---------	---------	---------	---------	---------	---------	---------	---------	---------	---------	---------	---------	---------	---------	---------	---------	---------	---------	---------	---------	---------	---------	---------	---------	---------	---------	---------	---------	---------	---------	---------	---------	---------	---------	---------	---------	---------	---------	---------	---------	---------	---------	---------	---------	---------	---------	---------	---------	---------	---------	---------	---------	---------	---------	---------	---------	---------	---------	---------	---------	---------	---------	---------	---------	---------	---------	---------	---------	---------	---------	---------	---------	---------	---------	---------	---------	---------	---------	---------	---------	---------	---------	---------	---------	---------	---------	---------	---------	---------	---------	---------	---------	---------	---------	---------	----------	----------	----------	----------	----------	----------	----------	----------	----------	----------	----------	----------	----------	----------	----------	----------	----------	----------	----------	----------	----------	----------	----------	----------	----------	----------	----------	----------	----------	----------	----------	----------	----------	----------	----------	----------	----------	----------	----------	----------	----------	----------	----------	----------	----------	----------	----------	----------



a

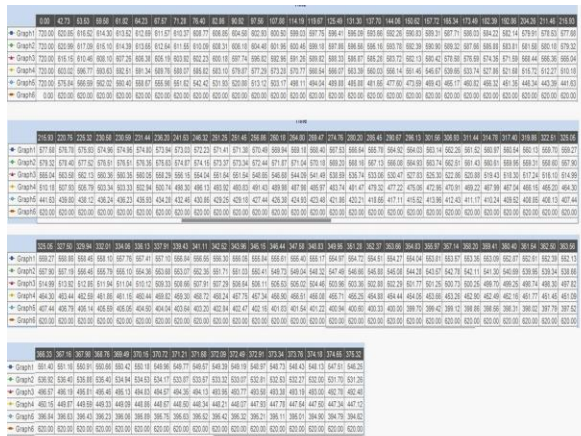
b



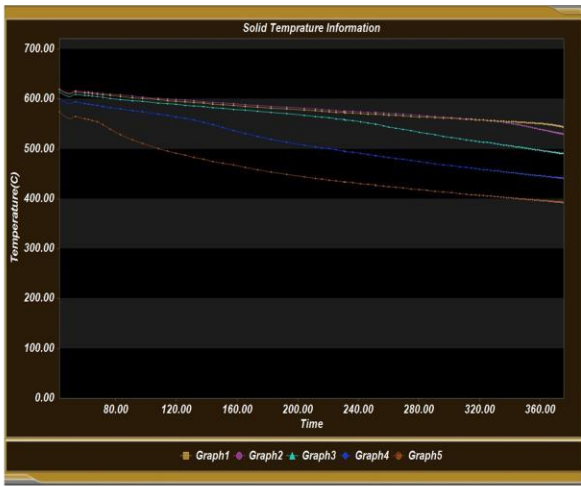
c

d

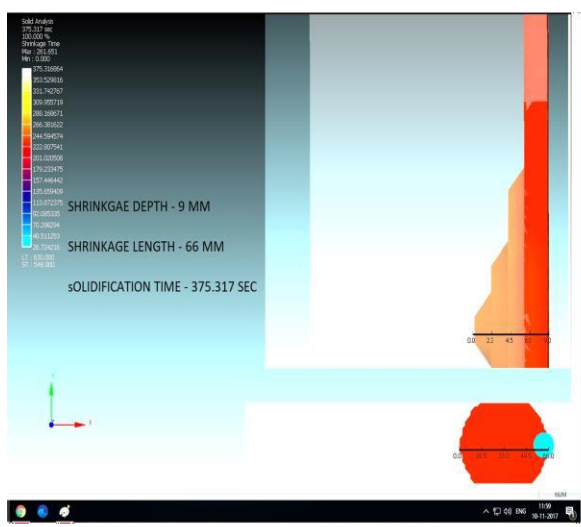
Figure 4.37 Sand casting simulation for A2



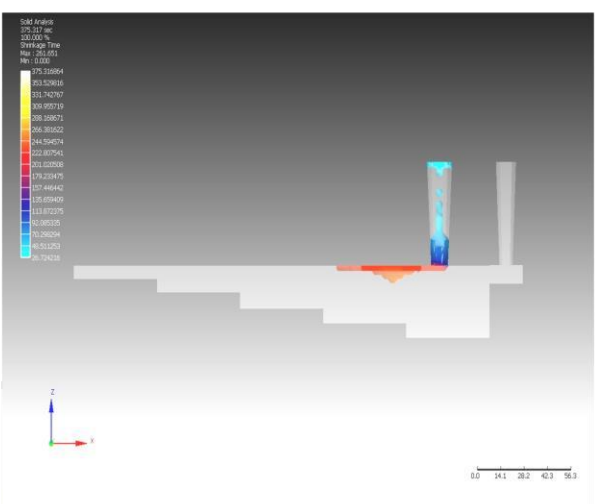
a



b



c



d

Figure 4.38 Sand casting simulation for A3

4.6.2 Simulation results of gravity die casting

The solidification simulation results of gravity die casting detected shrinkage cavities at the base of the riser for the existing riser dimension. Solidification simulation results predicted shrinkage defects for each composition at the base of the riser for our present analysis. The defects are mainly due to inadequate feeding. Present analysis aims at comparing the accuracy of the predicted results (including defects) with the actual casting results. So, components were casted with the existing riser dimensions [existing riser dimension produce defect free casting for LM6 alloy containing silicon]. Study of simulation results indicate different sizes and shapes of shrinkage for each alloy composition. Shrinkage cavity position in simulation images marked as 1', 2' and 3' and for actual components marked as 1, 2, 3. [Fig. 4.39-4.41] For alloy A1 color pattern of temperature from simulation implies cooling direction is from thinnest S-5 to thickest S-1 section. The solidification process initiates from the thinnest section which is also the farthest from the riser and proceeds towards the thickest part. After 25% solidification is completed as shown in the Fig 4.39 (b) and (c) the section S-1 close to riser is still above the solidus temperature (550°C for the composition). During progress of solidification at this section (mushy zone) lack of molten metal due to insufficient feeding from the riser may lead to shrinkage cavities. Similarly, simulation images for A2 reveal Fig 4.40 b & c after completion of 60% of solidification the temperature at sections S-1, S-2 is well above solidus temperature. These sections take longer time to solidify and feeding

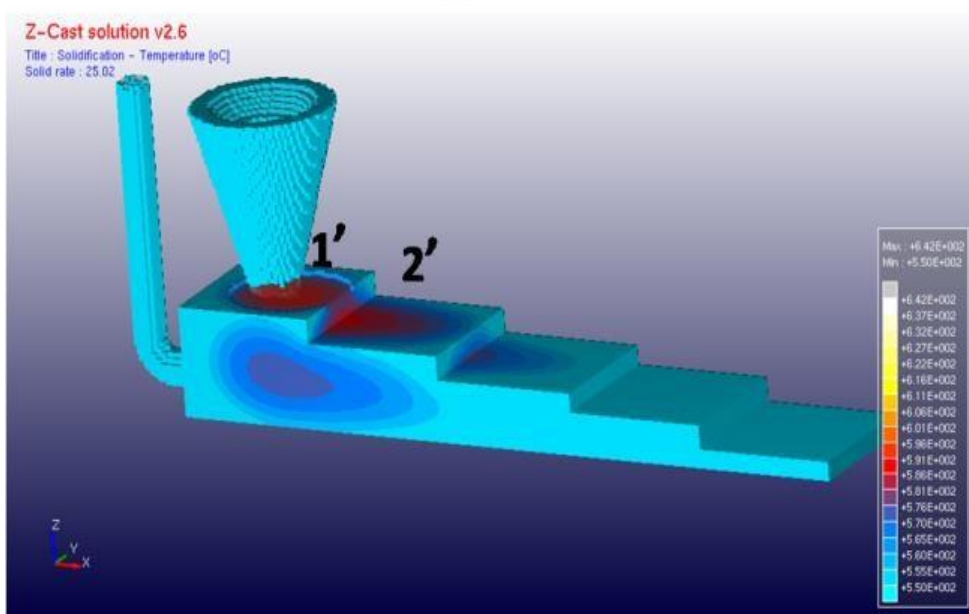
from the riser is halted. This happened as the riser solidified earlier to the component and no metal flows to compensate for the shrinkage. It may be noted that riser solidifies earlier to the component for all the compositions under consideration. This condition leads to insufficient feeding of molten metal. In the paper by Lee et al it is experimentally established that increasing riser size can favor better feeding and avoidance of surface collapse for Al-Cu alloy [127]. These predictions from simulation analysis can be used to rectify riser position and dimension which may lead to defect free castings. For alloy A3 similar condition is being observed. For this composition as can be seen from [Fig 4.41b & c] even after 80% of solidification is completed section near riser is at much above the solidus temperature. The alloy A3 has observed bigger hot spot zone as compared to other alloy composition. It can be said that the position of shrinkage due to poor riser design can be predicted from the solidification simulation. The change in shrinkage size due to addition of copper is also predicted from the simulation results. Simulation predictions can be used to avoid defects by focusing on the problem areas and by proper feeding to this area.

The cooling graphs obtained from simulated thermocouple data for sections S-1 and S-5 have different rate of cooling for each alloy composition [Fig 4.42-4.44] The cooling curves (cc-S1, cc-S5) and their first derivative curve (fdc-S1, fdc-S5) derived from simulation graphs are shown in Fig [4.42a-4.44a] The start of α -phase is marked with the peak 'a' and 'b' of first derivative curves for section S-5 and S-1 respectively. Similarly, the points marked as 'a1' and 'b1' on the cooling curves correspond to start of α -phase at section S-1 and S-5 respectively. The peak of the first derivative curve is the result of latent heat released when solidification starts. The rate of cooling calculated from the simulation graphs is the slope marked as cc-S1 for section S-1 and cc-S5 for section S-5 in [Fig 4.42b-4.44b]. The simulation predictions show faster cooling rate for thin section S-5 than thick section S-1. The simulation cooling curve clearly predicts different rate of cooling both for change in composition and change in dimension. The rate of cooling for different composition at section S-1 is predicted to be between 3.0-3.5^oC/sec. Therefore, from simulation prediction it can be concluded that the rate of cooling is not affecting the size of shrinkage variations at the riser base. This is because prediction of cooling rate at riser base for all the compositions is not varying too much. Therefore, variation in shrinkage may be attributed to copper concentration in aluminium from simulation results.

Cooling graphs prediction from simulation is validated with the metallographic and XRD analysis. It is observed that for section S-5 dendrite arm spacings are smaller as compared to section S-1 irrespective of the alloy composition. This can be explained from the cooling curves which clearly show rate of cooling is faster for S-5. Section S-5 of alloy A1 having the highest cooling rate [Fig. 4. 42b]. The thickness of sections affects the cooling rate as it is predicted from the simulation curves. By changing process parameters desired sound castings can be produced and for this simulation can be used as an effective tool. Research shows that shrinkage porosity grows where solid fraction is the lowest [128].

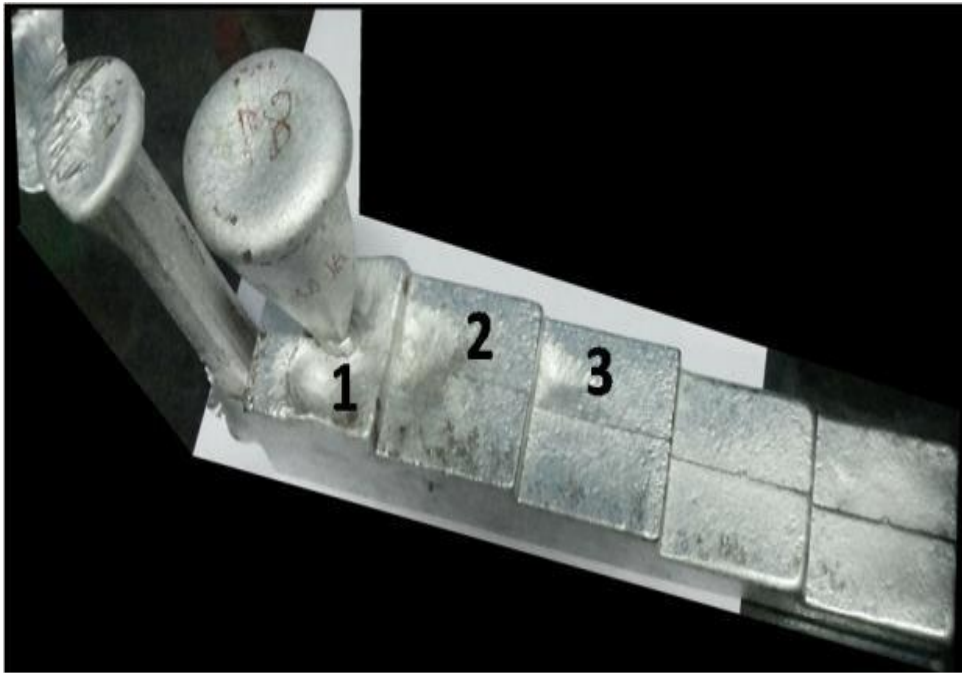


a

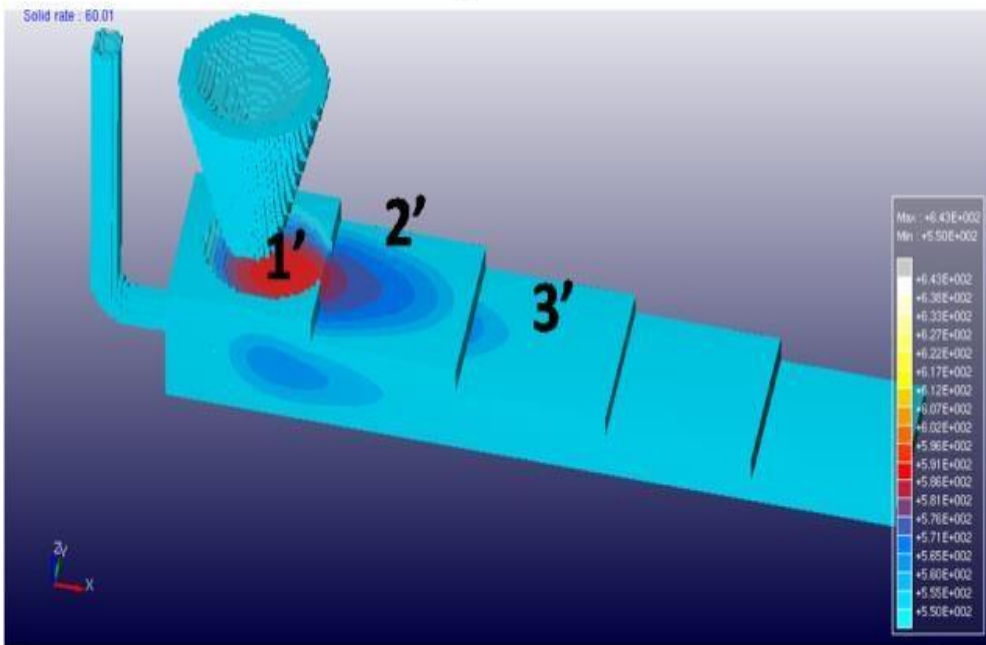


c

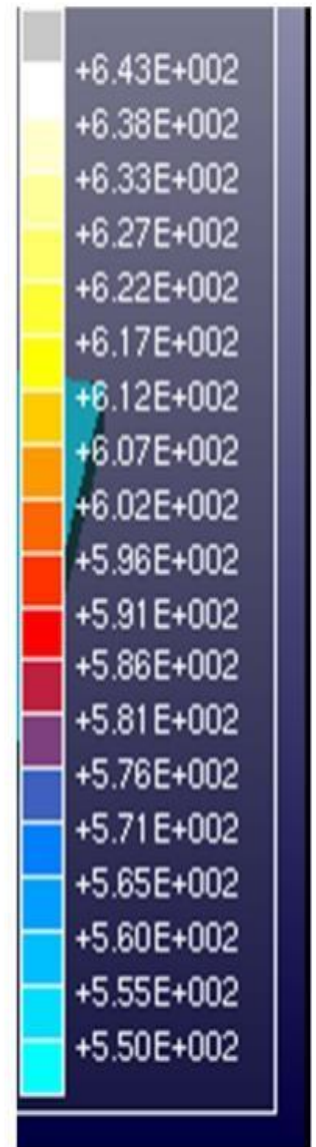
b
 Figure 4.39 Die casting simulation for A1



a



b

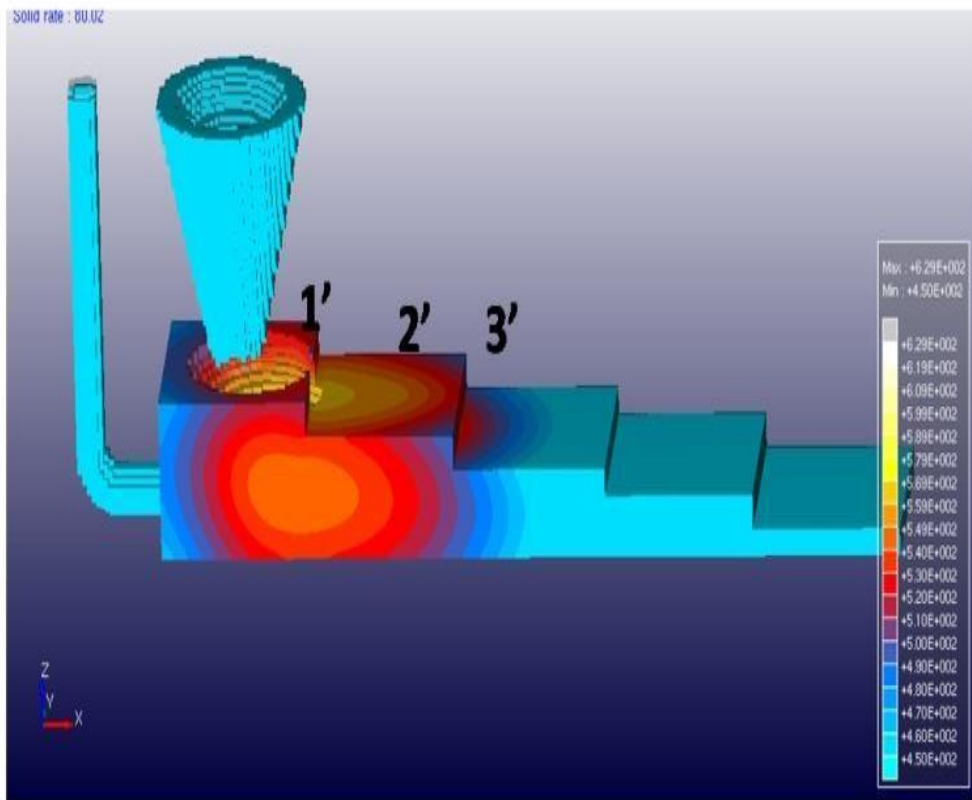


c

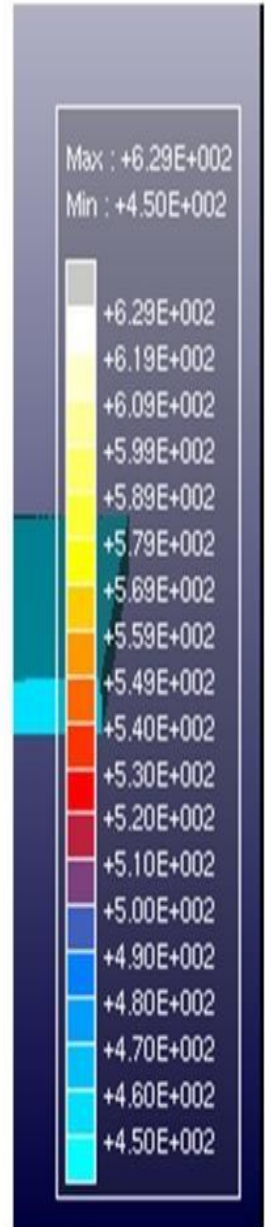
Figure 4.40 Die casting simulation for A2



a

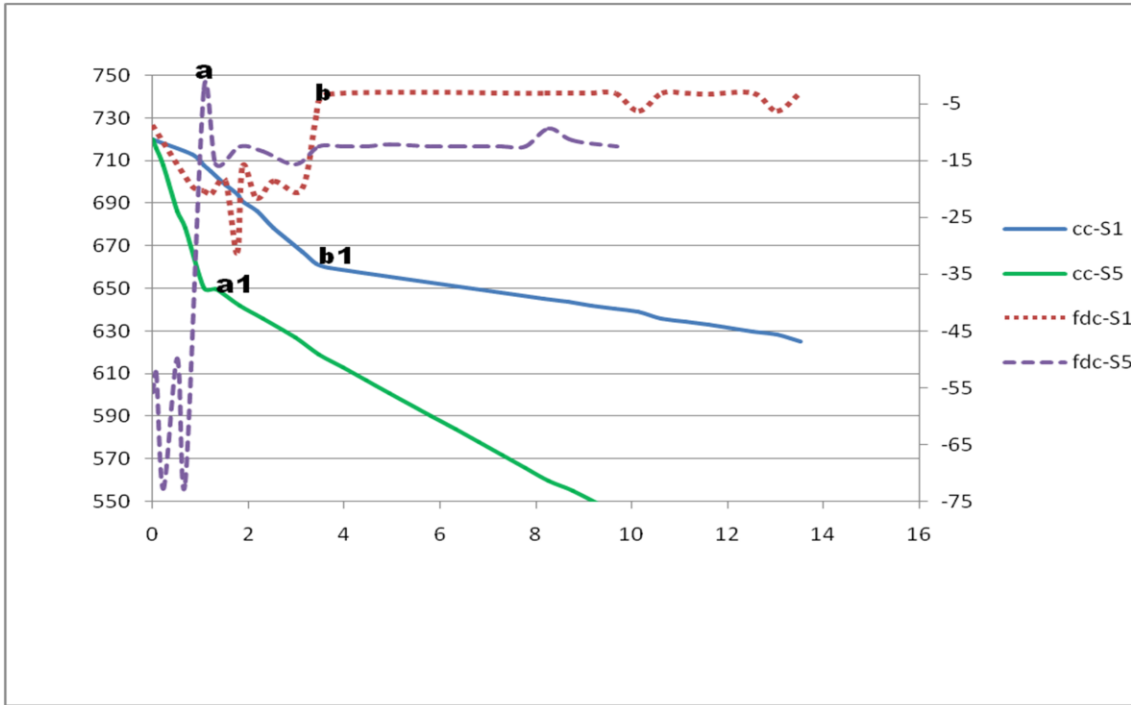


b

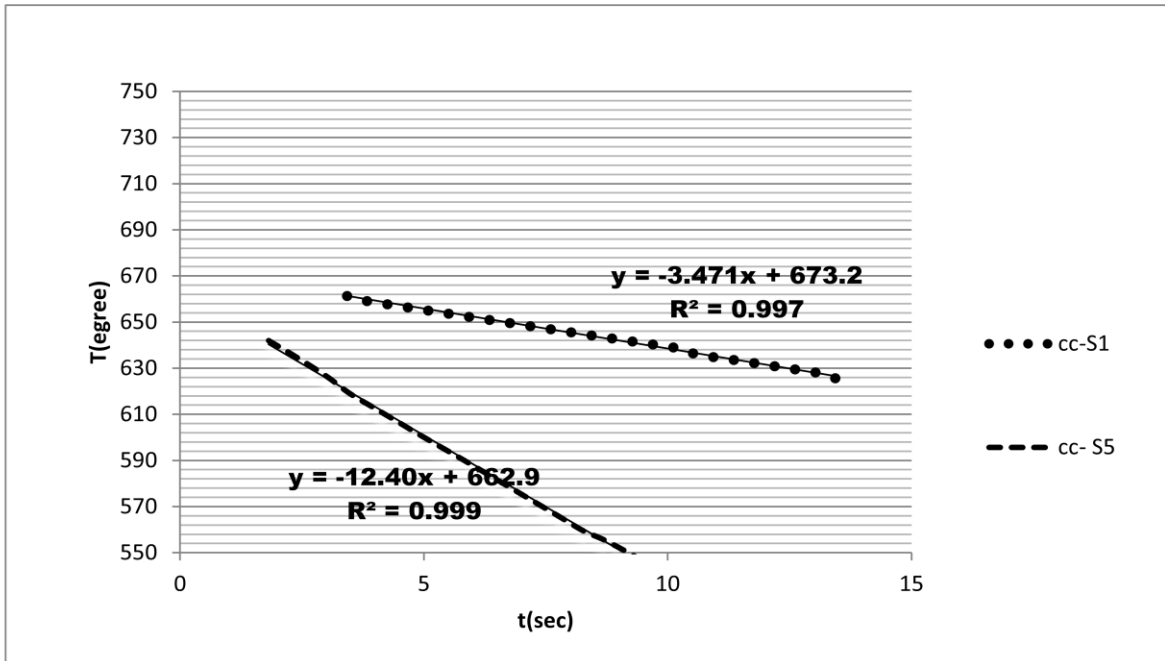


c

Figure 4.41 Die casting simulation for A3

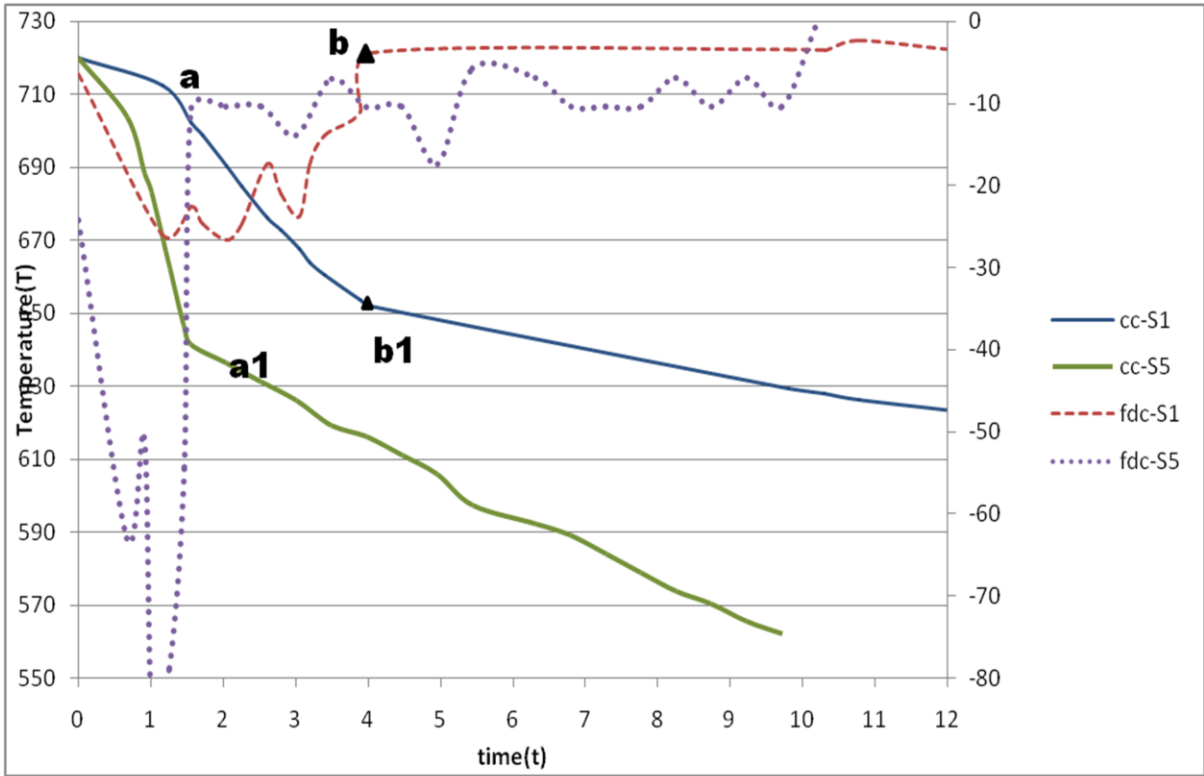


a

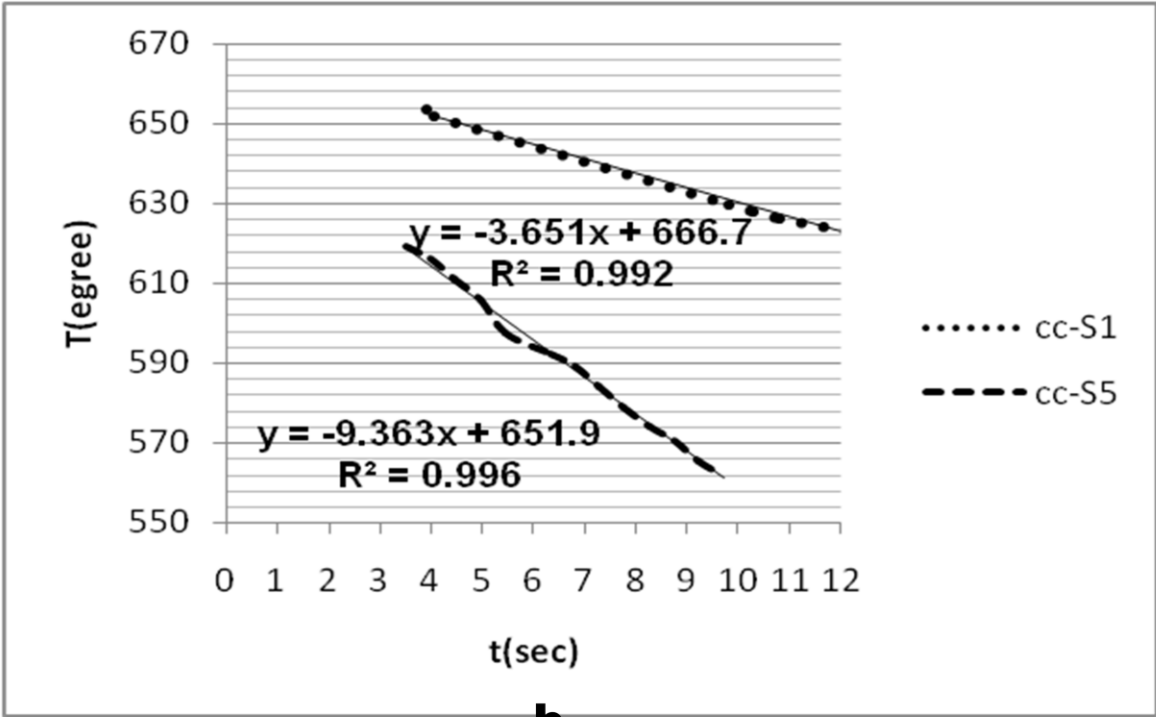


b

Figure 4.42 Simulation cooling curve for A1

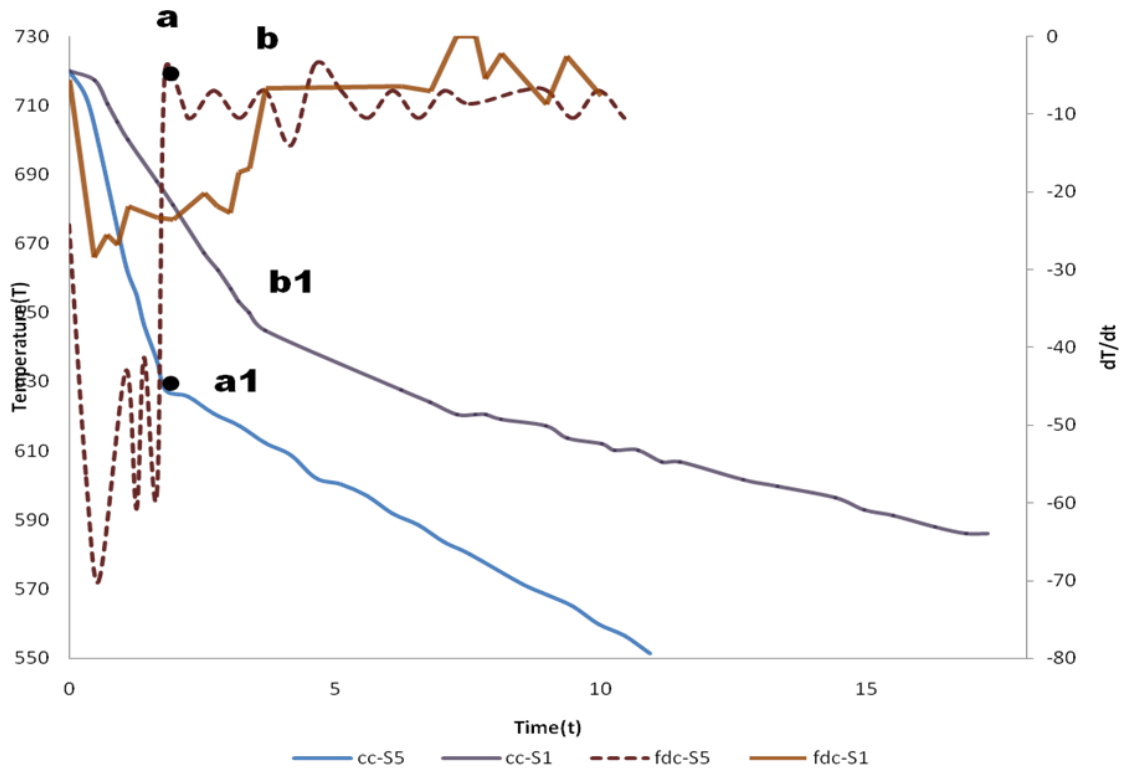


a

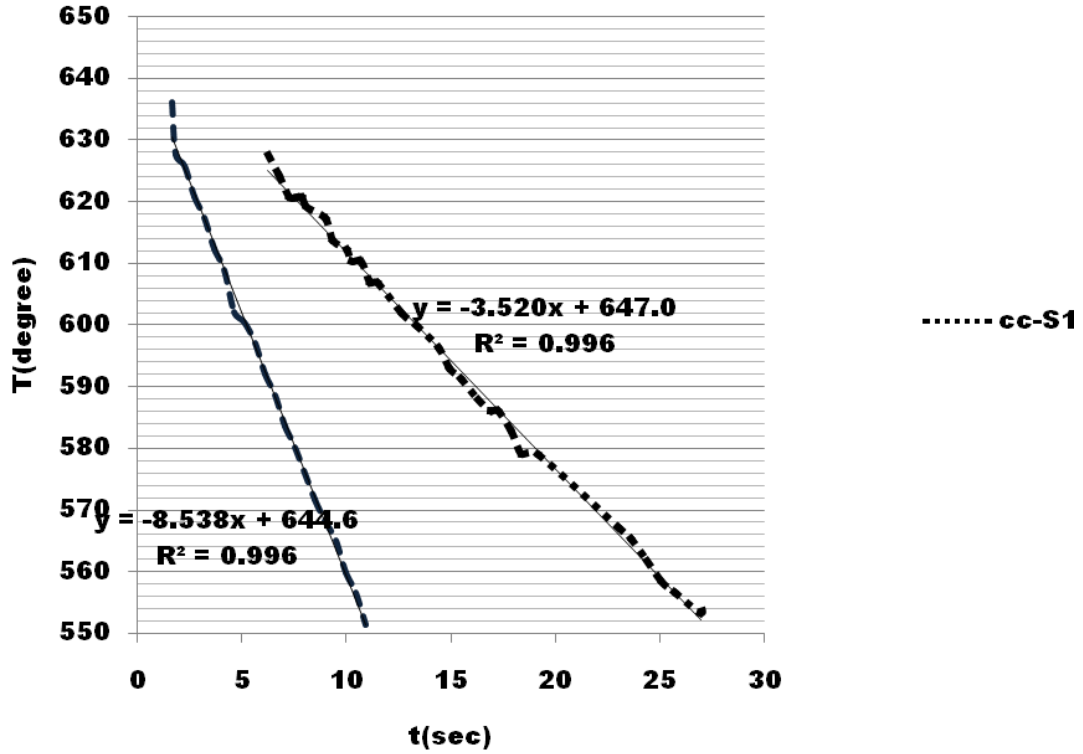


b

Figure 4.43 Simulation cooling curve for A2



a



b

Figure 4.44 Simulation cooling curve for A3

4.6.3 Simulation and Experimental results discussion

The cooling curves obtained from simulation analysis and experimental results of different alloy compositions are in good agreement with each other. The cooling rate for different thickness calculated from virtual cooling curves and grain size obtained from microstructure analysis show that for smaller thickness cooling rate is higher and consequently grain sizes are smaller. It can be clearly seen from physical examination of the cast components the shrinkage defects are at exact position that were predicted from the simulation for different compositions of alloy.

The study of cooling rate and corresponding first derivative curves from simulation analysis goes very well with the microstructure analysis. The relationship between the experimentally calculated SDAS of alloy A2 and A3 and cooling rate calculated from simulation cooling curves can be represented by the co-efficient equation as shown in [Equation 4. 1].

$$SDAS = Av^{-n} \quad (4.1)$$

Where SDAS is in μm , 'A' and 'n' are alloy dependent parameters. 'v' is the cooling rate in [Equation 4.1].

Taking $n = 1/3$ the expression for alloy A2 and A3 are given in Table 4.17.

Table 4.17 Comparison of actual and simulation SDAS

Section/Alloy composition	A2 [SDAS] simulation	A3[SDAS] simulation	A2[SDAS] actual	A3[SDAS] actual
S-5	$39(8.5)^{-1/3}=19.1$	$51(9.2)^{-1/3}=24.33$	18	26
S-1	$39(3.5)^{-1/3}=25.686$	$51(3.5)^{-1/3}=33.59$	25	31

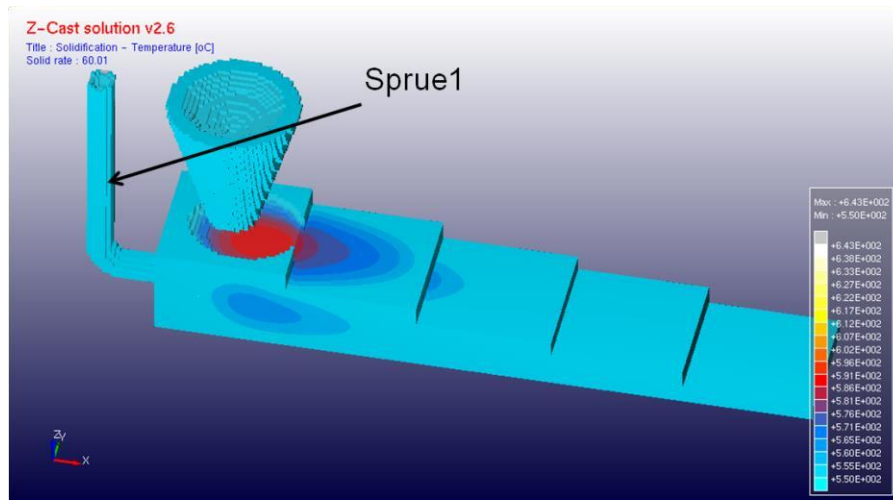
For A2 alloy, $A=39$ and for A3 alloy, $A=51$. Research shows that coefficient 'A' strongly depends on copper concentration [129]. The cooling rate calculated from simulation results are incorporated in the coefficient equation and the results obtained for grain sizes are close to the experimentally obtained grain size. The coefficient 'A' can be used to predict grain size from the cooling rate for a definite composition.

4.6.4 Simulation results to make defect free cast components

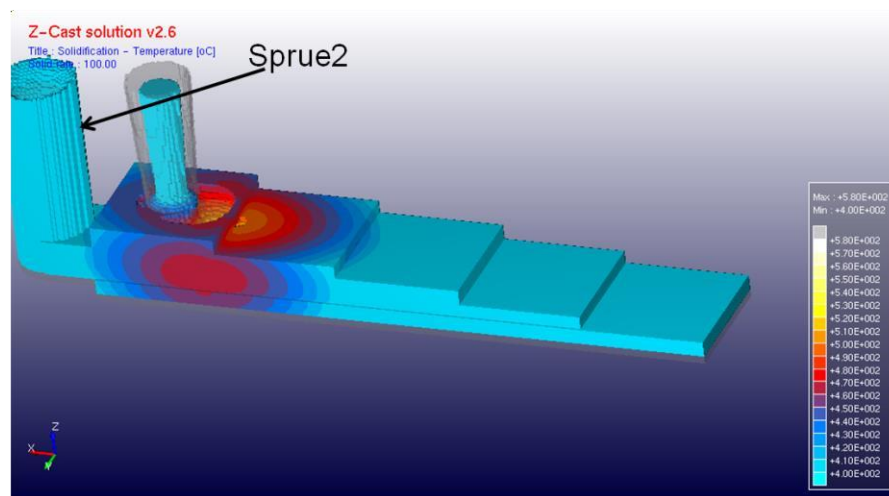
Virtual casting process has its advantage of avoiding wastage of material, money and time. Iterations for change in riser dimensions resulted in components having no shrinkage at the base of the riser. Simulation predictions can be used to avoid defects by focusing on the problem areas and by proper feeding to this area the iterations for both sand casting and die casting suggested a change in riser dimension can make components shrinkage free at the riser base.

Increasing the sprue size [Alloy A2]

Initial virtual trials made with changing the sprue size. Though increasing the sprue dimension resulted in shrinkage size reduction but it did not make the component defect free. It can be seen in the Fig 4.45.



a

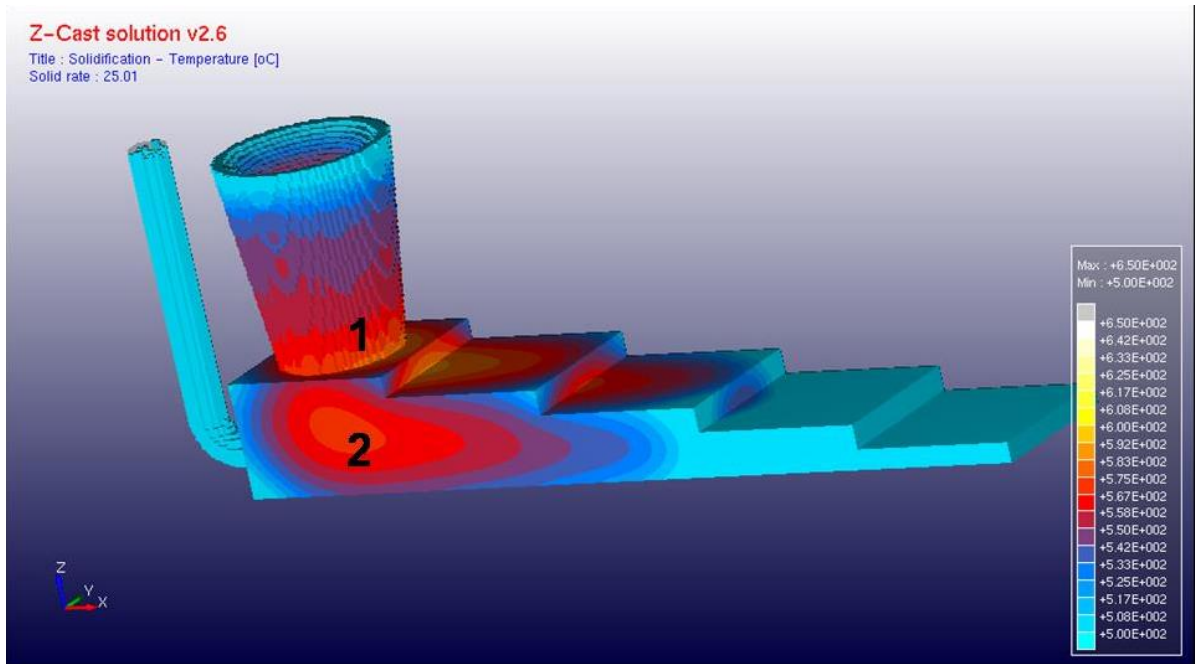


b

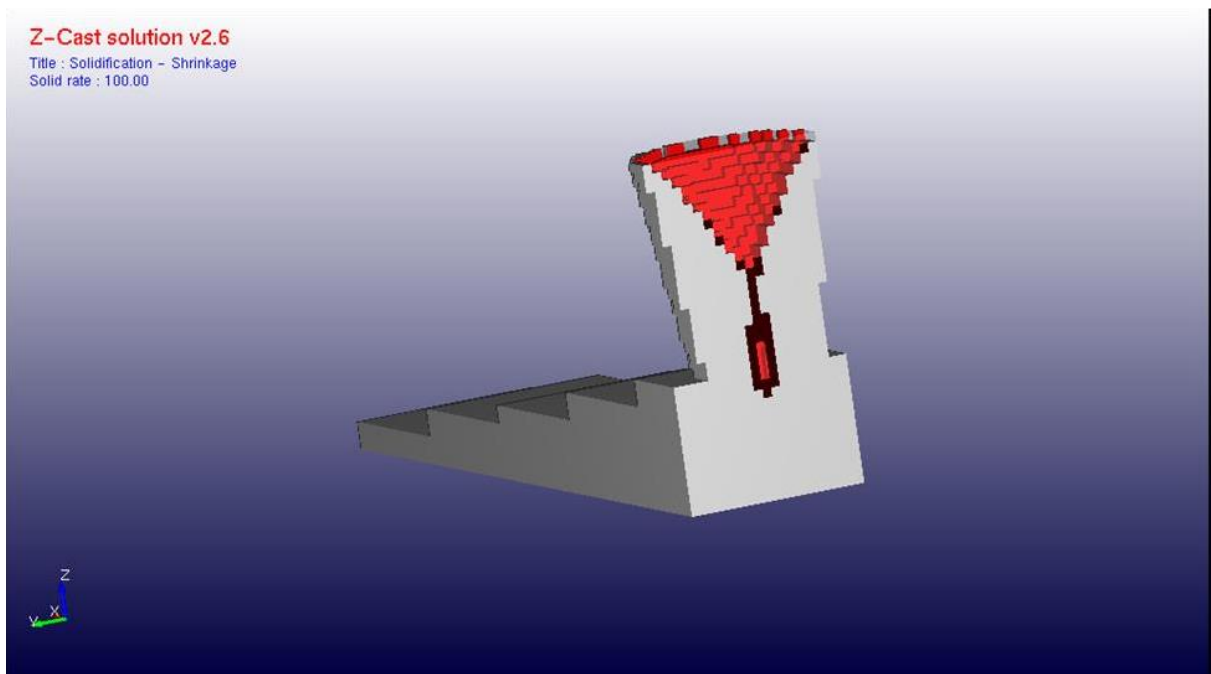
Figure 4.45 Solidification simulation iteration [sprue size change]

Changing the riser dimension [Alloy A2]

The diameter at the base of the riser for the existing cast iron mold is 20 mm and through iteration [virtual] process the base diameter was modified to 30 mm. Many virtual trials for riser dimensions done and as shown in 4.46 the shrinkage was finally eliminated from the component. It can be seen from Fig. 4.46(a) after 25% of solidification of the component the riser still having metal in liquid condition (marked 1 in the figure) and supplying the molten metal required. In Fig. 4.46(a) the hot spot marked '2' is eliminated completely. It can be seen in Fig. 4.46(b) there is no shrinkage at the base of the riser after 100% solidification. The simulation done for the A2 alloy successfully eliminated the shrinkage from the riser base.



a



b

Figure 4.46 Solidification for modified riser base diameter

4.6.5 Simulation results for spiral [fluidity] tests

The simulation results for spiral–shape fluidity test clearly reveal the length of spiral is smallest for the alloy A2. The scale for spiral length showing 77mm (right bottom corner). For alloy composition A1 and A3 the scale is showing 82.9 and 82.4 mm respectively [Fig. 4.47-4.49], scale used is 1mm=1cm for simulation. The phase diagram for Al-Cu alloy obtained using “Thermocalc Software” as shown in the [Fig.1.2] clearly indicates that freezing range for A2

is maximum as compared to other compositions i.e. A1 and A3. It is very well known that the lower the freezing range the higher the fluidity. Therefore, the fluidity simulation result for the composition goes well with the phase diagram for Al-Cu alloy.

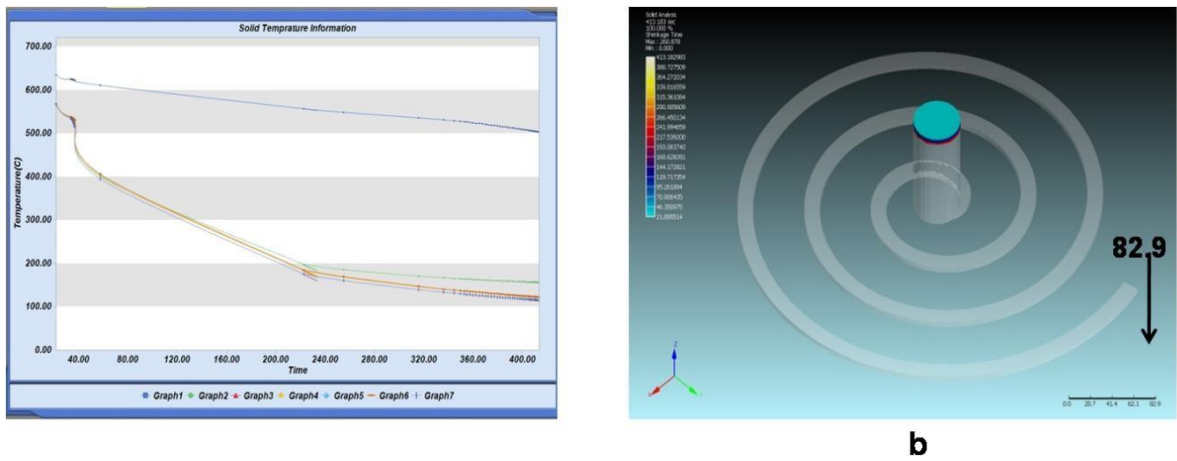


Figure 4.47 Simulation (a)cooling curve (b)length of spiral for A1

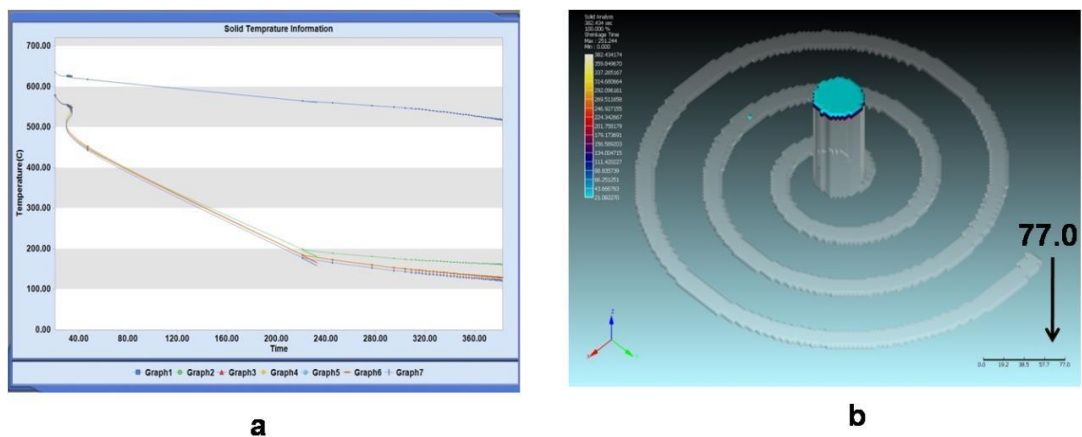


Figure 4.48 Simulation (a)cooling curve (b)length of spiral for A2

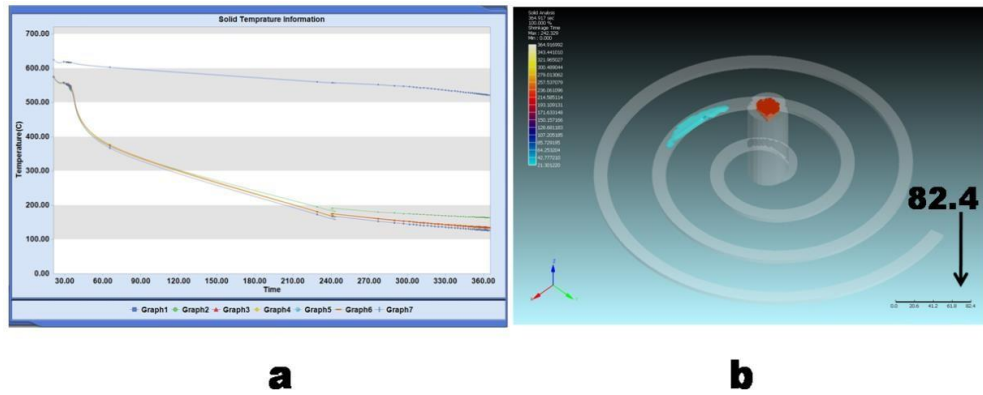


Figure 4.49 Simulation (a)cooling curve (b)length of spiral for A3

Table 4.18 Simulation shrinkage dimensions (in mm)

Alloy	Length(l)	Depth(d)	l x d
A1	65.3	8.8	574.6
A2	62.3	9.4	585.6
A3	66	9	594

The simulation results go very well with experimental shrinkage

5. CHAPTER 5 **CONCLUSION**

5.1 Variation in casting quality with varying composition

The analysis and study from various aspects of Al-Cu cast alloys developed; such as using different casting processes, varying compositions and varying thickness with their effects on cast components led to many important findings. The microstructure analysis and the mechanical behaviour of Al-Cu alloys having copper in the range of 4-12 wt% [in the absence of silicon] are suitable to use in automotive industries. Based on microstructure and mechanical characteristics following conclusions has been listed for developed alloy compositions.

Alloy A1:

The alloy containing copper 4wt% in aluminium is one of the most preferred cast alloys and also many researches are already done for this alloy. Both in presence and absence of silicon the aluminium alloy containing 4 wt% of copper [below its maximum solid solubility limit at eutectic]; ease of casting is not much affected. This property is due to less copper which during solidification form more eutectic Al₂Cu intermetallic. During cooling when α -aluminium formation pushes the remaining liquid towards eutectic composition Al₂Cu is formed, but as copper is less for the alloy time taken for mushy zone to completely solidify is less. This led to better quality of cast components.

Alloy A2:

Aluminium having copper 8wt% in the absence of silicon exhibit poor quality of cast components. Both for green sand and gravity die casting processes shrinkage cavities at the base of the riser has been noticed. As compared to alloy A1 the size (length and width) the shrinkage cavities are bigger for alloy A2. Keeping other factors such as mold temperature, riser size, pouring temperature constant and only increase in copper wt% affected the cast quality. The increase in solidification range and mushy zone formation during solidification for the alloy are responsible for poor castability.

Alloy A3:

Alloy A3 having 12wt% of copper and in the absence of silicon exhibit very poor castability. Keeping all other parameters same for the casting with addition of copper shrinkage sizes increase at the base of the riser. It can be noted that shrinkage formed at the thickest sections decrease gradually with decrease in thickness. The shrinkage cavities formed are smaller for sand casting as compared to die casting. For sand casting the rate of cooling is less which allows liquid metal to be available for longer time. Even for high wt% of copper the shrinkage formed at thickest section is smaller as compared to the die cast counterpart. In case of gravity die cast component with 12 wt% of copper the riser solidifies faster due to higher rate of cooling and shrinkages formed are much larger. Use of casting simulation software suggested to avoid shrinkage formation by changing casting parameters such as change in riser dimension.

The present study helps in deciding to choose the casting process for components with complicated shapes. Green sand casting are preferable over gravity die casting for complicated shapes.

5.2 Variation in mechanical properties with varying composition

Alloy A1:

Aluminium alloy with 4 wt% of copper i.e. alloy A1 is having ultimate tensile strength of

126MPa for gravity die cast component. For sand cast component the ultimate tensile strength of alloy A1 found to be 70MPa. Tensile properties of alloy A1 improved upon heat treatment. SEM images of fractured surface revealed mostly ductile fracture for this alloy.

Alloy A2: This alloy has ultimate tensile strength of 136MPa for gravity die cast component (as cast condition). The UTS improved to 210Mpa after heat treatment. It is discussed in the section 4.2.1 as the percent area covered by θ -phase is maximum for this alloy. The fractured surface of the tensile sample reveals mixed ductile and brittle type fracture. The %elongation also reported for this alloy is less than alloy A1. So ductility of alloy A2 is less compared to A1. The study suggest gravity die casting over green sand casting for this alloy when strength is the deciding factor. The analysis findings also suggest heat treatment response of alloy A2 is best among all the three compositions.

Alloy A3: The alloy A3 having 12 wt% of copper tensile strength is less than alloy A1. With increase in copper wt% from 8% to 12% the ultimate tensile strength decreases both for sand cast and die cast component. The % elongation also decreases due to presence of blocky θ -phase at grain boundaries. Heat treatment improves the tensile properties of alloy A3. When it comes to hardness alloy A3 exhibit highest hardness among all the three compositions. Both for sand cast and die cast component the hardness of alloy A3 is highest.

Aluminium alloy with 4wt% of copper has better casting properties as compared to other two compositions. Al₂Cu intermetallics are known to impart better strength at high temperature application as compared to Al-Si-Cu [ternary] intermetallics that is formed due to addition of silicon.

5.3 Wear properties

The alloy having 8wt% of copper exhibit highest wear resistance under dry-sliding condition. The optimum wear variable combination found for alloy A2 at 30N load and 500 rpm. Addition of copper beyond 8wt% affect the wear properties adversely due to coarser grain structure.

5.4 Casting simulation

Casting simulation is the future of modern foundries. The validation of simulation results with experimental results can make such software more reliable for industries. The current alloys under consideration are very well responsive to simulation results. Alloys with better mechanical behaviour and poor to fair castability enhance their yield by using “casting simulation software”. The data base of the simulation software used for the present analysis has been updated with the developed compositions as these compositions are not commercially available. So it can be used for research purpose to predict alloy behaviour with customized compositions. The external shrinkage cavity positions, size predicted from simulation and from shop floor experiments were in good agreement with each other for all the composition.

6. CHAPTER 6

FUTURE SCOPE OF WORK

The developed aluminium copper alloys without addition of silicon especially the composition having 8wt% of copper possess excellent mechanical and wear properties. Use of such alloy where strength at elevated temperature is required can be very economical. Using simulation software to produce sound casting with the composition having poor to fair castability is necessary before practical implementation.

The alloy properties of A3 having 12wt% of copper can be enhanced by using grain refiner. The alloy though has good tensile strength and better response to heat treatment; refining grains can enhance it further.

Optimising heat treatment can enhance the tensile properties further as response of the entire developed alloy was excellent.

Further research and analysis to improve soundness of casting and refining grains with optimised heat treatment process can help in use of the alloy which is comparatively cost effective in the area of high temperature applications for automobile industries.

REFERENCES

- [1] Cole, G. S., & Sherman, A. M. (1995). Lightweight materials for automotive applications. *Materials characterization*, 35(1), 3-9.
- [2] Ye, H. (2003). An overview of the development of Al-Si-alloy based material for engine applications. *Journal of Materials Engineering and Performance*, 12(3), 288-297.
- [3] Hirsch, J. (1997). Aluminium alloys for automotive application. In *Materials Science Forum* (Vol. 242, pp. 33-50). Trans Tech Publications Ltd.
- [4] Huda, Z., Taib, N. I., & Zaharinie, T. (2009). Characterization of 2024-T3: An aerospace aluminum alloy. *Materials Chemistry and Physics*, 113(2-3), 515-517.
- [5] Adeoti, M. O., Bongfa, B., & Olaiya, K. A. (2015). Microstructural analysis of sand and gravity die cast aluminium scraps.
- [6] Totten, G. E., & MacKenzie, D. S. (Eds.). (2003). *Handbook of aluminum: vol. 1: physical metallurgy and processes*. CRC press.
- [7] Nwaeju, C. C., Odo, J. U., Jisieike, S.C. Edoziuno, F. O. (2016) “Effect Of Copper Addition On The Structure And Mechanical properties Of Al-4%Zn Alloy” *International Journal of Scientific Research Engineering & Technology (IJSRET)*, ISSN 2278 – 0882 Volume 5, Issue 1.
- [8] Rodak, K., Kuc, D., & Mikuszewski, T. (2020). Superplastic Deformation of Al–Cu Alloys after Grain Refinement by Extrusion Combined with Reversible Torsion. *Materials*, 13(24), 5803.
- [9] Stadler, F., Antrekowitsch, H., Fragner, W., Kaufmann, H., & Uggowitzer, P. J. (2012). Effect of main alloying elements on strength of Al–Si foundry alloys at elevated temperatures. *International Journal of Cast Metals Research*, 25(4), 215-224.
- [10] Jeong, C. Y. (2012). Effect of alloying elements on high temperature mechanical properties for piston alloy. *Materials Transactions*, 53(1), 234-239.
- [11] J.E. Hatch, Aluminum Association. (1984). *Aluminum: Properties and Physical Metallurgy* (Vol. 1). ASM International., OH,1984, pp. 322-388
- [12] T. Gladman (1999) Precipitation hardening in metals, *Materials Science and Technology*, 15:1, 30-36, DOI: [10.1179/026708399773002782](https://doi.org/10.1179/026708399773002782)
- [13] Abdelaziz, M. H., Samuel, A. M., Doty, H. W., Songmene, V., & Samuel, F. H. (2022). Mechanical performance and precipitation behavior in Al-Si-Cu-Mg cast alloys: Effect of prolonged thermal exposure. *Materials*, 15(8), 2830.
- [14] Ilangovan, S. (2014). Effects of Solidification time on mechanical properties and wear behaviour of sand cast Aluminium alloy. *International Journal of Research in Engineering and Technology*, 3(2), 71-75.

- [15] Akhyar H, arhan A, Cooling rate, hardness and microstructure of aluminium cast alloys. www.Researchgate.net, May 2018, 2019
- [16] Reddy, K. S. Casting Simulation of Automotive Wheel Rim Using Procast. *Journal of Mechanical and Civil Engineering, IOSR-JMCE*, 11(6), 11-14.
- [17] Sun, T. T., Geng, J. W., Bian, Z. Y., Yi, W. U., Wang, M. L., Dong, C. H. E. N., & WANG, H. W. (2022). Enhanced thermal stability and mechanical properties of high-temperature resistant Al– Cu alloy with Zr and Mn micro-alloying. *Transactions of Nonferrous Metals Society of China*, 32(1), 64-78.
- [18] Molina R., Amalberto P. (2011) Mechanical charecterisation of aluminium alloy for high temperature applications Part2: Al-Cu, Al-Mg , Teksid Aluminum M. Rosso Politecnico di Torino ,(Vol. 29-2 - Ed2011)
- [19] J. Datta, Ed. (2002) *Aluminium Schlüssel: Key to Aluminum Alloy: 6th ed.* Aluminum Verlag, Düsseldorf, Germany.
- [20] Kang, B. K., & Sohn, I. (2018). Effects of Cu and Si contents on the fluidity, hot tearing, and mechanical properties of Al-Cu-Si alloys. *Metallurgical and Materials Transactions A*, 49(10), 5137-5145.
- [21] Ravi, K. R., Pillai, R. M., Amaranathan, K. R., Pai, B. C., & Chakraborty, M. (2008). Fluidity of aluminum alloys and composites: A review. *Journal of Alloys and Compounds*, 456(1-2), 201-210.
- [22] Zamani, M. (2017). *Al-Si Cast alloys-microstructure and mechanical properties at ambient and elevated temperatures* (Doctoral dissertation, Jönköping University, School of Engineering).
- [23] Molina, R., Amalberto, P., & Rosso, M. (2011). Mechanical characterization of aluminium alloys for high temperature applications Part1: Al-Si-Cu alloys. *Metallurgical Science and Tecnology*, 29(1).
- [24] Shabestari, S. G., & Moemeni, H. (2004). Effect of copper and solidification conditions on the microstructure and mechanical properties of Al–Si–Mg alloys. *Journal of Materials Processing Technology*, 153, 193-198.
- [25] Dahle, A. K., & Arnberg, L. (1996). The rheological properties of solidifying aluminum foundry alloys. *Jom*, 48(3), 34-37.
- [26] Davis, J. R. (1993). *Aluminum and aluminum alloys*. ASM international.
- [27] Sun, T. T., Geng, J. W., Bian, Z. Y., Yi, W. U., Wang, M. L., Dong, C. H. E. N., & WANG, H. W. (2022). Enhanced thermal stability and mechanical properties of high-temperature resistant Al– Cu alloy with Zr and Mn micro-alloying. *Transactions of Nonferrous Metals Society of China*, 32(1), 64-78.
- [28] Plaza, D., Asensio, J., Pero-Sanz, J. A., & Verdeja, J. I. (1998). Microstructure, a limiting parameter for determining the engineering range of compositions for light alloys: The Al-Cu-Si system. *Materials characterization*, 40(3), 145-158.
- [29] Piwonka, T.S. “Solidification of Metals and Alloy”, ASM HAND BOOK ONLINE

- [30] Sigworth, G., "Aluminum Casting Alloys and Casting Processes" ASM HAND BOOK ONLINE
- [31] Girgis, A., Samuel, A. M., Doty, H. W., Valtierra, S., & Samuel, F. H. (2019). On the Elevated Temperature, Tensile Properties of Al-Cu Cast Alloys: Role of Heat Treatment. *Advances in Materials Science and Engineering*, 2019.
- [32] Sabau, A. S., Mirmiran, S., Glaspie, C., Li, S., Apelian, D., Shyam, A., & Rodriguez, A.F. (2017). Hot-tearing of multicomponent Al-Cu alloys based on casting load measurements in a constrained permanent mold. In *TMS 2017 146th Annual Meeting & Exhibition Supplemental Proceedings* (pp. 465-473). Springer, Cham.
- [33] Easton, M. A., & StJohn, D. H. (2008). Improved prediction of the grain size of aluminum alloys that includes the effect of cooling rate. *Materials Science and Engineering: A*, 486(1-2), 8-13.
- [34] Zobac, O., Kroupa, A., Zemanova, A., & Richter, K. W. (2019). Experimental description of the Al-Cu binary phase diagram. *Metallurgical and Materials Transactions A*, 50(8), 3805-3815.
- [35] Zobac, O., Kroupa, A., Zemanova, A., & Richter, K. W. (2019). Experimental description of the Al-Cu binary phase diagram. *Metallurgical and Materials Transactions A*, 50(8), 3805-3815.
- [36] Xu, H., Xu, L. D., Zhang, S. J., & Han, Q. (2006). Effect of the alloy composition on the grain refinement of aluminum alloys. *Scripta materialia*, 54(12), 2191-2196.
- [37] Birol, Y. (2013). Effect of solute Si and Cu on grain size of aluminium alloys. *International Journal of cast metals research*, 26(1), 22-27.
- [38] Al-Rawajfeh A.E. & Al Qawabah, S.M.A. "Investigation Of Copper Addition On The Mechanical Properties And Corrosion Resistance Of Commercially Pure Aluminum", *Jordan Journal of Mechanical and Industrial Engineering*, Volume 9 Number 4, August.2015 ISSN 1995-6665 Pages 297- 301
- [39] Kaufman, J. G., & Rooy, E. L. (2004). *Aluminum alloy castings: properties, processes, and applications*. Asm International.
- [40] Bozorgi, S., & Anders, K. (2018). Mechanical Properties of High Copper Containing Al-Cu-Si Cast Alloys at Elevated Temperature. *Proceedings of ICAA-16 2018*.
- [41] Zhao, Q. L., Zhang, Q. Q., Zhang, W., Qiu, F., & Jiang, Q. C. (2018). Improved ductility and toughness of an Al-Cu casting alloy by changing the geometrical morphology of dendritic grains. *Materials Letters*, 214, 276-279.
- [42] Seifeddine, S., Sjgren, T., & Svensson, I. L. (2007). Variations In Microstructure And Mechanical Properties Of Cast Aluminum EN AC 43100 Alloy. *Metallurgical Science and Tecnology*, 25(1).

- [43] Santosh, M. V., Suresh, K. R., & Aithal, S. K. (2017). Mechanical Characterization and Microstructure analysis of Al C355.0 by Sand Casting, Die Casting and Centrifugal Casting Techniques. *Materials Today: Proceedings*, 4(10), 10987-10993.
- [44] Okayasu, M., Ohkura, Y., Takeuchi, S., Takasu, S., Ohfuji, H., & Shiraishi, T. (2012). A study of the mechanical properties of an Al–Si–Cu alloy (ADC12) produced by various casting processes. *Materials Science and Engineering: A*, 543, 185-192.
- [45] Liang, G., Ali, Y., You, G., & Zhang, M. X. (2018). Effect of cooling rate on grain refinement of cast aluminium alloys. *Materialia*, 3, 113-121.
- [46] He, C., Yu, W., Li, Y., Wang, Z., Wu, D., & Xu, G. (2020). Relationship between cooling rate, microstructure evolution, and performance improvement of an Al–Cu alloy prepared using different methods. *Materials Research Express*, 7(11), 116501.
- [47] Caceres, C. H., Djurdjevic, M. B., Stockwell, T. J., & Sokolowski, J. H. (1999). The effect of Cu content on the level of microporosity in Al-Si-Cu-Mg casting alloys. *Scripta Materialia*, 40(5), 631-637.
- [48] Di Giovanni, M. T., Cerri, E., Saito, T., Akhtar, S., Åsholt, P., Li, Y., & Di Sabatino, M. (2018). How slight solidification rate variations within cast plate affect mechanical response: a study on as-cast A356 alloy with Cu additions. *Advances in Materials Science and Engineering*, 2018.
- [49] Fornaro, O., & Palacio, H. A. (2009). Study of dilute Al–Cu solidification by cooling curve analysis. *Journal of materials science*, 44(16), 4342-4347.
- [50] Gao, K., Zhang, Z., Zhao, J., Sun, D., & Wang, F. (2020). Orientation and Microstructure Evolution of Al-Al₂Cu Regular Eutectic Lamellar Bifurcating in an Abruptly Changing Velocity under Directional Solidification. *Materials*, 13(4), 1004.
- [51] Neuser, M., Grydin, O., Andreiev, A., & Schaper, M. (2021). Effect of solidification rates at sand casting on the mechanical joinability of a cast aluminium alloy. *Metals*, 11(8), 1304.
- [52] Beroual, S., Boumerzoug, Z., Paillard, P., & Borjon-Piron, Y. (2019). Comparative study on the microstructures and hardness of the AlSi10.6CuMg alloy produced by sand casting and high pressure die casting. *International Journal of Cast Metals Research*.
- [53] Akhil, K. T., Arul, S., & Sellamuthu, R. (2014). The effect of section size on cooling rate, microstructure and mechanical properties of A356 aluminium alloy in casting. *Procedia Materials Science*, 5, 362-368.
- [54] Wierzbinska, M., & Sieniawski, J. (2011). *Microstructural Changes of Al-Cu alloys after prolonged annealing at elevated temperature*. INTECH Open Access Publisher.
- [55] Staszczyk, A., Sawicki, J., & Adameczyk-Cieslak, B. (2019). A study of second-phase precipitates and dispersoid particles in 2024 aluminum alloy after different aging treatments. *Materials*, 12(24), 4168.

- [56] Tash, M., Samuel, F. H., Mucciardi, F., & Doty, H. W. (2007). Effect of metallurgical parameters on the hardness and microstructural characterization of as-cast and heat-treated 356 and 319 aluminum alloys. *Materials Science and Engineering: A*, 443(1-2), 185-201.
- [57] Tsao, C. S., Huang, E. W., Wen, M. H., Kuo, T. Y., Jeng, S. L., Jeng, U. S., & Sun, Y.S. (2013). Phase transformation and precipitation of an Al–Cu alloy during non-isothermal heating studied by in situ small-angle and wide-angle scattering. *Journal of alloys and compounds*, 579, 138-146.
- [58] Shanmugasundaram, T., Heilmaier, M., Murty, B. S., & Sarma, V. S. (2010). On the Hall–Petch relationship in a nanostructured Al–Cu alloy. *Materials Science and Engineering:A*, 527(29-30), 7821-7825.
- [59] Rana, R. S., Purohit, R., & Das, S. (2012). Reviews on the influences of alloying elements on the microstructure and mechanical properties of aluminum alloys and aluminum alloy composites. *International Journal of Scientific and research publications*, 2(6), 1-7.
- [60] Abo-Elsoud, M., Esmail, H., & Sobhy, M. S. (2007). Correlation between elastic modulus of Al–Cu alloys and metallurgical characteristics of their constituent elements. *Radiation Effects & Defects in Solids*, 162(9), 685-690.
- [61] Talamantes-Silva, M. A., Rodriguez, A., Talamantes-Silva, J., Valtierra, S., & Colás, R. (2008). Characterization of an Al–Cu cast alloy. *Materials Characterization*, 59(10), 1434- 1439.
- [62] Lee, E., & Mishra, B. (2017). Effect of solidification cooling rate on mechanical properties and microstructure of Al-Si-Mn-Mg alloy. *Materials Transactions*, 58(11), 1624- 1627.
- [63] Mehdi, H., Sharma, S. , Anas, M., Sharma, N., “The Influences of Variation of Copper Content on the Mechanical Properties of Aluminium Alloy”, *International Journal of MaterialScience Innovations (IJMSI)* 3 (3): 74-86, 2015
- [64] Jin, P., Liu, Y., Li, F., & Sun, Q. (2021). Realization of synergistic enhancement for fracture strength and ductility by adding TiC particles in wire and arc additive manufacturing 2219 aluminium alloy. *Composites Part B: Engineering*, 219, 108921.
- [65] Lin C., Zhang H., Bi L., Wang Y.,2016. Research status of casting defects of cast Al-Cu alloys. 30(21): pp 143-149
- [66] Razaz G. and Carlberg T.,2019.,Hot Tearing Susceptibility of AA3000 Aluminum AlloyContaining Cu, Ti, and Zr .*Metallurgical and Materials Transactions A*, 50, pp 3842–3854.
- [67] Fan, Y.Y. and Makhlof, M.M., 2013. Castable aluminium alloys for high temperature applications. In *Materials Science Forum* (Vol. 765, pp. 8-12). Trans Tech Publications Ltd.
- [68] Lasagni, F., Lasagni, A., Marks, E., Holzapfel, C., Mücklich, F. and Degischer,

H.P., 2007. Three-dimensional characterization of ‘as-cast’ and solution-treated AlSi12 (Sr) alloys by high-resolution FIB tomography. *Acta materialia*, 55(11), pp.3875-3882.

[69] Jankowski, J. (2019). *Development of novel high temperature aluminum alloys*. Colorado School of Mines.]

[70] Xiao, D.H.; Wang, J.N.; Ding, D.Y. & S.P. Chen. (2002). Effect of Cu content on the mechanical properties of an Al–Cu–Mg–Ag alloy, *Journal of Alloys and Compounds*, 343, pp77–81.

[71] Mohamed, I. F., Yonenaga, Y., Lee, S., Edalati, K., & Horita, Z. (2015). Age hardening and thermal stability of Al–Cu alloy processed by high-pressure torsion. *Materials Science and Engineering: A*, 627, 111-118.

[72] Nwaokafor, P., Okeoma, K. B., & Mbamala, E. C. Investigation of The Effects of Varying Copper Concentrations on The Mechanical Properties of Aluminium.

[73] Molina, R., Leghissa, M., & Mastrogiacomo, L. (2004). New developments in high performance cylinder heads: application of LHIP and SPLIT cylinder head concept. *Metallurgical Science and Technology*, 22(2).

[74] Nunney, M. J. (2007). *Light and heavy vehicle technology*. Routledge.

[75] Karthikeya, G. V & Apparao K. Ch. (2019) Enhancement of Fluidity and Mechanical Properties of Al – Si cast Alloy, *International Journal of Innovative Technology and Exploring Engineering (IJITEE) ISSN: 2278-3075 (Online), Volume-9 Issue-2, December 2019*

[76] Barros, A. S., Magno, I. A., Souza, F. A., Mota, C. A., Moreira, A. L., Silva, M. A., & Rocha, O. L. (2015). Measurements of microhardness during transient horizontal directional solidification of Al-Rich Al-Cu alloys: Effect of thermal parameters, primary dendrite arm spacing and Al₂Cu intermetallic phase. *Metals and Materials International*, 21(3), 429-439.

[77] Özen, F., Fiçici, F., DüNDAR, M., & ÇOLAK, M. (2017). Effect of copper addition to aluminium alloys on surface roughness in terms of turning operation. *Acta Physica Polonica A*, 131(3), 467-469.

[78] Vasconcelos, A. J., Kikuchi, R. H., Barros, A. S., Costa, T. A., Dias, M., Moreira, A. L., ... & Rocha, O. L. (2016). Interconnection between microstructure and microhardness of directionally solidified binary Al-6wt.% Cu and multicomponent Al-6wt.% Cu-8wt.% Si alloys. *Anais da Academia Brasileira de Ciências*, 88, 1099-1111.

[79] Soliman, N. F., Ramadan, D. O., & Yagoob, J. A. (2021). Influence of Mould Thickness on Microstructure, Hardness and Wear of Al-Cu Cast Alloys. *International Journal of Engineering*, 34(8).

[80] Effect of Fe content on microstructure and mechanical properties of A206 alloy Cheng- jung Tseng, Sheng-Long Lee, Ten-Fu Wu and Jing-chie Lin

- [81] Abo-Elsoud, M., Esmail, H., & Sobhy, M. S. (2007). Correlation between elastic modulus of Al–Cu alloys and metallurgical characteristics of their constituent elements. *Radiation Effects & Defects in Solids*, 162(9), 685-690.
- [82] Rakhmonov, J., Liu, K., Pan, L., Breton, F., & Chen, X. G. (2020). Enhanced mechanical properties of high-temperature-resistant Al–Cu cast alloy by microalloying with Mg. *Journal of Alloys and Compounds*, 827, 154305.
- [83] Zhao, J., Yuan, Y., & Cui, F. (2017). Relationship between the Cu content and thermal properties of Al–Cu alloys for latent heat energy storage. *Journal of Thermal Analysis and Calorimetry*, 129(1), 109-115.
- [84] Bozorgi, S., & Anders, K. (2018). Mechanical Properties of High Copper Containing Al-Cu-Si Cast Alloys at Elevated Temperature. *Proceedings of ICAA-16 2018*.
- [85] Tanaka, T., & Kamitakahara, Y. (2017). Highly heat-resistant aluminum alloy “KS2000”. *KOBELCO Technol. Rev*, 35, 28-33.
- [86] Kasprzak, W., Emadi, D., Sahoo, M., & Aniolek, M. (2009). Development of aluminium alloys for high temperature applications in diesel engines. In *Materials Science Forum* (Vol. 618, pp. 595-600). Trans Tech Publications Ltd.
- [87] ASM Handbook, Volume 4: Heat Treating ASM Handbook Committee, p 841-879 DOI: 10.1361/asmhba0001205
- [88] Peng, J. H., Tang, X. L., He, J. T., & Xu, D. Y. (2011). Effect of heat treatment on microstructure and tensile properties of A356 alloys. *Transactions of Nonferrous Metals Society of China*, 21(9), 1950-1956.
- [89] Souissi, N., Souissi, S., Lecompte, J. P., Amar, M. B., Bradai, C., & Halouani, F. (2015). Improvement of ductility for squeeze cast 2017 A wrought aluminum alloy using the Taguchi method. *The International Journal of Advanced Manufacturing Technology*, 78, 2069-2077.
- [90] Heat Treating of Aluminum Alloys, ASM Handbook, Volume 4: Heat Treating ASM Handbook Committee, p 841-879, DOI: 10.1361/asmhba0001205
- [91] Arslankaya, S. (2020). Estimating the effects of heat treatment on aluminum alloy with artificial neural networks. *Emerging Materials Research*, 9(2), 540-549.
- [92] Jae-Ho, J. A. N. G., Dae-Geun, N. A. M., Yong-Ho, P. A. R. K., & Ik-Min, P. A. R. K. (2013). Effect of solution treatment and artificial aging on microstructure and mechanical properties of Al–Cu alloy. *Transactions of Nonferrous Metals Society of China*, 23(3), 631- 635.
- [93] Hamasha, M. M., Mayyas, A. T., Hassan, A. M., & Hayajneh, M. T. (2012). The effect of time, percent of copper and nickel on naturally aged Al-Cu-Ni cast alloys. *Journal of Minerals and Materials Characterization and Engineering*, 11(02), 117.
- [94] Paulisch, M. C., Wanderka, N., Haupt, M., Selve, S., Driehorst, I., & Reimers, W. (2015). The influence of heat treatments on the microstructure and the mechanical

properties in commercial 7020 alloys. *Materials Science and Engineering: A*, 626, 254-262.

[95] Bogdanoff, T., & Dahlström, J. (2009). The influence of copper on an Al-Si-Mg alloy (A356)-Microstructure and mechanical properties.

[96] Iswanto, P. T., & Pambekti, A. (2020). Heat treatment T4 and T6 effects on mechanical properties in Al-Cu alloy after remelt with different pouring temperatures. *Metalurgija*, 59(2), 171-174.

[97] Wang, H., Yi, Y., & Huang, S. (2017). Microstructure evolution and mechanical properties of 2219 Al alloy during aging treatment. *Journal of Materials Engineering and Performance*, 26(4), 1475-1482.

[98] Mohamed, A. M. A., & Samuel, F. H. (2012). A review on the heat treatment of Al-Si- Cu/Mg casting alloys. In *Heat Treatment-Conventional and Novel Applications* (Vol. 1, pp. 55-72). Rijeka, Croatia: InTech.

[99] Zamani, M., Belov, I., Sjölander, E., Bjurenstedt, A., Ghassemali, E., & Seifeddine, S. (2020). Study on dissolution of Al₂Cu in al-4.3 cu and a205 cast alloys. *Metals*, 10(7), 900.

[100] Reiso, O., Øverlie, H. G., & Ryum, N. (1990). Dissolution and melting of secondary Al₂Cu phase particles in an AlCu alloy. *Metallurgical Transactions A*, 21(6), 1689-1695.

[101] Ymanoğlu, R., Karakulak, E., Zeren, A., & Zeren, M. (2013). Effect of heat treatment on the tribological properties of Al-Cu-Mg/nanoSiC composites. *Materials & Design*, 49, 820-825.

[102] Chen, J., Liao, H., & Xu, H. (2018). Uneven Precipitation Behavior during the Solutionizing Course of Al-Cu-Mn Alloys and Their Contribution to High Temperature Strength. *Advances in Materials Science and Engineering*.

[103] H. Zoller and A. Ried, (1971) "Metallurgical aspects in development of AL MG SI alloys with a low sensitivity to quenching," *Z Metallkd*, vol. 62, pp. 354-358.

[104] Mondolfo, L. F. (1976). „Aluminium alloys: structure and properties“, Butterworths, London, 1. Ausgabe, S, 72.

[105] Kavalco, P. M., & Canale, L. C. (2009). Quenching of aluminum alloys. *Heat treating progress*, 23.

[106] Kassner, M. E., Geantil, P., & Li, X. (2011). A Study of the Quench Sensitivity of 6061-T6 and 6069-T6 Aluminum Alloys. *Journal of Metallurgy*, 2011.

[107] Tan, C. F., & Radzai, S. M. (2009). Effect of hardness test on precipitation hardening aluminium alloy 6061-T6. *Chiang Mai Journal of Science*, 36(3), 276-286.

[108] Samuel, F. H. (1998). Incipient melting of Al₅Mg₈Si₆Cu₂ and Al₂Cu intermetallics in unmodified and strontium-modified Al-Si-Cu-Mg (319) alloys during solution heat treatment. *Journal of Materials Science*, 33(9), 2283-2297.

- [109] Subramanian C, (1985), Proc. Int Conf on Aluminium, New Delhi, India, 568–572
- [110] Beesley, C., & Eyre, T. S. (1976). Friction and wear of aluminium alloys containing copper and zinc. *TRIBOLOGY international*, 9(2), 63-69.
- [111] Rao, K. N., & Sekhar, J. A. (1986). Comparative wear behaviour of aluminium alloys. *Journal of materials science letters*, 5(11), 1186-1188.
- [112] Sekar, K., & Vasanthakumar, P. (2019). Mechanical properties of Al-Cu alloy metal matrix composite reinforced with B4C, Graphite and Wear Rate Modeling by Taguchi Method. *Materials Today: Proceedings*, 18, 3150-3159.
- [113] Dai, W., Zhang, X., Li, C., & Yao, G. (2022). Effect of thermal conductivity on micro- arc oxidation coatings. *Surface Engineering*, 38(1), 44-53. *Surface Engineering* 38:1, pages 44-53.
- [114] Abd El Aal, M. I., El Mahallawy, N., Shehata, F. A., Abd El Hameed, M., Yoon, E. Y., & Kim, H. S. (2010). Wear properties of ECAP-processed ultrafine grained Al–Cu alloys. *Materials Science and Engineering: A*, 527(16-17), 3726-3732. <https://doi.org/10.1016/j.msea.2010.03.057>
- [115] Zhang, J., & Alpas, A. T. (1997). Transition between mild and severe wear in aluminium alloys. *Acta materialia*, 45(2), 513-528. [https://doi.org/10.1016/S1359-6454\(96\)00191-7](https://doi.org/10.1016/S1359-6454(96)00191-7)
- [116] P. Haldar and G. Sutradhar, (2021) Simulation and validation of castings in shopfloor. In casting processes and modelling of metallic materials. IntechOpen.
- [117] Sultana N., Md. Uzzaman R., YounosurRahman Y., and Das A. (2019). Solidification and Filling Related Defects Analysis Using Casting Simulation Technique with Experimental Validation, *International Journal of Mechanical Engineering and Applications*, 6(6), 150-160. <http://www.sciencepublishinggroup.com/j/ijmea>
- [118] Boeira, A. P., Ferreira, I. L., & Garcia, A. (2009). Alloy composition and metal/mold heat transfer efficiency affecting inverse segregation and porosity of as-cast Al–Cu alloys. *Materials & Design*, 30(6), 2090-2098. <https://doi.org/10.1016/j.matdes.2008.08.032>
- [119] Yin, Y., Zhou, J., Guo, Z., Wang, H., Liao, D., & Chen, T. (2015). The Through Process Simulation of Mold filling, Solidification, and Heat Treatment of the Al Alloy Bending Beam Low-pressure Casting. In *IOP Conference Series: Materials Science and Engineering* (Vol. 84, No. 1, p. 012043). IOP Publishing.
- [120] Jain S.K., Jain V¹, and Jain V². (2014) Effect of Chill Size and Material on Temperature Gradient in Aluminium, Alloys Casting *Journal of Material Science and Mechanical Engineering*, 1(2). <http://www.krishisanskriti.org/jmsme.html>
- [121] Dehnavi, M., Vafaenezhad, H., & Sabzevar, M. H. (2014). Investigation the solidification of Al-4.8 wt.% Cu alloy at different cooling rate by computer-aided cooling curve analysis. *Metallurgical and Materials Engineering*, 20(2), 107-118.

<https://dx.doi.org/10.5937/metmateng14>

[122] Farahany, S., Ourdjini, A., Idris, M. H., & Shabestari, S. G. (2013). Computer-aided cooling curve thermal analysis of near eutectic Al–Si–Cu–Fe alloy. *Journal of thermal analysis and calorimetry*, 114(2), 705-717. <http://dx.doi.org/10.1007/s10973-013-3005-7>

[123] Djurdjevic, M. B., Vicario, I., & Huber, G. (2014). Review of thermal analysis applications in aluminium casting plants. *Revista de Metalurgia*, 50(1), 1- 12.: doi: <http://dx.doi.org/10.3989/revmetalm.004>

[124] Seifeddine, S., Wessen, M., & Svensson, I. L. (2006). Use of simulation to predict microstructure and mechanical properties in an as-cast aluminium cylinder head comparison- with experiments. *Metallurgical Science and Tecnology*, 24(2).

[125] Raneetpongprung, C. & Hassamontr, Jaramporn. (2003). Analysis of grain size measurement methods in semiautomatic image analysis setup. Transactions of the North American Manufacturing Research Institution of SME. 31. 499-506.

[126] Aguilar Rivas, R. & Biloni, H. (1980). Fluidity of Al-Cu AlloyswithZeroSuperheat. *International Journal of Materials Research*, 71(4), 264-268. <https://doi.org/10.1515/ijmr-1980-71041>

[127] Kayal, S., Behera, R., & Sutradhar, G. (2011). Effect of SiCp on fluidity of the LM6/SiCp metal matrix composites. *International Journal of Emerging Trends in Engineering and Development*, 3(1), 172-180.

[128] Roy, S., Allard, L. F., Rodriguez, A., Porter, W. D., & Shyam, A. (2017). Comparative evaluation of cast aluminum alloys for automotive cylinder heads: Part II—mechanical and thermal properties. *Metallurgical and Materials Transactions A*, 48(5), 2543-2562.

[129] Grugel, R. N. (1993). Secondary and tertiary dendrite arm spacing relationships in directionally solidified Al-Si alloys. *Journal of materials science*, 28(3), 677-683.

